ADVECTIVE-DISPERSIVE CONTAMINANT TRANSPORT TOWARDS A PUMPING WELL

Jaco Johannes Adriaan van Kooten

Promotor: Dr.Ir. J. Grasman
Hoogleraar in de Wiskunde, inclusief de Numerieke Wiskunde

Co-promotor: Dr. M. de Gee
Universitair hoofddocent bij de vakgroep Wiskunde

Jaco Johannes Adriaan van Kooten

ADVECTIVE-DISPERSIVE CONTAMINANT TRANSPORT TOWARDS A PUMPING WELL

PROEFSCHRIFT

ter verkrijging van de graad van doctor
in de landbouw- en milieuwetenschappen
op gezag van de rector magnificus,
dr. C.M. Karssen,
in het openbaar te verdedigen
op woensdag 31 januari 1996
des namiddags te één uur dertig in de Aula
van de Landbouwuniversiteit te Wageningen.

ACKNOWLEDGEMENTS

The research described in this thesis was carried out at the Department of Mathematics, Agricultural University, Wageningen, the Netherlands. The research was financially supported by the Dutch Foundation for Technical Sciences STW (Stichting Technische Wetenschappen) which is subsidized by the Dutch Organization for Scientific Research NWO (Nederlandse Organisatie voor Wetenschappelijk Onderzoek).

Nederlandse vertaling titel:
ADVECTIEF-DISPERSIEF TRANSPORT VAN EEN VERONTREINIGING NAAR EEN POMPPUT

NWO

CIP-DATA KONINKLIJKE BIBLIOTHEEK, DEN HAAG

Kooten, Jaco Johannes Adriaan van

Advective-dispersive contaminant transport towards a pumping well /
Jaco Johannes Adriaan van Kooten. - [S.l.:s.n.]
Thesis Landbouwuniversiteit Wageningen. - With ref. - With summary in Dutch.
ISBN 90-5485-472-3
Subject Headings: Contamination of Wells / analytical approximation method / dispersion.

STELLINGEN

1. Transversale dispersie kan wel degelijk een belangrijk effect hebben op het transport van een verontreiniging. *(Dit proefschrift)*

2. Hoewel in de in hoofdstuk 3 gepresenteerde gemengd numeriek-analytische methode voor het oplossen van de transportvergelijkingen voor een kinetisch adsorberende stof geen fouten worden geïntroduceerd als gevolg van tijdsdiscretisatie van de adsorptie-isotherm, heeft een gemengde oplossing dezelfde nauwkeurigheid als een volledig numerieke oplossing; de dominerende fout is afkomstig van de ruimte-tijd discretisatie van de parabolische advectie-dispersie vergelijking (1a).
(J.J.A van Kooten, A method to solve the advection-dispersion equation with a kinetic adsorption isotherm, To appear in Advances in Water Resources, 1995).

3. We beschouwen het advectie-dispersie model met twee mobiele fasen:

$$\frac{\partial C_1}{\partial t} = -v_1\frac{\partial C_1}{\partial x} + D_1\frac{\partial^2 C_1}{\partial x^2} - (k_1+\lambda_1)C_1 + k_2C_2$$

$$\frac{\partial C_2}{\partial t} = -v_2\frac{\partial C_2}{\partial x} + D_2\frac{\partial^2 C_2}{\partial x^2} - (k_2+\lambda_2)C_2 + k_1C_1$$

waarin

C_i = concentratie van stof in fase i $[M/L^3]$,
v_i = advectiesnelheid in fase i $[L/T]$,
D_i = dispersiecoëfficiënt in fase i $[L^2/T]$,
λ_i = vervalcoëfficiënt in fase i $[T^{-1}]$,
k_i = kinetische uitwisselingscoëfficiënten tussen fase 1 en 2 $[T^{-1}]$.

De oplossing van bovenstaand stelsel voor een Diracpuls in fase 1

$$C_1(x,0) = \delta(x) \quad , \qquad C_2(x,0) = 0 \quad ,$$

luidt

$$C_1(x,t) = \tilde{C}(x,t)e^{-(k_1+\lambda_1)t} + \int_0^t \tilde{C}(x,\tau)h_{11}(t,\tau)e^{-\lambda_1\tau-\lambda_2(t-\tau)}d\tau \quad ,$$

$$C_2(x,t) = \int_0^t \tilde{C}(x,\tau)h_{12}(\tau,t)e^{-\lambda_1\tau-\lambda_2(t-\tau)}d\tau.$$

met

$$\tilde{C}(x,\tau,t) = \frac{1}{2\sqrt{\pi(D_1\tau+D_2(t-\tau))}}\exp\{-\frac{(x_1-v_1\tau-v_2(t-\tau))^2}{4(D_1\tau+D_2(t-\tau))}\}$$

en waarin h_{11} en h_{12} als gedefinieerd in hoofdstuk 3 van dit proefschrift (uitdrukking (2) and (3)). *(recent resultaat)*

4. Evenals voor (massa)media blijkt voor simulatiemodellen te gelden dat een gekleurde presentatie hoger gewaardeerd wordt dan eenvoudigweg diepgang.

5. Bij het implementeren van een algoritme in programmacode dient men ter bevordering van de inzichtelijkheid en betrouwbaarheid te streven naar zo'n klein mogelijk aantal statements.

6. De smogvorming in de stratosfeer illustreert dat onze welvaart een te hoge vlucht heeft genomen. Vliegtuiggebruik dient daarom ontmoedigd te worden, zeker voor vakantiedoeleinden. *(N.a.v. Volkskrant 18 november 1995, pag. 19)*

7. Het geven van zindelijkheidstraining voordat kinderen kunnen lopen, is dweilen met de kraan open. Zindelijkheid is een vorm van gedrag dat pas mag worden aangeleerd als de parasympathische vezels vanuit het centrale zenuwstelsel naar de blaas zijn aangelegd. *(prof.dr. J.A.R. Sanders-Wouters et al., Leerboek kinder- en jeugdpsychiatrie, 3e gewijzigde druk, Assen/Maastricht, 1990)*

8. Hoewel van den Beukel terecht constateert dat "natuurwetenschap (ver)wordt tot pseudoreligie, waarvan de wetenschappers de priesters zijn", mogen wetenschap en techniek niet geïdentificeerd worden met de anti-christ.
(prof.dr.ir. A. van den Beukel, "De dingen hebben hun geheim", Baarn, 1990; 2 Thess. 2).

9. Het feit dat een wiskundig model een fysisch verschijnsel slechts kan beschrijven maar niet kan verklaren, zou natuurwetenschappers bescheiden moeten stemmen.
(N.a.v. Stephen Hawking, "A brief history of time", Ned. vert. "Het Heelal", A'dam, 1988).

10. Ook non-conformisme kan een vorm van conformisme zijn.

11. Het ontbreken van diversiteit in een kerkelijke gemeente duidt eerder op niet-wezenlijke betrokkenheid van de leden dan op eensgezindheid.

12. Het is onmogelijk een goed interpreet van Bachs religieuze werken te zijn, zonder kennis te hebben van de Lutherse of gereformeerde theologie en de waarde hiervan aan te voelen. *(Casper Honders, Over Bachs schouder, Groningen, 1986).*

13. Veelal geldt: Wie promoveert is niet wijs.

J.J.A van Kooten

Abstract

In this thesis we describe an analytical approximation method for predicting the advective-dispersive transport of a contaminant towards a pumping well. The groundwater flow is assumed to be stationary and essentially horizontal. Due to dispersion contaminant transport is a stochastic process. We derive approximations for the arrival probability (or fraction) of particles at a well, for the mean and variance of the arrival time and for the arrival time distribution at a well. The advective flow yields first order approximations. The effect of longitudinal dispersion is included by expanding the first and second moment of the arrival time in power series of the longitudinal dispersion coefficient. Transversal dispersion only plays a crucial role near the separating streamlines bounding the catchment area of a well. Its effect is analyzed locally with boundary layer techniques. The incorporation of linear equilibrium adsorption and first order decay is rather straightforward. The asymptotic approximations are compared with the results of random walk simulations.

A self-contained part of this thesis is devoted to the transport of a kinetically adsorbing contaminant. We show that once the transport of a non-adsorbing contaminant has been computed, the effect of first order kinetics can be incorporated naturally by utilizing a stochastic description of the residence time of particles in the free phase.

The results of our research have been implemented in the software package ECOWELL. The input of ECOWELL consists of a head field generated with a numerical flow model. The technical documentation of ECOWELL is part of this thesis. The use of ECOWELL is demonstrated in a case study.

Key words: advective-dispersive contaminant transport, arrival fraction at well, arrival time, asymptotic approximations, random walk, first order decay, kinetic adsorption.

Ontmoeting bij een put in Samaria:

"Jezus antwoordde en zeide tot haar: Een ieder die van dit water drinkt zal wederom dorsten, maar zo wie gedronken zal hebben van het water dat ik hem geven zal, die zal in eeuwigheid niet dorsten, maar het water dat ik hem zal geven, zal in hem worden een fontein van water springende tot in het eeuwige leven".

(Johannes 4 : 13 en 14)

Voor MARJA
en onze kinderen
RUBEN en ARNOUD

DANKWOORD

Een proefschrift schrijven doe je niet alleen. Vele personen dragen direkt of indirekt bij aan de totstandkoming ervan. In de eerste plaats denk ik dan aan mijn promotor prof.dr.ir. J. Grasman en co-promotor dr. M. de Gee. Zij waren de initiatiefnemers van het door STW-gefinancierde onderzoeksproject. Gedurende vier jaar waren zij mijn dagelijkse begeleiders. Vrijwel iedere woensdag hadden we werkbespreking. Dit hield vaart in het project. Regelmatig streefden Oscar en ik ernaar om voor de werkbespreking iets af te hebben. Johan en Maarten, het was een voorrecht om door jullie begeleid te worden. Johan hield de grote lijn in de gaten. Maarten waakte over de correcte uitwerking van deelonderwerpen. Deze combinatie heeft zeker bijgedragen aan het welslagen van het project. Door jullie scherpzinnigheid werd menige hobbel in het onderzoek snel genomen. Hartelijk dank!

Met Oscar Buse heb ik heel intensief samengewerkt. Oscar heeft het grootste deel van het programmeerwerk aan ons software pakket ECOWELL voor zijn rekening genomen. Dankzij hem is het een gebruiksvriendelijk en robuust pakket geworden. Oscar heeft voor menige vrolijke noot gezorgd. Door zijn levenslustige uitstraling weet hij een ontspannen sfeer te scheppen. Trouwens, ook bedankt voor de vele bakjes koffie die je hebt gezet. Vrijwel iedere morgen kwam de koffiegeur ons reeds tegemoet.

Om in het onderzoeksonderwerp thuis te raken, heb ik van januari tot en met mei 1992 stage gelopen aan het RIVM. De gastvrijheid op het LBG was groot. Gerard Uffink wil ik bedanken voor zijn begeleiding en voor het gebruik van zijn kamer en computer. Met de METROPOL-code heb ik simulaties uitgevoerd van een tracer-experiment in een diepe kleilaag in Mol (België).

Eens per halfjaar hadden we een bijeenkomst van de STW-begeleidingscommissie, bestaande uit: W. (Wim) Aspers (STW/SMC), ir. C. (Cors) van den Brink (IWACO), dr. R. (Rik) Kaasschieter (TU Eindhoven), dr.ir. R.W.R. (Ruurd) Koopmans (Vakgroep Hydrology, LUW), dr.ir. G.J.M. (Gerard Uffink) (RIVM), dr.ir. E.J.M. (Ed) Veling (RIVM) en mr. A. Philippo (STW/jurist). Allen vriendelijk dank voor de (geheel vrijwillige!) deelname. Jullie interesse was merkbaar. De bijeenkomsten hebben duidelijk richting gegeven aan het onderzoek; door jullie bijdragen heb ik meer dan eens nieuwe inspiratie opgedaan.

Aan de vakgroep Wiskunde van de LU heb ik met plezier gewerkt. Mijn temperamentvolle kamergenoot Joris Maree bracht veel gezelligheid met zich mee. Ik bewaar goede herinneringen aan onze gesprekken. Behalve wiskunde blijken er nog vele andere onderwerpen te zijn die ons beide interesseren. Op deze wijze zijn heel wat ervaringen gedeeld. Ik heb dankbaar gebruik gemaakt van een basisstroompatroon getekend door Onno van Herwaarden (bijv. Omslag en Hoofdstuk 2 fig. 2 tm 5). Adwin Vervuurt heeft enkele lastige integratieroutines uitgewerkt en geïmplementeerd in ons software pakket (zie Hoofdstuk 4, Appendix A). Het secretariaat ben ik erkentelijk voor het uittikken van mijn eerste en tweede artikel.

Ook ieders meeleven in de spannende tijd rond de geboorte van Arnoud heeft ons goed gedaan. De jaarlijkse excursie met "Bloemlezingen" en de decemberavond kwamen het vakgroepsleven ten goede.

Op initiatief van prof.dr.ir. P.A.C. (Pieter) Raats werd in het voorjaar van 1993 een studiegroep georganiseerd over stochastische modellering van waterstroming en stoftransport in heterogene poreuze media. Het waren leerzame bijeenkomsten; ik heb kennis gemaakt met een voor mij toen nog onbekend terrein. Ook heeft Pieter verschillende van mijn artikelen kritisch doorgelezen. De data voor de casestudie in hoofdstuk 5 werden aangeleverd door ir. Rien Pastoors.

De basis voor dit proefschrift is reeds in mijn jeugd gelegd. Mijn ouders wil ik daarom hartelijk danken voor alles wat zij mij hebben meegegeven. Ook de belangstelling van broers, zussen en schoonfamilie heb ik erg gewaardeerd. De zeeuwse zeewind die ik bij mijn schoonouders mocht opsnuiven, werkte verfrissend op de geest.

Marja, de dank die ik jou verschuldigd ben, laat zich eigenlijk niet in een paar zinnen uitdrukken. Dit proefschrift is geschreven in een tijd waarin ook jij het heel druk had met je werk, je studie en onze kinderen. Daarnaast wist je altijd belangstelling op te brengen voor de mensen om je heen. Ik bewonder je geduld, werklust en doorzettingsvermogen. Af en toe moest je mij dwingen om niet helemaal in het onderzoek weg te dromen. Zonder jouw steun was dit proefschrift nooit verschenen.

Jaco van Kooten
Lunteren, oktober 1995

CONTENTS

General Introduction 2

Chapter 1
Groundwater contaminant transport including adsorption and first-order decay
Published in Stochastic Hydrology and Hydraulics, 8, 185-205, 1994 7

Chapter 2
An asymptotic method to predict the contamination of a pumping well
Published in Advances in Water Resources, 18 (5), 295-313, 1995 31

Chapter 3
A method to solve the advection dispersion equation with kinetic adsorption
In revised form to appear in Advances in Water Resources 63

Chapter 4
ECOWELL, A computer package to estimate the contamination of a pumping well, Technical Documentation 81

Chapter 5
Case study: Delineation of a protection zone near pumping station Lochem 109

Samenvatting 117

Curriculum Vitae 120

GENERAL INTRODUCTION

Knowledge is as the waters,
some descending from above, some springing from beneath.

(Francis Bacon, 1561-1626)

MODELLING GROUNDWATER FLOW AND CONTAMINANT TRANSPORT

In many countries in the world groundwater is pumped up for consumption purposes. In the Netherlands 70% of the drinking water is groundwater. Despite the protecting and purifying character of the soil groundwater can be polluted. Biological or chemical pollutants (such as bacteria, viruses, nitrates, heavy metals, radioactive materials and toxic compounds) produced by domestic, agricultural and industrial activities may penetrate the soil and reach the groundwater system. Examples are the leaching of landfills, penetration of fertilizers by rain water, oil spills and the infiltration of industrial waste from rivers, streams and lakes. To control the groundwater quality engineers and decision-makers need models that predict water flow and contaminant transport. The growing concern about the environment has stimulated the research in this field. Together with the advances in computer technology this research has resulted in the development of a large number of simulation models. An extensive review of computer models is given in Mangold & Tsang (1991). Restricting ourselves to the saturated zone we can distinguish two types: flow models and solute transport models.

Flow models describe the macroscopic path lines of the water through the porous medium. Groundwater flow is a potential flow: Darcy's law gives a linear relationship between the flow velocity and the gradient of the hydraulic head. The hydraulic head can be solved from the law of mass conservation. For an interesting class of configurations the hydraulic head and the flow velocity can be expressed in an analytical formula. In the past decade the analytical element method of Strack (1989) has been widely used. The analytical element method can be applied to porous formations consisting of blocks with different hydraulic conductivities. To deal with irregular geometries and arbitrary boundary conditions finite element and finite different models have been developed. Flow models may be used to get an impression of the flow pattern in aquifer or to study the change in the hydraulic head (the drawdown) near a pumping well.

Solute transport is governed by advection and dispersion. Advection is the displacement of a solute in the macroscopic flow direction. Dispersion is the spreading in longitudinal and transversal direction due to the complex movement of particles through tortuous pores with varying microscopic velocities. Almost all transport models assume that the dispersion can be described by a Fickian law. The resulting differential equation is commonly referred to as "the advection-dispersion equation" (ADE). The ADE may be coupled to isotherms that describe adsorption or chemical reactions. Analytical solutions of the ADE has been derived for various initial and boundary conditions (see e.g. van Genuchten & Alves, 1982, Leij et al. 1991). Almost all solutions are based on a uniform velocity field. More complex flow patterns can be dealt with by finite element, finite difference and random walk models.

ADVECTIVE-DISPERSIVE TRANSPORT TOWARDS A PUMPING WELL

In this thesis we mainly focus on contaminant transport towards a pumping well. Pumping wells are used to extract water both for human use and for remediation purposes. This class of problems is worth being studied in more detail than it has been done up to now. Currently, protection zones and remediation strategies are almost always determined with flow models. Flow models are easy to use and provide results quickly. However, to analyze contaminant transport to a well adequately also the effects of both transversal and longitudinal dispersion should be incorporated. Although in many application the dispersion terms are small compared with the advection terms, their effect may be large. Due to transversal dispersion contamination spilled outside the catchment area may cross a separating streamline and enter the well. Or in remediation context: contamination may escape from the catchment area, so that the groundwater remains (partially) polluted. Furthermore longitudinal dispersion affects the time that contamination keeps seeping into the well.

Of course, the dispersive transport towards a well can be computed with currently existing finite element or finite difference methods. However, this is a time-consuming job that requires much computer capacity. Because the ADE is a parabolic differential equation numerical solution methods are prone to numerical dispersion, especially if the dispersivities are small. To reduce numerical dispersion a large grid and a small time step are required.

The random walk method may provide more satisfying results. By carrying out many simulations of the stochastic motion of a particle, an estimate can be obtained for the fraction of a contaminant that eventually enters a well and for the breakthrough curve. A disadvantage is that the random walk method costs much computer time. Moreover, it provides less general information; from the simulation results no formulae can be derived that, for example, express the arrival fraction at the well or the breakthrough curve as function of the dispersivities.

RESEARCH OBJECTIVE

Uffink (1989) has shown the usefulness of Kolmogorov's backward equation in the study of dispersive contaminant transport. Given the present state of a particle the backward equation describes where the particle might have been coming from. One of Uffink's examples concerns contaminant transport in horizontal stationary flow towards a well. This example has been worked out further by Van Herwaarden & Grasman (1991) and Van der Hoek (1992). From the backward Kolmogorov equation they have derived a boundary value problem for the arrival fraction of a contaminant at a well. Solving this problem with perturbation techniques they have obtained an analytical approximation for the arrival fraction in which the effect of transversal dispersion is included. A first extension was made by van Herwaarden (1994), who presented an asymptotic approximation for the mean arrival time.

The objective of the research in this thesis is to develop the asymptotic method of Van Herwaarden & Grasman further and to implement it in a software package. Beside transversal dispersion we also take into account longitudinal dispersion. Moreover we allow the dispersivities to vary in space. Because chemical reactions and interactions with the soil may highly affect the transport of a contaminant we also incorporate the effect of linear equilibrium adsorption, first order decay and linear kinetic adsorption. We have

succeeded in deriving analytical approximations for
- the arrival fraction at a well,
- the mean and variance of the arrival time
- and for the arrival time distribution at the well.

The approximations can be applied to arbitrary (numerically or analytically computed) flow patterns with wells. The regional background needs not necessarily to be uniform. The results have been derived for a point spill of pollution. By integrating the approximations in space they can also be applied to a contaminant that already has spread out over a certain area.

In comparison with a finite element, a finite difference or random walk method the advantage of the asymptotic method is considerable. Because the effects of dispersion and adsorption are incorporated analytically, the approximations can be evaluated efficiently and free of numerical dispersion. The time that is needed to evaluate the approximations is of the same order as one random walk simulation.

APPLICATION AND IMPLEMENTATION OF THE RESULTS

The asymptotic method may be used for the following purposes:
- to delineate a protection zone near a pumping station more accurately,
- to design a remediation strategy,
- to analyze the risk of e.g. placing a factory or landfill at a certain location.
- to estimate the effective porosity or the dispersivities, by fitting theoretical and observed breakthrough curves in tracer tests. In this context our results may be considered as an extension of the work of Guvanasen & Guvanasen (1987), who describe a semi-analytical method to estimate parameters from a tracer experiment in radial flow to a well. They neglect the effect of the regional background flow.

In order to make the method easy applicable for engineers and decision-makers we have implemented it in a software package, called ECOWELL (which stands for Estimating Contamination Of WELLs). The package will be distributed by the International Ground Water Modelling Centre (IGWMC) in Colorado. The input of ECOWELL consist of a head field generated with a finite element or finite difference code for groundwater flow. The flow pattern may contain various pumping and injection wells. With ECOWELL the effects of dispersion, adsorption and decay on the transport of a contaminant can be analyzed. In chapter 5 we discuss a case study.

For completeness it is mentioned that the method has also been implemented in a program that has a complex-analytical potential as starting point. This version, however, is not yet available for direct use.

OUTLINE OF THE THESIS

This thesis is composed of three scientific papers, published in or submitted to international journals, a technical description of the program ECOWELL and a case study. We give a brief overview of the contents.

Chapter 1 deals with the transport of a linearly decaying contaminant. We start with summarizing some theoretical results on the validity of the advection-dispersion equation at field scale. Using that the mass flux of a contaminant satisfies the backward Kolmogorov equation we derive boundary value problems for the arrival rate and the mean arrival time of a decaying contaminant at the boundary of a domain. These boundary value problems are solved asymptotically for flow towards a well. The advective flow pattern yields first order approximations. In a boundary layer near a separating streamline we have to compute a correction accounting for the effect of transversal dispersion. Because longitudinal dispersion hardly affects the arrival rate and the mean arrival time, it does not have to be taken into consideration.

Without information on the spreading of the arrival time of a contaminant, the mean arrival time is an unreliable guideline for e.g. the clean up time of an aquifer. In particular one will be interested in the arrival time distribution. Therefore, in Chapter 2 we derive approximations for the variance of the arrival time and for the arrival time distribution. Now, also longitudinal dispersion has to be taken into account. We expand the moments of the arrival time in power series of the longitudinal dispersivity. Longitudinal dispersion is a one-dimensional process. Therefore, we expect that the arrival time distribution at the well can be parameterized by the probability distribution of a particle at the endpoint of a column. Near a separating streamline the effect of transversal dispersion is taken into account by generalizing the results of chapter 1.

Chapter 3 is a more general chapter; it is not primarily devoted to contaminant transport toward a well. We study the advection-dispersion model for the transport of a kinetically adsorbing contaminant. Kinetic interactions of a contaminant with the soil may explain the long tail in the breakthrough profile that is often observed in remediation projects (see also van den Brink, 1995). We show that once the transport of a non-adsorbing contaminant has been computed, the kinetic adsorption can be incorporated naturally by utilizing a stochastic description of the residence time of particles in the fluid phase. The method is demonstrated in various examples, among which the special case of transport towards a pumping well.

Chapter 5 is the technical documentation of the software package ECOWELL. We describe how ECOWELL determines the stagnation points and separating streamlines in the flow, and how it evaluates the asymptotic approximations for the arrival fraction and arrival time of a contaminant at a well. We also give estimates for the first and last entering time.

In chapter 6 we discuss a field study. We demonstrate how ECOWELL may be applied to delineate a protection zone near pumping station Lochem in the Achterhoek. With a finite element program the flow field near Lochem has been computed. With ECOWELL we analyze the effect of dispersion on the arrival fraction of a contaminant at the pumping station and on the 1, 10, 25, 100 and 250 year travelling time zones.

REFERENCES

van den Brink, C. and W.J. Zaadnoordijk: Non-equilibrium transport and sorption of organic chemicals during aquifer remediation. To appear in Ground Water, 1995.

van Genuchten, M.Th. and W.J. Alves, Analytical solutions of the one-dimensional convective-dispersive solute transport equation, Tech. Bull. 1661, 151 pp., U.S. Dep. of Agric. Riverside, California, 1982.

de Gee, M., J. Grasman, O.A. van Herwaarden, C.J. van der Hoek and J.J.A. van Kooten: Groundwater contaminant transport: Estimating the pollution at a well, in "Stochastic and Statistical Methods in Hydrology and Environmental Engineering", proceedings of the 1993 Unny Conference in Waterloo (Canada), Kluwer, Dordrecht, 1994.

van Kooten, J.J.A., J. Grasman, M. de Gee: A new mathematical method to predict groundwater quality in pumping wells, Acta Universitatis Carolinae Praag, Geologica 39, 243-254, 1995.

M. de Gee, J. Grasman, J.J.A. van Kooten and O.A. Buse: Voorspelling van de mate van verontreiniging van opgepompt grondwater, H2O (28) 15, 463-464, 1995.

Guvanasen, V. and V.M. Guvanasen: An approximate semi-analytical solution for tracer injection tests in a confined aquifer with a radially converging flow field and finite volume of tracer and chase fluid, Water Resour. Res. 23, 1607-1619, 1987.

van Herwaarden, O.A. and J. Grasman: Dispersive groundwater flow and pollution, Math. Models and Methods in Appl. Sci., 1, 61-81, 1991.

van Herwaarden, O.A.: Spread of pollution by dispersive groundwater flow, SIAM. J. of Appl. Math. 54 (1), 26-41, 1994.

van der Hoek, C.J: Contamination of a well in a uniform background flow, Stochastic Hydrol. Hydraul. 6, 191-208, 1992.

Mangold, D.C. and C.F. Tsang: A summary of subsurface hydrological and hydrochemical models, Reviews of Geophysics, 29 (1), 51-79, 1991.

Leij, F.J., J.H. Skags, M.Th. van Genuchten: Analytical solutions for transport in three-dimensional semi-infinite porous media, Water Resour. Res. 27, 2719-2734, 1991.

Strack, O.D.L.: Groundwater Mechanics, Prentice Hall, New Yersey, 1989.

Uffink, G.J.M.: Application of Kolmogorov's backward equation in random walk simulation of groundwater contaminant transport, in Kobus & Kinzelbach (eds.), Balkema Rotterdam, 1989.

CHAPTER 1

GROUNDWATER CONTAMINANT TRANSPORT INCLUDING ADSORPTION AND FIRST ORDER DECAY

(By J.J.A. van Kooten, Stochastic Hydrology and Hydraulics, 8, 185-205, 1994)

Abstract: This study deals with the transport of a contaminant in groundwater. The contaminant is subject to first order decay or linear adsorption. Its displacement can be modeled by a random walk process in which particles are killed at exponentially distributed times. Dirichlet problems are derived for the rate and mean time at which contaminated particles reach a particular part of the boundary of a certain domain. These Dirichlet problems are solved asymptotically for two types of 2D-flow patterns: flow parallel to the boundary of a domain and arbitrary flow towards a well in an aquifer.

Key words : contaminant transport, adsorption, decay, random walk, killing, Kolmogorov equations, contamination of a well

1. INTRODUCTION

Groundwater confined in aquifers is an important source of water supply for domestic, industrial and agricultural use. In order to control the quality of the groundwater prediction tools are needed. In this study we present a method to predict the fraction of a pollution that enters a protected zone or a well where groundwater is pumped up. We also give an estimate of the mean travelling time of particles. If a contaminant does not interact with the solid or is not subject to decay these problems have already been dealt with by Van Herwaarden & Grasman (1991), Van Herwaarden (1994) and Van der Hoek (1992). However, adsorption and decay may be factors of importance; because of the large residence times of water in an aquifer adsorption and decay may have a non-negligible effect upon the rate and mean time at which contaminated particles cross a certain boundary or are pumped up at a well.

Starting point of our analysis is the advection-dispersion equation containing terms that account for linear (non-) equilibrium adsorption and first order decay. In a dispersive flow a single particle makes a random walk. This random walk is modelled by a stochastic differential equation of which the corresponding Fokker-Planck equation equals the advection-dispersion equation without adsorption or decay terms (Uffink, 1990). Linear equilibrium adsorption only retards the spread of the contaminated particles. Linear irreversible adsorption and first order decay cause a fixed fraction of the contaminated particles to be "killed" in each time step. The spread of contaminated particles can be simulated by the aforementioned random walk process in which the particles have an

exponentially distributed life time. The Dirichlet problems formulated in section 4 are based on the backward Kolmogorov equation of this random walk process. The solutions of these problems give the rate and mean time at which particles cross a particular part of the boundary of a certain domain. These Dirichlet problems are applicable to various types of flow patterns.

In section 6 we solve the Dirichlet problems to approximate the rate and mean time at which particles hit the boundary of a domain in which the flow is parallel to that boundary. In section 7 the Dirichlet problems are solved to predict what fraction of a pollutant will enter a well operating in a confined aquifer and its mean travelling time. In both cases the Dirichlet problems are solved with the use of singular perturbation techniques. Because dispersion contributes considerably less to the displacement of a particle than advection, the advective flow field yields a first order approximation of the solutions. Where necessary we introduce a boundary layer in which we compute second order approximations which take into account the effects of dispersion. In this way analytical expressions are obtained which may be used to approximate the rate and mean time at which particles hit a certain boundary or enter a well in arbitrary 2D-flow. In chapter 8 the latter case is worked out for a well in a uniform background flow. The accuracy of the approximations is tested by making a comparison with random walk simulations.

2. THE SOLUTE TRANSPORT EQUATION

We analyse the spread of a non-conservative contaminant by stationary groundwater flow in a saturated porous formation. We restrict ourselves to linearly interacting solutes. The transport of the contaminant may be influenced by local equilibrium adsorption (also called linear Freundlich sorption), which occurs in many applications. Linear equilibrium adsorption is a reversible process, which only makes that the solute transport is retarded (see, for example, Bear and Verruyt, 1987). In Valocchi (1985) criteria are presented to assess the validity of the local equilibrium assumption (LEA). The LEA is often used to describe adsorption processes in which the reaction rate with the porous matrix is much faster than the advective flow rate.

In addition to local equilibrium adsorption, we allow for loss of mass due to linear irreversible adsorption or first order reactions/decay. These processes make that in each time step a certain fraction of the solute disappears. It is assumed that the adsorption/decay rate is a constant, which is realistic for radioactive and several reactive organic compounds.

Under these assumptions it is well known that at local scale the solute concentration $c(y,t)$ (M/L^N, $y \in \mathbb{R}^N$, N = 2 or 3) satisfies the advection-dispersion equation (ADE)

$$\frac{\partial c}{\partial t} = -\frac{\partial}{\partial y_i}\left(\frac{v_i}{R}c\right) + \frac{\partial}{\partial y_i}\left(\frac{D_{ij}}{R}\frac{\partial c}{\partial y_j}\right) - \frac{\lambda}{R}c \,, \tag{2.1}$$

where v_i is the average pore velocity (L/T) and λ is the adsorption/decay rate coefficient (T^{-1}). With respect to the indices in (2.1) we use the Einstein summation convention. The retardation factor R is related to the distribution factor K_d which characterizes the equilibrium adsorption, and to the porosity n and the solid's density ρ_s:

$$R = 1+\frac{1-n}{n}\,\rho_s K_d \ . \tag{2.2}$$

For an isotropic porous medium the hydrodynamic dispersion tensor is given by

$$D_{ij} = a_T|v|\delta_{ij} + (a_L-a_T)v_i v_j/|v| \ , \tag{2.3}$$

where respectively a_L and a_T denote the longitudinal and transversal dispersion coefficient (see Bear and Verruyt, 1987).

We are especially interested in the transport of a contaminant in an aquifer, which is a field-scale process. At field-scale a porous formation is often heterogeneous, i.e. the hydraulic properties of the formation display spatial variability. Heterogeneity enhances the spread of a contaminant (especially in the longitudinal direction). This phenomenon is called "macro-dispersion". Flow and transport in a heterogeneous formation can be modelled by introduction of random space functions (RSF) for the velocity field v, the retardation factor R and the first order reaction/decay coefficient λ (Dagan, 1987). The heterogeneity of the formation is characterized by the auto-correlations and cross-correlations of v, R and λ. Because v, R and λ are RSF the ADE (2.1) becomes a stochastic differential equation, and consequently the point value of the concentration becomes uncertain. Therefore, we are more interested in the expected value of the concentration. Assuming that v, R and λ are stationary random fields Kabala and Sposito (1991) proved that the mean transport equation still is approximately an ADE of form (2.1), where v_i/R, D_{ij}/R and λ/R have to be replaced by their "field-scale values". Because of the heterogeneity these field-scale values are functions of the auto- and cross-correlations of v, R and λ. This results in time-dependent transport parameters. However, if the correlation scales are finite, it can be shown that at the long term the time dependency vanishes and the transport parameters tend to constants (see also Dagan, 1987, Neumann, 1991).

In this study we assume that the scale of heterogeneity is small compared to the geometry of the aquifer, so that we may take as starting point of our analysis the equation

$$\frac{\partial c}{\partial t} = -\frac{\partial}{\partial y_i}\,(v_i^f\, c) + \frac{\partial}{\partial y_i}\,(D_{ij}^f\,\frac{\partial c}{\partial y_j}) - \lambda^f\, c \ , \tag{2.4}$$

where respectively v_i^f, D_{ij}^f and λ^f denote the field-scale values of v_i/R, D_{ij}/R and λ/R at the long term. The field-scale dispersion is still assumed to be proportional to the velocity, so that the dispersion tensor is given by Eq.(2.3), where the pore-scale dispersivities a_T and a_L have to be replaced by their asymptotic field-scale values a_T^f and a_L^f. For small values of variance of the logconductivity Dagan derived approximations for this dispersivities (Dagan, 1987, p. 308-326, see also Gelhar and Axness, 1983). These approximation show that $a_L^f >> a_L$, whereas (at the long term) $a_T^f = a_T$. The transversal dipersivity a_T^f turns out to play a crucial role in this study.

It is noted that it is not always realistic to assume that the transport parameters tend to their asymptotic values rapidly. Sposito and Barry (1990) applied the Dagan model of solute transport to a tracer experiment at the Borden site. It turned out that at the Borden site the transversal dispersivities do not reach their asymptotic values on any realistic time scale. Roberts et al. (1986) found that for the Borden aquifer the scale of time dependency of the field-scale retardation factor is more than two years.

In this study we answer the question at what rate and mean time a contaminant, the expected concentration of which satisfies Eq.(2.4), will enter a protected domain. For that purpose the concentration function $c(y,t)$ is interpreted as the space-time probability density function for a contaminated particle as it makes a random walk through the groundwater. (In the remainder of this study the superscripts f in (2.4) will be omitted.)

Remark. The LEA or the assumption that a solute undergoes first order decay do not always accurately describe the physical, chemical or biological processes in an aquifer (Valocchi, 1985, Cameron and Klute, 1977). In such cases kinetic non-equilibrium models are needed to describe the mass transfers. A random walk method for simulating the spread of a kinetic adsorbing solute is described by Andricevic and Foufoula-Georgiou (1991).

3 COMPARISON WITH A DIFFUSION PROCESS WITH KILLING

For the subsequent analysis of the transport of a contaminant, it is more convenient to rewrite Eq. (2.4) in the following form:

$$\frac{\partial c}{\partial t} = M_\lambda c \tag{3.1a}$$

with

$$M_\lambda = -\frac{\partial}{\partial y_i}(a_i(y).) + \frac{1}{2}\frac{\partial^2}{\partial y_i \partial y_j}(b_{ij}(y).) - \lambda \tag{3.1b}$$

and

$$a_i = v_i + \frac{\partial}{\partial y_j} D_{ij}\,, \qquad \frac{1}{2} b_{ij} = D_{ij}\,. \tag{3.1cd}$$

Setting $c = c_0\, e^{-\lambda t}$ we find that c_0 has to satisfy the ADE without adsorption or decay terms:

$$\frac{\partial c_0}{\partial t} = M_0 c_0\,. \tag{3.2}$$

If no adsorption or decay takes place it is known that the dispersive spread of a contaminant in groundwater can be simulated by a random walk process. Contaminated particles are released at some point $x \in \mathbb{R}^N$ and their motion consists of a deterministic part, the drift, and a stochastic part that accounts for the dispersion: the position of the particles at time t is only known with some probability. The probability density function $p_0(y,t \mid x)$ for particles released in $x \in \mathbb{R}^N$ has to satisfy the same equation as $c_0(y,t)$, so that

$$\frac{\partial p_0}{\partial t} = M_0 p_0, \qquad p_0(y,0 \mid x) = \delta(x-y)\,. \tag{3.3}$$

Eq. (3.3) is the Fokker-Planck equation or forward Kolmogorov equation that corresponds with the diffusion process described by the Ito stochastic differential equation

$$dy_i = a_i(y)dt + F_{ij}dW_j \,, \tag{3.4a}$$

where W_j are independent Wiener processes and F_{ij} is a tensor so that

$$F_{ik}F_{kj} = b_{ij} \,, \tag{3.4b}$$

see Gardiner (1983) and Uffink (1990).

Linear non-equilibrium adsorption or first order decay cause contaminated particles to be "killed". This killing process has an exponential distribution; the probability that a particle has not been killed before time t equals $e^{-\lambda t}$. With this killing process, the probability density function for finding a particle in $y \in \mathbb{R}^N$ at time t is

$$p(y,t|x) = p_0(y,t|x)\, e^{-\lambda t} \,. \tag{3.5}$$

It is noticed that p is a defective, or deficient, probability density function. The defect is $1\text{-}e^{-\lambda t}$, being the probability that a particle has been killed before time t. The probability density function p satisfies the ADE (3.1). So we can simulate the spread of a contaminant that is subject to adsorption or first order decay by a random walk process with killing.

Eq. (3.3) describes where a particle that was released in the point x, might be some time later. We may also reverse the situation. Given that a particle is found in y at time t, we may ask where the particle's initial position might have been. Beside the forward Kolmogorov equation (3.3) $p_0(y,t\,|\,x)$ satisfies the backward Kolmogorov equation that refers to the particle's position in the past:

$$\frac{\partial p_0}{\partial t} = L_0 p_0 \,, \tag{3.6a}$$

where

$$L_\lambda = M_\lambda^* = a_i(x)\frac{\partial}{\partial x_i} + \frac{1}{2}b_{ij}(x)\frac{\partial^2}{\partial x_i \partial x_j} - \lambda \,. \tag{3.6b}$$

The backward equation plays an important role in finding expressions for the probability and mean time of entering or leaving a given domain in $\mathbb{R}^N$.

Remark. In the above approach of the spread of pollution in a porous medium where adsorption or a first order decay takes place, it is essential that λ is space independent. If the killing is space dependent the probability of finding a particle at a certain place at a certain time depends on the path followed by that particle. In that case the diffusion process and the killing process are not any longer independent.

4. PROBABILITY AND MEAN TIME OF EXIT THROUGH A CERTAIN BOUNDARY

Let us consider a domain $\Omega \in \mathbb{R}^N$ (N = 2 or 3) with boundary $\partial\Omega$. We assume that $\partial\Omega$ is an absorbing boundary; a particle is removed when it reaches $\partial\Omega$, i.e. $p(y,t\,|\,x)=0$ if $y \in \partial\Omega$. Let $\partial\Omega_0$ and $\partial\Omega_1$ be parts of $\partial\Omega$, i.e. $\partial\Omega_0 \cap \partial\Omega_1 = \phi$ and $\partial\Omega_0 \cup \partial\Omega_1 = \partial\Omega$ (fig.1).

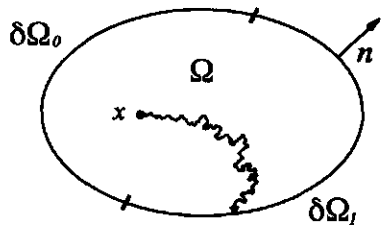

Figure 1 Example of the region Ω considered in section 4.

We want to know the probability that a particle that was released in $x \in \Omega$, exits through $\partial\Omega_1$. In a diffusion process without killing the (defective) probability density function for leaving Ω through $\partial\Omega_1$ at time t is

$$\int_{\partial\Omega_1} n_i J_i(y,t|x)dSy \ , \tag{4.1}$$

where n is the outward normal vector on $\partial\Omega$, and J is the so-called probability current:

$$J_i(y,t|x) = a_i(y)p_0(y,t|x) - \frac{1}{2}\frac{\partial}{\partial y_j}b_{ij}(y)p_0(y,t|x), \tag{4.2}$$

see Gardiner (1983), Sec. 5.2 and 5.4. It follows that the probability density function for exit through $\partial\Omega_1$ at time t for a diffusion process with exponentially distributed killing is

$$q(x,t) = \left(\int_{\partial\Omega_1} n_i J_i(y,t|x)\,dSy\right)e^{-\lambda t} \ . \tag{4.3}$$

A particle starting at $\partial\Omega$ is absorbed immediately, so that a particle starting at $\partial\Omega_0$ cannot exit through $\partial\Omega_1$ anymore. So, at the boundary we have

$$\begin{aligned} q(x,t) &= 0 \qquad \text{if } x \in \partial\Omega_0, \\ q(x,t) &= \delta(t) \qquad \text{if } x \in \partial\Omega_1. \end{aligned} \tag{4.4}$$

Let $u(x)$ be the probability that a particle starting in $x \in \Omega$ exits through $\partial\Omega_1$. By partial integration we find

$$\begin{aligned} u(x) &= \int_0^\infty q(x,t)\,dt \\ &= \left\{-\frac{1}{\lambda}\left(\int_{\partial\Omega_1} n_i J_i dSy\right)e^{-\lambda t}\Big|_0^\infty\right\} + \frac{1}{\lambda}\int_0^\infty \frac{d}{dt}\left(\int_{\partial\Omega_1} n_i J_i dSy\right)e^{-\lambda t}dt \ . \end{aligned} \tag{4.5}$$

The term between braces cancels because $J(y,0)\,|\,x) = 0$ at $\partial\Omega_1$. Because p_0 satisfies the backward Kolmogorov equation, J satisfies this equation too. Making use of this fact we conclude that

$$u(x) = \frac{1}{\lambda}\int_0^\infty \left(\int_{\partial\Omega_1} n_i\left(a_i(x)\frac{\partial}{\partial x_i}J_i + \frac{1}{2}b_{ij}(x)\frac{\partial^2}{\partial x_i \partial x_j}J_i\right) dSy\right) e^{-\lambda t} dt$$
$$= \frac{1}{\lambda}\left(a_i(x)\frac{\partial}{\partial x_i}u(x) + \frac{1}{2}b_{ij}(x)\frac{\partial^2}{\partial x_i \partial x_j}u(x)\right). \tag{4.6}$$

Thus, the probability that a particle starting in $x \in \Omega$ exits through $\partial\Omega_1$ satisfies the homogeneous Dirichlet problem

$$L_\lambda u = 0 \text{ in } \Omega \tag{4.7a}$$

with the boundary conditions immediately following from (4.4):

$$\begin{aligned} u &= 1 \text{ at } \partial\Omega_1, \\ u &= 0 \text{ at } \partial\Omega_0. \end{aligned} \tag{4.7b}$$

Let $T_1(x)$ be the mean exit time of a particle starting in $x \in \Omega$, under the condition that the particle exits Ω through $\partial\Omega_1$

$$T_1(x) = \int_0^\infty t\frac{q(x,t)}{u(x)}dt = \frac{T(x)}{u(x)}, \tag{4.8a}$$

where

$$T(x) = \int_0^\infty t q(x,t)dt. \tag{4.8b}$$

Partial integration of T gives

$$T(x) = \frac{1}{\lambda}u(x) + \frac{1}{\lambda}\int_0^\infty t\left(\int_{\partial\Omega_1} n_i \frac{d}{dt}J_i dSy\right)e^{-\lambda t}dt\ . \tag{4.9}$$

Again, because J satisfies the backward Kolmogorov equation, it follows that

$$T(x) = \frac{1}{\lambda}u(x) + \frac{1}{\lambda}\left(a_i(x)\frac{\partial}{\partial x_i}T + \frac{1}{2}b_{ij}(x)\frac{\partial^2}{\partial x_i \partial x_j}T\right). \tag{4.10}$$

From (4.4) we obtain as boundary condition: $T = 0$ at $\partial\Omega$. Thus, $T(x)$ is the solution of the nonhomogeneous Dirichlet problem

$$\begin{cases} L_\lambda T(x) = -u(x) \text{ in } \Omega \\ T = 0 \qquad\quad \text{at } \partial\Omega\ . \end{cases} \tag{4.11}$$

We mention that in the same way as we derived the Dirichlet problem (4.11) related to the first moment T_1 of the conditional exit time we can derive the Dirichlet problem related to the mth moment T_1^m of the conditional exit time. We do not work this out, because we do not use these higher order moments in this study.

In section 6 and 7 the Dirichlet problems (4.7) and (4.11) will be solved approximately for two special 2D cases. Using singular perturbation techniques we derive approximations for the rate and mean time at which particles reach a given boundary. We test the accuracy of the asymptotic approximations by comparing them with the outcomes of random walk simulations.

5. RANDOM WALK SIMULATION WITH KILLING

In two dimensions the stochastic differential equation (3.2) reads

$$dX = \left(v_x + \frac{\partial}{\partial x}D_{xx} + \frac{\partial}{\partial y}D_{xy}\right)dt + \sqrt{2a_L|v|}\frac{v_x}{|v|}dW_L + \sqrt{2a_T|v|}\frac{v_y}{|v|}dW_T\,, \tag{5.1a}$$

$$dY = \left(v_y + \frac{\partial}{\partial x}D_{yx} + \frac{\partial}{\partial y}D_{yy}\right)dt + \sqrt{2a_L|v|}\frac{v_y}{|v|}dW_L - \sqrt{2a_T|v|}\frac{v_x}{|v|}dW_T\,. \tag{5.1b}$$

Because the Wiener processes W_L and W_T are independent, their increments dW_L and dW_T are also independent. The increment of a Wiener process has variance dt:

$$\left\langle dW_L^2\right\rangle = \left\langle dW_T^2\right\rangle = dt, \tag{5.2}$$

see Gardiner (1983), sec 4.2. Let z_i be a uniformly distributed variable with mean zero and variance σ. Then, according to the central limit theorem, the variable $z = \sum_{i=1}^{N} z_i$, with N sufficiently large, has approximately a normal distribution with mean zero and variance $\sqrt{N\sigma}$. So we can simulate the motion of a particle in a specified domain $\Omega \subset \mathbb{R}^2$ on the computer by

$$\Delta X = \left(v_x + \frac{\partial}{\partial x}D_{xx} + \frac{\partial}{\partial y}D_{xy}\right)\Delta t + \sqrt{2a_L|v|}\frac{v_x}{|v|}z_L\sqrt{\Delta t} + \sqrt{2a_T|v|}\frac{v_y}{|v|}z_T\sqrt{\Delta t} \tag{5.3a}$$

$$\Delta Y = \left(v_y + \frac{\partial}{\partial x}D_{xy} + \frac{\partial}{\partial y}D_{yy}\right)\Delta t + \sqrt{2a_L|v|}\frac{v_y}{|v|}z_L\sqrt{\Delta t} + \sqrt{2a_T|v|}\frac{v_x}{|v|}z_T\sqrt{\Delta t} \tag{5.3b}$$

where z_L and z_T are uniformly distributed variables with mean zero and variance one (see also Kinzelbach, 1988). The time step Δt is taken sufficiently small. Furthermore, the particles are killed at exponentially distributed times. Therefore, before we start simulating the motion of a particle by (5.3), we choose a random variable τ which is uniformly distributed at [0,1]. Then $t = -\log(\tau)/\lambda$ is exponentially distributed; we call t the killing time of this particular particle. We stop simulating the motion of a particle if it exits the domain Ω, or if its simulated travelling time exceeds the killing time t. By counting the particles that exit Ω across a particular part $\partial\Omega_1$ of the boundary $\partial\Omega$ an estimate is obtained of the probability of exit through $\partial\Omega_1$. By taking the mean of the exit time of these particles we obtain an estimate of the conditional mean exit time T_1.

Now the question arises how small the time step Δt and how large the number of simulations has to be taken to obtain accurate estimates from the random walk simulations. The first part of the question must be answered empirically: we take Δt sufficiently small, such that the result is independent of the chosen step size. The second part of the question can be answered with the use of a theoretical argument.

Let μ_i be the outcome of the i'th random walk; $\mu_i = 1$ if the particle exits through $\partial\Omega_1$, $\mu_i = 0$ if not. Let τ_j be the exit time of the j'th particle that exits through $\partial\Omega_1$. The mean of μ_i is u and the mean of τ_j is T_1. The sample means are

$$\bar{\mu} = \sum_{i=1}^{N} \frac{\mu_i}{N} \quad \text{and} \quad \bar{\tau} = \sum_{j=1}^{M} \frac{\tau_j}{M} , \tag{5.4}$$

where N is the number of simulations and $M \leq N$ the number of particles that exit Ω through $\partial\Omega_1$. Let σ_u^2 and σ_T^2 be the variances of μ_i an τ_j, respectively. From statistics it is known that the random variables

$$\sqrt{N}\frac{(\bar{\mu}-u)}{\sigma_u} \quad \text{and} \quad \sqrt{M}\frac{(\bar{\tau}-T_1)}{\sigma_T} , \tag{5.5}$$

have a limiting normal distribution with zero mean and unit variance. This fact can be used to construct confidence domains for u and T_1. For that purpose estimates for σ_u^2 and σ_T^2 are needed. Unbiased estimators for them are respectively

$$S_u^2 = \sum_{i=1}^{N} \frac{(\mu_i-\bar{\mu})^2}{N-1} \quad \text{and} \quad S_T^2 = \sum_{j=1}^{M} \frac{(\tau_j-\bar{\tau})^2}{M-1} . \tag{5.6}$$

It is easy to verify that 95% confidence intervals for u and T_1 are approximately:

$$\bar{\mu}-d_u < u < \bar{\mu} + d_u , \tag{5.7a}$$

$$\bar{\tau} - d_T < T_1 < \bar{\tau} + d_T \tag{5.7b}$$

with $$d_u = \frac{1.96\, S_u}{\sqrt{N}} \text{ and } d_T = \frac{1.96\, S_T}{\sqrt{M}} . \tag{5.7c}$$

6. UNIFORM PARALLEL FLOW

As a first example we consider a uniform 2D flow through the domain

$$\Omega = \{(x,y) | x < 0,\ y > 0\} \tag{6.1a}$$

with boundaries

$$\partial\Omega_0 = \{(x,y) | x = 0,\ y > 0\} \text{ and } \partial\Omega_1 = \{(x,y) | x < 0,\ y = 0\} . \tag{6.1b}$$

The uniform advective flow is in the x-direction. Due to dispersion a particle released somewhere in Ω may hit the boundary $\partial\Omega_1$. While moving through Ω particles may be absorbed or may undergo first order decay. We use the Dirichlet problem (4.7) to compute

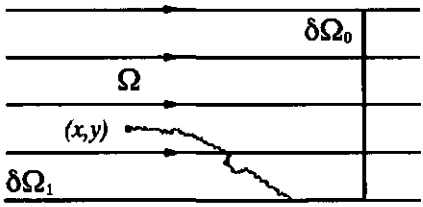

Figure 2. Uniform flow parallel to the boundary $\partial\Omega_1$.

an approximation of the probability $u(x,y)$ that a particle released in $(x,y) \in \Omega$ hits the boundary $\partial\Omega_1$. Neglecting the probability that a particle starting at $\partial\Omega_0$ may hit $\partial\Omega_1$, we find that $u(x,y)$ is the solution of the problem

$$\begin{cases} v\dfrac{\partial u}{\partial x} + a_L v\dfrac{\partial_2 u}{\partial x_2} + a_T v\dfrac{\partial^2 u}{\partial y^2} - \lambda u = 0 \text{ in } \Omega \\ u(x,0) = 1 \quad \text{for } x < 0 \\ u(0,y) = 0 \quad \text{for } y > 0\ . \end{cases} \tag{6.2}$$

Due to the advective flow in the x-direction, which dominates the dispersion, particles released far away from $\partial\Omega_1$ have probability zero of reaching $\partial\Omega_1$. One may expect that only near $\partial\Omega_1$ the probability of reaching $\partial\Omega_1$ differs significantly from zero. Therefore, a boundary layer around $\partial\Omega_1$ may occur in which the qualitative behaviour of u changes. We expect that in this layer the transversal dispersion is important, because it allows particles to cross streamlines. The layer is stretched by introducing the boundary layer coordinate

$$\eta = y/\sqrt{a_T}\ . \tag{6.3}$$

Substitution in (6.2) yields for $a_L, a_T \to 0$

$$v\frac{\partial \bar{u}}{\partial x} + v\frac{\partial^2 \bar{u}}{\partial \eta^2} - \lambda \bar{u} = 0 \quad \text{in} \quad \Omega \tag{6.4a}$$

with

$$\bar{u}(0,\eta) = 0, \quad \bar{u}(x,0) = 1 \tag{6.4b}$$

and with matching condition

$$\lim_{\eta \to \infty} \bar{u}(x,\eta) = 0\ . \tag{6.4c}$$

Using a Laplace transform in the x-direction we find that the solution of (6.4) reads

$$\bar{u}(x,\eta) = \frac{1}{2}\exp\{\eta\sqrt{\lambda/v}\}\,\mathrm{Erfc}\left\{\frac{\frac{1}{2}\eta + \sqrt{-\lambda/v}}{\sqrt{-x}}\right\} + \frac{1}{2}\exp\{-\eta\sqrt{\lambda/v}\}\,\mathrm{Erfc}\left\{\frac{\frac{1}{2}\eta - \sqrt{-\lambda/v}}{\sqrt{-x}}\right\}. \tag{6.5}$$

	$y = 0.04$			$y = 0.08$			$y = 0.12$		
x	u_{asymp}	u_{simul}	d_u	u_{asymp}	u_{simul}	d_u	u_{asymp}	u_{simul}	d_u
-0.5	55.2	53.7	1.382	24.4	23.5	1.175	8.4	7.9	1.605
-1.0	65.4	64.0	1.331	38.7	38.1	1.346	20.5	19.4	1.096
-1.5	69.7	68.9	1.283	45.8	45.5	1.380	28.1	26.9	1.229
-2.0	72.0	71.9	1.246	49.9	50.0	1.386	33.0	31.9	1.292
-2.5	73.5	73.0	1.231	52.5	52.3	1.385	36.3	36.0	1.331
-3.0	74.5	74.2	1.213	54.3	53.9	1.382	38.6	37.8	1.344
-3.5	75.2	74.6	1.207	55.6	56.7	1.374	40.3	40.1	1.359
-4.0	75.7	76.1	1.182	56.6	56.6	1.374	41.6	41.0	1.363

TABLE I. Probabilities of hitting $\partial\Omega_1$ (in %) calculated from the asymptotic approximation (6.5), compared with the probabilities from $N = 5000$ simulations at different points ($v = 1$, $a_L = 1/32$, $a_T = 1/200$, $\lambda = 0.2$, $\Delta t = 0.0005$).

We have simulated the spread of particles by the random walk method with killing as described in section 5. In table I the rate at which particles hit the boundary $\partial\Omega_1$ as calculated from (6.5) and as obtained from simulations are compared. Because the rate obtained from the simulations is also an approximation of the real rate u, table I contains the coefficient d_u calculated from (5.7c). The probability that u differ less then d_u from u_{simul} is 0.95. One may notice that in almost all cases $|u_{simul}-u_{asymp}| \le 0.95$. From the table we may conclude that formula (6.5) gives a good approximation of the rate at which particles hit $\partial\Omega_1$. We emphasize that in this formula a_L does not occur. So the Brownian motion in the x-direction plays a minor role in answering the question at what rate particles hit $\partial\Omega_1$.

From the Dirichlet problem (4.11) we may find an approximation for the conditional mean of the first time that a particle hits $\partial\Omega_1$. However, we may also try to derive an approximation in a different way. Ignoring the Brownian motion in the x-direction there only remains a stochastic motion in the y-direction, which is described by

$$d\eta = \sqrt{2v}\, dW_T . \tag{6.6}$$

For a particle released in $(x,\eta) \in \Omega$ the probability density function for reaching the axis $\eta = 0$ at time t equals

$$f(t,\eta) = \frac{1}{2\sqrt{\pi v}} \frac{\eta}{t^{3/2}} e^{-\eta^2/4vt} , \tag{6.7}$$

see Karlin (1960). Starting at $(x,\eta) \in \Omega$ the boundary $\partial\Omega_1$ can only be reached if $t < -x/v$, otherwise the boundary $\partial\Omega_0$ has been passed. Furthermore, the probability that a particle has not been killed at time t is $e^{-\lambda t}$. So the conditional mean first hitting time of $\partial\Omega_1$ equals

$$\bar{T}_1(x,\eta) = \frac{1}{2\sqrt{\pi v}} \int_0^{-\frac{x}{v}} \frac{\eta}{t^{1/2}} e^{-(\eta^2/4vt)-\lambda t} dt / \bar{u}(x,\eta) . \tag{6.8}$$

Table II contains the mean first hitting time obtained from random walk simulations and calculated from (6.8). A comparison shows that $\bar{T}_1(x,\eta)$ is a good approximation for the real mean first hitting time T_1. To support our confidence in T_{simul} table II also contains d_T calculated from (5.7d); the probability that T_1 differs less then d_T from T_{simul} is 0.95 (see §5). We notice that in almost all cases $|T_{simul}-T_{asymp}| \leq 0.95$.

	$y = 0.04$			$y = 0.08$			$y = 0.12$		
x	T_{asymp}	T_{simul}	d_T	T_{asymp}	T_{simul}	d_T	T_{asymp}	T_{simul}	d_T
-0.5	0.173	0.179	$5.22.10^{-3}$	0.280	0.301	$8.86.10^{-3}$	0.347	0.395	$7.49.10^{-3}$
-1.0	0.256	0.260	$8.32.10^{-3}$	0.442	0.442	$1.17.10^{-3}$	0.575	0.592	$1.66.10^{-2}$
-1.5	0.316	0.321	$1.10.10^{-2}$	0.562	0.571	$1.58.10^{-2}$	0.752	0.759	$2.08.10^{-2}$
-2.0	0.362	0.364	$1.34.10^{-2}$	0.658	0.672	$1.95.10^{-2}$	0.897	0.906	$2.47.10^{-2}$
-2.5	0.400	0.406	$1.57.10^{-2}$	0.737	0.753	$2.27.10^{-2}$	1.019	1.026	$2.88.10^{-2}$
-3.0	0.431	0.452	$1.82.10^{-2}$	0.804	0.829	$2.58.10^{-2}$	1.123	1.140	$3.33.10^{-2}$
-3.5	0.457	0.474	$1.99.10^{-2}$	0.861	0.866	$2.82.10^{-2}$	1.213	1.231	$3.68.10^{-2}$
-4.0	0.479	0.491	$2.14.10^{-2}$	0.909	0.910	$3.12.10^{-2}$	1.292	1.305	$4.01.10^{-2}$

TABLE II. Mean time of hitting $\partial\Omega_1$ computed by the asymptotic approximation (6.8), compared with the mean time obtained from $N = 5000$ simulations at different points ($v = 1$, $a_L = 1/32$, $a_T = 1/200$, $\lambda = 0.2$, $\Delta t = 0.0005$).

7. EXIT PROBLEM IN A DOMAIN WITH SEPARATING STREAMLINE

The Dirichlet problems (4.7) and (4.11) play a crucial role in answering the question at what rate and mean time a certain pollution will enter a drinking water well. Drinking water is often pumped up from layers from confined aquifers. The thickness of the aquifer is assumed to be small relative to its horizontal dimensions, so that the groundwater flow we consider is essentially 2D. Domains containing a well have the important characteristic

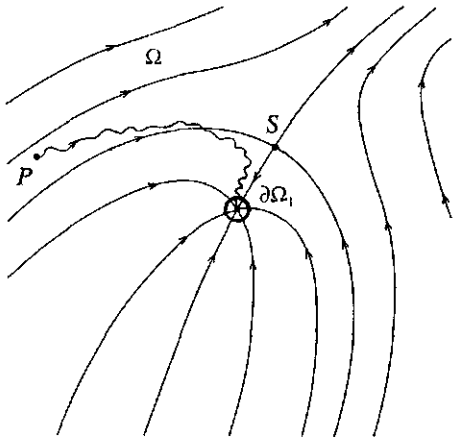

Fig.3. Example of a flow field in a domain containing a well. The catchment area of the well is bounded by two separating streamlines ending in the stagnation point S. Due to dispersion a particle released outside the catchment area may enter the well.

that the flow field contains separating streamlines ending in a stagnation point. These separating streamlines bound the region of advective flow towards the well, called the catchment area. Therefore we now analyse the exit problem in a domain $\Omega \subset \mathbb{R}^2$ with arbitrary flow containing separating streamlines ending in a stagnation point. To force that the flow is divergence free we assume that Ω is free of sources or sinks; we simply exclude them as in figure 3 ($\partial\Omega_1$ may consist of the well only).

7.1 Away from a separating streamline

The solution $u(x,y)$ of the Dirichlet problem (4.7) gives the probability that a contaminated particle released in $(x,y) \in \Omega$ exits Ω through $\partial\Omega_1$ (e.g. enters a well). We will solve this problem asymptotically. Since dispersion contributes considerably less to the displacement of a particle than advection, we take as a first order approximation for the probability of exit, the solution of the advective part of problem (4.7)

$$\begin{cases} v_1(x,y)\dfrac{\partial u_{adv}}{\partial x} + v_2(x,y)\dfrac{\partial u_{adv}}{\partial y} - \lambda u_{adv} = 0 , \\ u_{adv} = 1 \quad \text{at } \partial\Omega_1 , \end{cases} \tag{7.1}$$

where $v_1(x,y)$ and $v_2(x,y)$ denote the velocity of the flow in (x,y) in respectively the x- and y-direction. Notice that outside the catchment area no streamline is ending at $\partial\Omega_1$, so that outside the catchment area

$$u_{adv} = 0 . \tag{7.2}$$

Inside the catchment area all streamlines are ending at $\partial\Omega_1$. Putting $u_{adv} = \exp(-\lambda T)$ we find that T satisfies

$$\begin{cases} v_1(x,y)\dfrac{\partial T}{\partial x} + v_2(x,y)\dfrac{\partial T}{\partial y} = -1 \quad \text{in } \Omega \\ T = 0 \quad \text{at } \partial\Omega_1 . \end{cases} \tag{7.3}$$

The solution of (7.3) is the advective travelling time T_{adv} to $\partial\Omega_1$. So inside the catchment area we have

$$u_{adv} = \exp(-\lambda T_{adv}) , \tag{7.4}$$

i.e. u_{adv} is the probability that a particle has not been killed at $t = T_{adv}$.

7.2 Near a separating streamline

We expect that near a separating streamline u_{adv} will need a correction. Due to transversal dispersion a particle released outside the catchment area and not too far away from a separating streamline may cross the separating streamline and enter the well. Or in the opposite way: a particle released inside the catchment area and not too far away from a separating streamline may cross the separating streamline, which would reduce the particles probability of reaching the well. Furthermore, the advective travelling time towards the well along a streamline, that ends into the well and that is close to a separating streamline, is very large, because this streamline passes the stagnation point very closely. Due to the killing a particle moving along this streamline has a very small probability of reaching the well. Transversal dispersion, however, may bring a particle into

a streamline further away from a separating streamline, which shortens the travelling time towards the well and, thus, enlarges the probability of reaching the well. So, near a separating streamline we may not neglect the influence of transversal dispersion; a boundary layer around such streamline is to be expected. Before we analyse the exit probability u in this boundary layer we carry out some preliminary coordinate transformations.

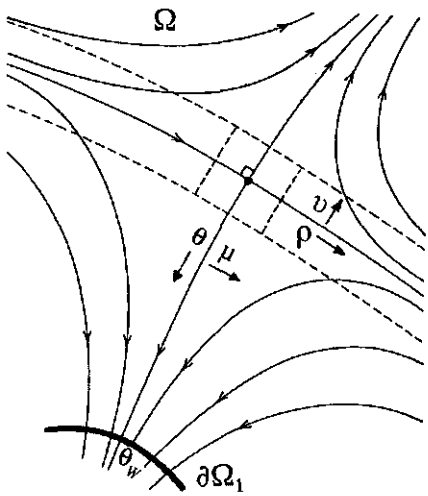

Fig. 4 The coordinates ρ and υ are taken along and perpendicular to a separating streamline leading towards the stagnation point. The coordinates θ and μ are taken along and perpendicular to the separating streamline leading away from the stagnation point.

Around a separating streamline we introduce some new (local) coordinates ρ and υ: $\rho > 0$ is a coordinate along the separating streamline and υ a coordinate perpendicular to it, see figure 4. The stagnation point is in $(\rho,\upsilon) = (0,0)$. The velocity near the separating streamline in this new coordinates is given by

$$(v(\rho,\upsilon),\ w(\rho,\upsilon)) \ . \tag{7.5}$$

Furthermore, we allow the dispersion coefficients to vary in space. We decompose the transversal dispersion coefficient in the following form:

$$a_T(\rho,\upsilon) = \bar{a}_T\ \alpha(\rho,\upsilon) \ . \tag{7.6}$$

where $\bar{a}_T$ is a (spatial) average of a_T and $\alpha(\rho,\upsilon)$ accounts for the spatial variability. (In a homogeneous medium $\bar{a}_T = a_T$ and $\alpha(\rho,\upsilon) = 1$). At the end of this paragraph we will see that it is not important how the average $\bar{a}_T$ is taken. We only have to introduce it for computational reasons. A boundary layer of width $O(\sqrt{\bar{a}_T})$ is expected near a separating streamline. We therefore introduce the boundary layer coordinate

$$\eta = \upsilon/\sqrt{\bar{a}_T} \ . \tag{7.7}$$

Letting a_L, $\bar{a}_T \to 0$ we obtain that inside the boundary layer u approximately satisfies

$$v(\rho,0)\frac{\partial u_{bound}}{\partial \rho} + w_v(\rho,0)\eta\frac{\partial u_{bound}}{\partial \eta} - \alpha(\rho,0)v(\rho,0)\frac{\partial^2 u_{bound}}{\partial \eta^2} - \lambda u_{bound} = 0 \qquad (7.8a)$$

with u_{bound} to be matched with the outer solution u_{adv}:

$$u_{bound}(\rho,\eta) = 0 \text{ for } \eta \to \infty , \qquad (7.8b)$$

$$u_{bound}(\rho,\eta) = \exp(-\lambda T_{adv}(\rho,\eta)) \text{ for } \eta << -1 . \qquad (7.8c)$$

In order to find the solution u_{bound} we have to know T_{adv} just outside the boundary layer. For that purpose we again introduce new local coordinates.

Let $\theta > 0$ be a coordinate along the streamline leading away from the stagnation point and μ a coordinate perpendicular to θ, see figure 4. The stagnation point is in (0,0) and the streamline leading away from the stagnation point intersects $\partial\Omega_1$ in $(\theta_w,0)$. The velocity near this streamline in these coordinates is given by

$$(r(\theta,\mu),\ s(\theta,\mu)) \qquad (7.9)$$

We need these coordinates in an expression for T_{adv} just outside the boundary layer. Van Herwaarden (1994) proved that for $-1 << \upsilon < 0$

$$T_{adv}(\rho,\upsilon) = \frac{1}{v_\rho(0,0)}\ln\left(\frac{-\upsilon\ v(\rho,0)}{v_\rho(0,0)\rho\theta_w}\right) + h(\rho) \qquad (7.10a)$$

with

$$h(\rho) = \int_\rho^0 \left(\frac{1}{v(\bar{\rho},0)} - \frac{1}{v_\rho(0,0)\bar{\rho}}\right)d\bar{\rho} + \int_0^{\theta_w}\left(\frac{1}{r(\theta,0)} - \frac{1}{r_\theta(0,0)\theta}\right)d\theta . \qquad (7.10b)$$

We call the right-hand side of (7.10a) T_{match}. Let

$$u_{match} = \exp(-\lambda T_{match}) . \qquad (7.11)$$

We put

$$u_{bound} = \exp\{\lambda\int_\gamma^\rho \frac{1}{v(\bar{\rho},0)}d\bar{\rho}\}\tilde{u} , \qquad (7.12)$$

where γ is an integration constant. It follows that $\tilde{u}$ satisfies

$$\begin{cases} v(\rho,0)\dfrac{\partial \tilde{u}}{\partial \rho} + w_v(\rho,0)\eta\dfrac{\partial \tilde{u}}{\partial \eta} - \alpha(\rho,0)v(\rho,0)\dfrac{\partial^2 \tilde{u}}{\partial \eta^2} = 0, \\ \tilde{u}(\rho,\eta) = 0 \qquad \text{for} \quad \eta \to \infty, \\ \tilde{u}(\rho,\eta) = u_{match}\cdot\exp\{-\lambda\displaystyle\int_\gamma^\rho \frac{1}{v(\bar{\rho},0)}d\bar{\rho}\} = \exp\{-\lambda h(\gamma)\}\left(\frac{-\sqrt{\bar{a}_T}\,\eta v(\rho,0)}{v_\rho(0,0)\gamma\theta_w}\right)^{-\lambda/v_\rho(0,0)} \quad \text{for } \eta << -1 . \end{cases} \qquad (7.13)$$

We introduce the new coordinates

$$\tau = \int_0^{\rho} \nu(\bar{\rho},0)^2 d\bar{\rho} \quad \text{and} \quad \zeta = -\eta\nu(\rho,0) \tag{7.14}$$

and write $\tilde{\alpha}(\tau,\zeta) = \alpha(\rho,\upsilon)$. Using the fact that the flow is divergence free, which implies that $\nu_\rho(\rho,0) = -w_\upsilon(\rho,0)$, we obtain the following initial value problem for $\tilde{u}$:

$$\frac{\partial \tilde{u}}{\partial \tau} = \tilde{\alpha}(\tau,0)\frac{\partial^2 \tilde{u}}{\partial \zeta^2} \tag{7.15a}$$

with

$$\tilde{u}(0,\zeta) = 0 \quad \text{for } \zeta>0 \ , \tag{7.15b}$$

$$\tilde{u}(0,\zeta) = \exp\{-\lambda h(\gamma)\}\left(\frac{-\sqrt{\bar{a}_T}\,\zeta}{\nu_\rho(0,0)\gamma\theta_W}\right)^{-\lambda/\nu_\rho(0,0)} \quad \text{for } \zeta<0 \ . \tag{7.15c}$$

The solution of this initial value problem reads

$$\tilde{u}(\tau,\zeta) = \frac{1}{\sqrt{2\pi}} e^{-\lambda h(\gamma)} \int_{\zeta/\tilde{q}(\tau)}^{\infty} \left(\frac{-\sqrt{\bar{a}_T}\,(\zeta - t/\tilde{q}(\tau))}{\nu_\rho(0,0)\gamma\theta_W}\right)^{-\lambda/\nu_\rho(0,0)} e^{-\frac{1}{2}t^2} dt \ ,$$

where (7.16a)

$$\tilde{q}(\tau) = \{2\int_0^{\tau} \tilde{\alpha}(\bar{\tau},0)d\bar{\tau}\}^{-1/2} \ . \tag{7.16b}$$

Bringing this solution in (ρ,υ)-coordinates and using (7.6) and (7.12) we find the boundary layer solution for the rate of pollution that exits Ω through $\partial\Omega_1$:

$$u_{\text{bound}}(\rho,\upsilon) = \frac{1}{\sqrt{2\pi}} e^{-\lambda h(\rho)} \left(\frac{\nu(\rho,0)}{\nu_\rho(0,0)\rho\theta_W}\right)^{-\lambda/\nu_\rho(0,0)} \int_{\upsilon q(\rho)}^{\infty} \left(-\upsilon + t/q(\rho)\right)^{-\lambda/\nu_\rho(0,0)} e^{-\frac{1}{2}t^2} dt \tag{7.17a}$$

where

$$q(\rho) = \{2\int_0^{\rho} a_T(\bar{\rho},0)\nu(\bar{\rho},0)^2 d\bar{\rho}/\nu(\rho,0)^2\}^{-1/2} \ . \tag{7.17b}$$

Note that in this boundary layer solution only the velocity field and the transversal dispersion coefficient upon a separating streamline are used.

7.3 A composite approximation

Note that u_{bound} is an approximation for the exit rate u that is only valid in the boundary layer around a separating streamline. Outside the boundary layer we have the approximation $u \approx u_{\text{adv}}$. Because $u_{\text{adv}} = 0$ outside the catchment area of the well, we may use (7.17) as an approximation for u in the whole domain outside the catchment area. We are able to construct an approximation u_{comp} that is valid in the entire catchment area, inside and

outside the boundary layer, as follows

$$u_{comp} = u_{adv} + u_{bound} - u_{match} \tag{7.18}$$

Outside the boundary layer u_{match} cancels u_{bound}. Inside the boundary layer u_{match} cancels u_{adv}.

7.4 Mean time of exit

If a particle released in Ω exits through $\partial\Omega_1$, then its mean time of exit is $T_1 = T/u$, where T has to satisfy the nonhomogeneous Dirichlet problem (4.11). We solve problem (4.11) asymptotically. Again we start with neglecting the dispersion terms outside the boundary layer around a separating streamline. A first order approximation for T satisfies

$$\begin{cases} v_1(x,y)\dfrac{\partial T}{\partial x} + v_2(x,y)\dfrac{\partial T}{\partial y} - \lambda T = -u_{adv} \quad \text{in } \Omega\,, \\ T = 0 \quad \text{at } \partial\Omega_1\,. \end{cases} \tag{7.19}$$

Outside the catchment area (7.19) yields the approximation $T = 0$.
Inside the catchment area we find the approximation

$$T = T_{adv} \cdot u_{adv}, \tag{7.20}$$

which yields as an approximation for the conditional mean exit time

$$T_1 = T_{adv}. \tag{7.21}$$

Inside the boundary layer around a separating streamline T satisfies asymptotically

$$v(\rho,0)\frac{\partial T}{\partial \rho} + w_v(\rho,0)\eta\frac{\partial T}{\partial \eta} - \alpha(\rho,0)v(\rho,0)\frac{\partial^2 T}{\partial \eta^2} - \lambda T = -u_{bound}\,, \tag{7.22a}$$

with T to be matched as follows

$$T(\rho,\eta) = 0 \text{ for } \eta \to \infty\,, \tag{7.22b}$$

$$T(\rho,\eta) = T_{match}.u_{match} \text{ for } \eta \ll -1\,. \tag{7.22c}$$

A particular solution of (7.22a) is

$$T_p(\rho,\eta) = -\left(\int_{\gamma}^{\rho}\frac{1}{v(\bar{\rho},0)}d\bar{\rho}\right)u_{bound} \tag{7.23}$$

with γ a certain integration constant. Setting

$$T(\rho,\eta) = T_p(\rho,\eta) + T_h(\rho,\eta) \tag{7.24a}$$

and

$$T_h(\rho,\eta) = \exp\{\lambda\int_{\gamma}^{\rho}\frac{1}{v(\bar{\rho},0)}d\bar{\rho}\}\tilde{T}_h(\rho,\eta) \tag{7.24b}$$

one can easily check that $\tilde{T}_h$ is the solution of the homogeneous problem

$$\begin{cases} v(\rho,0)\dfrac{\partial \tilde{T}_h}{\partial \rho} + w_v(\rho,0)\eta\dfrac{\partial \tilde{T}_h}{\partial \eta} - \alpha(\rho,0)v(\rho,0)\dfrac{\partial^2 \tilde{T}_h}{\partial \eta^2} = 0, \\ \tilde{T}_h(\rho,\eta) = 0 \qquad \text{if} \quad \eta \to \infty, \\ \tilde{T}_h(\rho,\eta) = (T_{\text{match}} + \displaystyle\int_{\tilde{\rho}}^{\rho} \frac{1}{v(\bar{\rho},0)}d\bar{\rho})\exp\{-\lambda(T_{\text{match}} + \int_{\tilde{\rho}}^{\rho} \frac{1}{v(\bar{\rho},0)}d\bar{\rho})\} \qquad \text{for } \eta << -1\ . \end{cases} \tag{7.25}$$

Solving this problem in the same way as problem (7.13) and using (7.23) and (7.24) we find a boundary layer solution for T and thus for the conditional mean exit time T_{bound}:

$$T_{\text{bound}} = \frac{T}{u_{\text{bound}}} = \frac{1}{v_\rho(0,0)}\ln\left(\frac{v(\rho,0)}{v_\rho(0,0)\rho\theta_W}\right) + h(\rho) + \frac{1}{v_\rho(0,0)}\int_{v_q(\rho)}^{\infty} \frac{\ln\left(-v+t/q(\rho)\right)\left(-v+t/q(\rho)\right)^{-\lambda/v_\rho(0,0)}e^{-\frac{1}{2}t^2}dt}{\displaystyle\int_{v_q(\rho)}^{\infty}\left(-v+t/q(\rho)\right)^{-\lambda/v_\rho(0,0)}e^{-\frac{1}{2}t^2}dt}. \tag{7.26}$$

T_{bound} is an approximation for the conditional mean time of exit through $\partial\Omega_1$ for a particle released inside the boundary layer. For a particle released outside the boundary layer and inside the catchment area of the well we have the approximation (7.21). In the same way as we constructed u_{comp}, we can construct an approximation for the conditional mean exit time T_{comp} which is valid in the whole catchment area, both inside and outside the boundary layer.

$$\begin{aligned} T_{\text{comp}} &= T_{\text{adv}} + T_{\text{bound}} - T_{\text{match}} \\ &= T_{\text{adv}} - \frac{1}{v_\rho(0,0)}\ln(-v) + \frac{1}{v_\rho(0,0)}\int_{v_q(\rho)}^{\infty} \frac{\ln\left(-v+t/q(\rho)\right)\left(-v+t/q(\rho)\right)^{-\lambda/v_\rho(0,0)}e^{-\frac{1}{2}t^2}dt}{\displaystyle\int_{v_q(\rho)}^{\infty}\left(-v+t/q(\rho)\right)^{-\lambda/v_\rho(0,0)}e^{-\frac{1}{2}t^2}dt} \end{aligned} \tag{7.27}$$

We may use T_{bound} as an approximation for the conditional mean exit time that is valid in the whole domain outside the catchment area.

8. A WELL IN A UNIFORM BACKGROUND FLOW

As an example we apply the expressions derived in the previous section to calculate the exit rate and mean exit time to a well in a uniform background flow. We assume that the background flow is parallel to the x-axis and that the well is situated in the origin (0,0). The corresponding velocity field is described by

$$\begin{cases} v_1(x,y) = 1 - \dfrac{x}{x^2+y^2} \\ v_2(x,y) = \dfrac{-y}{x^2+y^2} \end{cases} \tag{8.1}$$

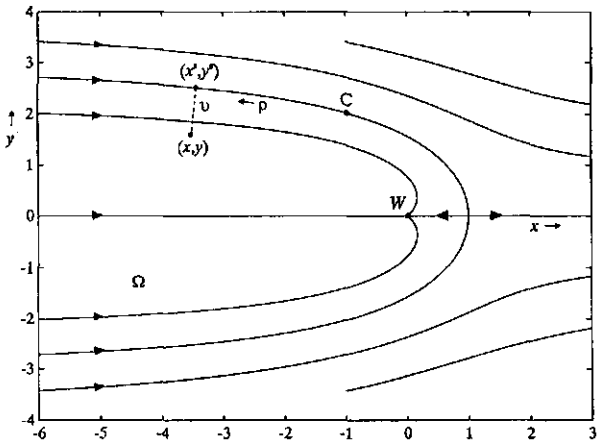

Figure 5 Stream pattern for a well in a uniform background flow.

We want to predict the rate and mean time at which a pollution, released somewhere in the xy-plane, reaches the well. Let Ω be the xy-plane with (0,0) excluded. So, $\partial\Omega_1$ consists of the well in (0,0) only. The stagnation point is in (1,0) and the separating streamline is given by

$$x = y/\tan(y) \ . \tag{8.2}$$

The (ρ,υ)-coordinates of a point (x,y) near the separating streamline are given by

$$\rho = \int_0^{y_s} \omega(y)dy \ , \qquad \upsilon = \left((x-x_s)^2 + (y-y_s)^2\right)^{1/2} \tag{8.3ab}$$

with

$$\omega(y) = \left\{1+\left(\frac{1}{\tan y} - \frac{y}{\sin^2 y}\right)^2\right\}^{\frac{1}{2}} , \tag{8.3c}$$

and where (x_s, y_s) is a point on the separating streamline so that $(x-x_s, y-y_s)^T$ is perpendicular to the separating streamline (see fig. 5). The velocity $v(\rho,0)$ along the separating streamline is

$$v(\rho,0) = -\left(1 + \left(\frac{1}{\tan y_s} - \frac{1}{y_s}\right)^2\right)^{\frac{1}{2}} \sin y_s \ . \tag{8.4}$$

The advective travelling time to the well from a point inside the catchment area of the well is

$$T_{adv}(x,y) = \ln\left(\frac{y}{\sin y}\right) - \ln\left(\frac{y}{\tan y} - x\right) - x \ , \tag{8.5}$$

see van der Hoek (1992). From (7.10) we obtain for the advective travelling time near the separating streamline

$$T_{match}(\rho,\upsilon) = -\ln(-\upsilon) - \frac{1}{2}\ln\left(1+\left(\frac{1}{\tan y_s}-\frac{1}{y_s}\right)^2\right) - x_s \,. \tag{8.6}$$

Assuming that the transversal dispersion coefficient is a constant and making use of (7.17) we find

$$u_{bound}(\rho,\upsilon) = \frac{1}{\sqrt{2\pi}} e^{\lambda x_s} \left(1+\left(\frac{1}{\tan y_s}-\frac{1}{y_s}\right)^2\right)^{\frac{1}{2}\lambda} \int_{\upsilon q(\rho)}^{\infty} \left(-\upsilon + t/q(\rho)\right)^{\lambda} e^{-\frac{1}{2}t^2} dt \tag{8.7a}$$

with

$$q(\rho) = \left\{2a_T \int_0^{y_s} v^2(\rho(y),0)\,\omega(y)\,dy / v^2(\rho,0)\right\}^{-1/2} \,. \tag{8.7b}$$

For pollution released inside the boundary layer or outside the catchment area of the well, u_{bound} is an approximation for the fraction of the pollution that will reach the well. The corresponding approximation for the mean arrival time is obtained from (7.26):

$$T_{bound}(\rho,\upsilon) = -\frac{1}{2}\ln\left(1+\left(\frac{1}{\tan y_s}-\frac{1}{y_s}\right)^2\right) - x_s - \frac{\int_{\upsilon q(\rho)}^{\infty} \ln\left(-\upsilon + t/q(\rho)\right)\left(-\upsilon + t/q(\rho)\right)^{\lambda} e^{-\frac{1}{2}t^2} dt}{\int_{\upsilon q(\rho)}^{\infty} \left(-\upsilon + t/q(\rho)\right)^{\lambda} e^{-\frac{1}{2}t^2} dt} \,. \tag{8.8}$$

From (7.18) we obtain an approximation for the rate of pollution that will reach the well, if the pollution is released in an arbitrary point inside the catchment area

$$u_{comp} = e^{-\lambda T_{adv}} + e^{\lambda x_s} \left(1+\left(\frac{1}{\tan y_s}-\frac{1}{y_s}\right)^2\right)^{\frac{1}{2}\lambda} \left\{\frac{1}{\sqrt{2\pi}} \int_{\upsilon q(\rho)}^{\infty} \left(-\upsilon + t/q(\rho)\right)^{\lambda} e^{-\frac{1}{2}t^2} dt - \left(-\upsilon\right)^{\lambda}\right\}. \tag{8.9}$$

An approximation for the mean arrival time of this pollution is

$$T_{comp} = T_{adv} + \ln\left(-\upsilon\right) - \frac{\int_{\upsilon q(\rho)}^{\infty} \ln\left(-\upsilon + t/q(\rho)\right)\left(-\upsilon + t/q(\rho)\right)^{\lambda} e^{-\frac{1}{2}t^2} dt}{\int_{\upsilon q(\rho)}^{\infty} \left(-\upsilon + t/q(\rho)\right)^{\lambda} e^{-\frac{1}{2}t^2} dt} \,. \tag{8.10}$$

We tested the accuracy of the asymptotic approximations by comparing them with results of random walk simulations. On the separating streamline we took the point C with coordinates $(\rho,\upsilon) = (2.958,0)$ corresponding with $(x,y) = (-0.915, 2.0)$. Carrying out some preliminary simulations, we obtained $\Delta t = 0.001$ as an appropriate time step to simulate the random walk motion of the particles in an accurate way. Next we carried out from C simulations consisting of respectively $N = 100$, 1000 and 15000 random walks, doing each simulation 10 times. In fig. 6 the rates and mean times at which particles reached the well are plotted. The figures visualise that the deviation in the random walk results is linear in respectively $1/\sqrt{N}$ and $1/\sqrt{N_w}$, see also section 5. If $N \to \infty$ the estimates for the probability and mean time of arrival obtained from random walk simulations will converge to their real values. Fig. 6 shows that these real values only slightly differ from the values

calculated from the asymptotic approximations. This implies that the asymptotic approximations for the probability and mean time of arrival are very good for this example.

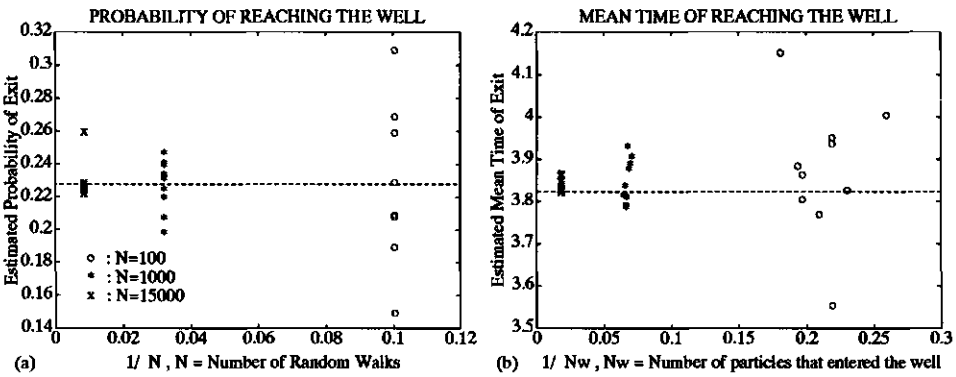

Fig. 6. Probability and mean time of arrival at a well in a uniform background flow for particles released in the point C (ρ,υ) = (2.958,0) as estimated from random walk simulations with N = 100, 1000 and 15000 respectively, and with a_L = 0.01, a_T = 0.001, λ = 0.2 and Δt = 0.001. The dashed lines denote asymptotic approximations for the probability and mean time of arrival as calculated form (8.7) and (8.8).

To enhance our confidence in the accuracy of the asymptotic approximations we carried out some additional simulations. On a line perpendicular to the separating streamline through C we took a number of points from which we carried out N = 15.000 random walk simulations. In fig. 7a the fraction of the particles that entered the well is compared with the asymptotic approximations (8.7) and (8.9) for the probability of arrival. In fig. 7b the mean arrival time of the particles that reached the well is compared with the asymptotic approximations (8.8) and (8.10) for the mean arrival time. If υ increases the number of particles that enter the well decreases. Therefore the mean arrival time as estimated from the simulations is subjected to increasing uncertainty. From the figures we may conclude that the approximations take into account the boundary layer behaviour of the probability and mean time of arrival in a surprisingly accurate way. The figures confirm that, although a_T is much smaller than a_L, the transversal dispersion plays a dominant role in predicting what fraction of a contaminant will enter a well.

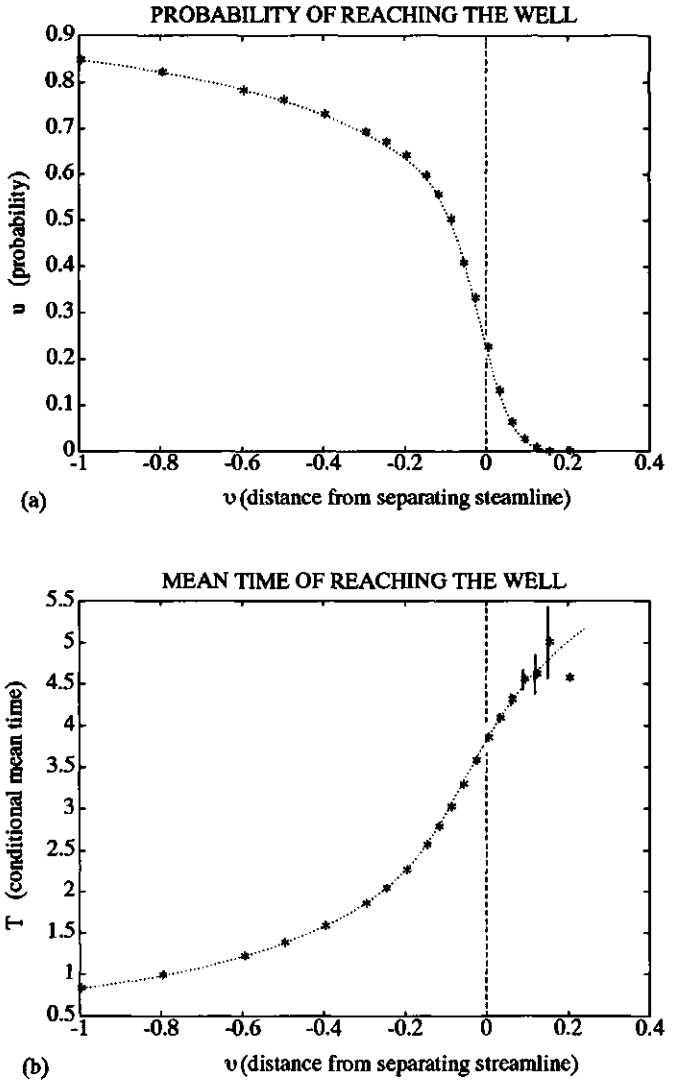

Fig. 7. Simulation results for particles released on a line perpendicular to the separating streamline through the point C obtained with N = 15.000, a_L = 0.01, a_T = 0.001, λ = 0.2 and Δt = 0.001. In fig. 7a the fraction of the particles that reached the well is compared with the asymptotic approximation for the probability of arrival calculated from (8.9) for $\upsilon < 0$ and from (8.7) for $\upsilon \geq 0$. For all simulations the 95% confidence domains for the real probability of arrival have a radius of less then 0.008. In fig. 7b the mean arrival time of the particles is compared with the asymptotic approximation calculated from (8.10) for $\upsilon < 0$ and from (8.8) for $\upsilon \geq 0$. For $\upsilon \geq -0.03$ the 95% confidence domains for the real mean arrival time are indicated. For $\upsilon < 0.03$ these domains are so narrow that they are not indicated.

CONCLUSIONS

When modelling the transport of pollution in aquifers the effects of adsorption or decay phenomena have to be taken into account. Restricting ourselves to space-independent linear (non-)equilibrium adsorption and first order decay/reactions, we answered the question at what rate and mean time particles of a source of pollution cross the boundary of a certain domain. In particular we considered a domain with arbitrary 2D-flow near separating streamlines ending in a stagnation point, which is typical for groundwater flow towards a well. We have constructed asymptotic approximations for the rate and mean time at which a contaminant, spilled somewhere in an aquifer, will enter the well. Far away from a separating streamline the advective flow field yields a first order approximation. Around a separating streamline boundary layer solutions are necessary which take into account the transversal dispersion. The approximations were worked out in the special case of a well in a uniform background flow. It was noticed that there is a good agreement with results from random walk simulations.

Substitution of $\lambda = 0$ and a_T = constant in the expressions (7.17), (7.18), (7.27) and (7.28) yields the same approximations for the rate and mean time of arrival at a well as obtained by van Herwaarden and Grasman (1991) and van Herwaarden (1994), who made a study of the spread of a mass conservative contaminant.

The expressions (7.17) and (7.18) we derived for the arrival rate not only give the fraction of a pollution produced by a point-source that will enter a well. If a pollution is distributed over a certain area Ω the expressions can also be used to compute approximately the amount of the pollution that will enter a well. Let $c(x)$ be the initial concentration of the pollution, then the amount of pollution that will be pumped up at well is

$$\int_{\Omega} c(x)u(x)dx \ ,$$

where $u(x)$ denotes the probability that a particle released in $x \in \Omega$ enters the well.

The analytical expressions for the rate of arrival ((7.16) and (7.17)) and for the mean arrival time ((7.27) and (7.28)) are quite powerful. Once an analytically or numerically obtained advective flow field is given, approximations for the rate and mean time at which a pollution will enter a well can be computed in an efficient and accurate way. The accuracy of the approximations increases when the ratio between advection and dispersion increases. The advantage above solving the advection-dispersion equation numerically is considerable. The latter method is very time and memory consuming and is subject to numerical dispersion, especially at high Peclet numbers, i.e. in cases where the ratio between advection and dispersion is large.

The expressions (7.16) and (7.17) can also be used to determine domains from which a certain fraction of the pollution will enter a well. Therefore these expressions may play an important role in the delineation of well head protection areas.

ACKNOWLEDGEMENTS

I am grateful to Johan Grasman and Maarten de Gee for the discussions concerning the subject treated in this paper and for reading the text critically. I also thank Onno van Herwaarden for the discussions we had and for his help with drawing the figures. Oscar Buse assisted me with programming the random walk routines, for which I am thankful.

REFERENCES

Andricevic, R. and M. Foufoula-Georgiou 1991: Modeling kinetic non-equilibrium using the first two moments of the residence time distribution. Stochastic Hydrol. Hydraul. 5, 155-171.

Bear, J. and A. Verruyt 1987: Modelling Groundwater Flow and Pollution, Dordrecht, Reidel

Cameron, D.R. and A. Klute 1977: Convective-Dispersive Solute Transport With a Combined Equilibrium and Kinetic Adsorption Model. Water Resour.Res. 13 (1): 183-188.

Dagan, G. 1989: Flow and transport in Porous Formations. Berlin Heidelberg, Springer

Gardiner, C.W. 1983: Handbook of Stochastic Methods for Physics, Chemistry and Natural Sciences, Berlin Heidelberg, Springer.

Gelhar, L.W. and C. Axness 1983: Three dimensional stochastic analysis of macrodispersion in aquifers. Water Resour.Res 19 (1) : 161-180.

van der Hoek, C.J. 1992: Contamination of a well in a uniform background flow. Stochastic Hydrol. Hydraul. 6: 191-208.

van Herwaarden, O.A. and J. Grasman 1991: Dispersive Groundwater Flow and Pollution. Math. Mod. and Meth. in Appl. Sci. 1:61-81.

van Herwaarden, O.A. 1994: Spread of Pollution by Dispersive Groundwater Flow. SIAM J. of Appl Math., 54 (1), 26-41.

Kabala, Z.J. and G. Sposito 1991: A Stochastic Model of Reactive Solute Transport With Time-Varying Velocity in a Heterogenous Aquifer. Water Resour.Res. 27 (3): 341-350.

Karlin, S. 1960: A First Course in Stochastic Processes, Academic Press.

Kinzelbach, W. 1986: The random walk method in pollutant transport simulation. In: Custodio,E. et al. (eds.) Groundwater flow and quality modelling, p 227-245. Reidel, Dordrecht.

Linderfelt, W.R. and J.L. Wilson 1993: Parameter uncertainty in capture zone analysis for a pumping well in an infinite domain. Manuscript, New Mexico Institute for Mining and Technology, Socorro, New Mexico.

Neumann, S.P. 1991: Eulerian-Lagrangian Theory of Transport in Space-Time Nonstationary Velocity Fields: Exact Nonlocal Formalism By Conditional Moments and Weak Approximations. Water Resour.Res. 29 (3), 633-645.

Roberts, P.V., M.N. Goltz and D.M. Mackay 1986: A natural gradient experiment on solute transport in a sand aquifer, 3, Retardation estimates and mass balances for organic solutes, Water Resour.Res. 22, 2247-2058.

Schuss, Z. 1980: Theory and Applications of Stochastic Differential Equations, Wiley.

Sposito, G. and D.A. Barry 1987 : On the Dagan Model of Solute Transport in Groundwater: Foundational Aspects. Water Resour.Res. 23 (10) : 1876-1875.

Uffink, G.J.M. 1990: Analysis of Dispersion by the Random Walk Method, Thesis, Technical University Delft.

Valocchi, A.J. 1985: Validity of the Local Equilibrium Assumption for Modelling Sorbing Solute Transport Through Homogeneous Soils. Water Resour.Res. 21 (6): 808-820.

CHAPTER 2

AN ASYMPTOTIC METHOD TO PREDICT THE CONTAMINATION OF A PUMPING WELL

(By J.J.A. van Kooten, published in Advances in Water Resources, 18 (5), 295-313, 1995)

Abstract: A method is presented to predict the advective-dispersive transport of a contaminant towards a well in a confined aquifer. Due to (macro-)dispersion particles carry out random walks through the porous formation. Using perturbation techniques we derive analytical approximations for the fraction of the particles that reaches the well and for the mean and variance of the arrival time. In particular, approximations for the breakthrough curve at the well are provided. The asymptotic approximations are shown to be in good agreement with results of random walk simulations. The method may be applied to any 2D-flow pattern.

Key words: advection, dispersion, contamination of a well, asymptotic approximations, breakthrough, random walk.

1. INTRODUCTION

Groundwater confined in aquifers is an important source of drinking water supply. In order to control groundwater quality in pumping wells, tools are needed which predict contaminant transport. Popular tools to delineate wellhead protection zones or to design aquifer remediation strategies are based on particle and front tracking techniques (e.g. Javandel and Tsang, 1986, Schafer and Wilson, 1991). These methods only take into account the advective transport of a contaminant. However, to control well water quality as accurately as possible one should also incorporate the effects of macro-dispersion. Recently, Van Herwaarden & Grasman (1991), Van der Hoek (1992), Van Herwaarden (1994) and Van Kooten (1994) have reported on an analytical method to study the effect of transversal dispersion on the fraction of a contaminant that enters a well. In the present paper this method is developed further. Taking into account both longitudinal and transversal dispersion we derive asymptotic approximations for the first and second moment of the arrival time at the well. The main aim of this study is to obtain expressions for the breakthrough curve.

We assume that contaminant transport can be modelled by the advection-dispersion equation (ADE), in which the dispersion may be a non-linear function of the velocity. The ADE can be interpreted as the Fokker-Planck equation corresponding with the random motion of a single particle (Uffink, 1989). Following this interpretation we formulate in section 4 boundary value problems both for the probability that a particle exits a certain region as for the moments of the exit time. In section 5 we show how these boundary value problems may be applied to a one-dimensional dispersion problem. In section 6 the boundary value problems are used to predict the arrival of a conservative contaminant at a well in a confined aquifer. Assuming that advection dominates dispersion we solve these

problems with the use of perturbation techniques. The advective flow yields first order approximations. These first order approximations can be improved by adding terms that account for longitudinal dispersion. Furthermore, we make use of the fact that transversal dispersion only plays a significant role in a boundary layer near the separating streamlines, which bound the catchment area. In section 7 the asymptotic approximations for the mean and variance of the arrival times at the well are used to obtain expressions for the arrival time distributions. In section 8 the results are generalised for a contaminant subject to linear equilibrium adsorption and first order decay. Finally, we consider the special case of a well in a uniform background flow. The asymptotic approximations are compared with results of random walk simulations.

2. SPREAD OF POLLUTION IN AN AQUIFER

2.1 The advection-dispersion equation

The conventional advection-dispersion model for the transport of a contaminant through a saturated porous formation is

$$\frac{\partial c}{\partial t} = -\frac{\partial}{\partial y_i}(v_i c) + \frac{\partial}{\partial y_i}\left(D_{ij}\frac{\partial c}{\partial y_j}\right) - \lambda c\,, \tag{2.1}$$

where $y \in \mathbb{R}^N$ (N = 1,2 or 3) is the vector of space coordinates, $c(y,t)$ $[M/L^3]$ is the solute concentration, v $[L/T]$ is the mean pore-velocity vector, D_{ij} $[L^2/T]$ is the dispersion tensor and λ $[T^{-1}]$ is the decay or reaction rate. With respect to the indices we use the Einstein summation convention. Linear equilibrium adsorption can be incorporated by replacing the parameters v_i and D_{ij} in (2.1) by their retarded values $v_i^R = v_i/R$, $D_{ij}^R = D_{ij}/R$, where R [-] is the retardation constant ($R \geq 1$).

The ADE has been derived from laboratory experiments. In this study we are especially interested in contaminant transport at aquifer scale. The soil properties in an aquifer will often be heterogeneous. Because at laboratory scale a porous medium is homogeneous, the applicability of the ADE to field scale processes is limited. In many experimental and theoretical studies (e.g. Roberts et al., 1986, Sudicky, 1986, Gelhar & Axness, 1983, Dagan, 1984, 1989) it has been demonstrated that physical and chemical heterogeneities have a large impact on solute transport. The irregular spatial variability of the velocity field and the chemical properties results in an enhanced spreading of the contaminant. This phenomenon is commonly referred to as "macro-dispersion". Another interpretation of the concept macro-dispersion is that it accounts for uncertainties in model prediction of the movement of a contaminant.

Important results with respect to flow and transport in heterogeneous porous formations have been obtained with stochastic modelling. Because the transport parameters vary in a random manner it is impossible to predict the actual transport of a contaminant. One can only try to predict the mean transport. If the velocity field, the decay rate and the retardation factor are assumed to be stationary (i.e. statistically homogeneous) random fields, the concentration expected value still satisfies an ADE of form (2.1) (Dagan, 1984, 1989, Kabala and Sposito, 1991). Because of the heterogeniety the field scale transport parameters show temporal growth. However, if the correlation scales of the random fields are finite, the time dependency vanishes after a certain time and the field-scale parameters tend to asymptotic values (see Gelhar & Axness, 1983, Neumann et al., 1987).

2.2 Basic assumptions

In this study we focus on contaminant transport through a confined aquifer with steady state flow towards a well. It is assumed that the scale of heterogeneity is small compared to the geometry of the aquifer. Under this assumption we expect that in many cases the transport parameters will reach their asymptotic values rapidly. So, as starting point of our analysis we may take ADE (2.1), where the parameters are time independent. We also assume that the thickness of the layer is small relative to the horizontal geometry, so that the flow is essentially two-dimensional. The velocity field is divergence free, except at the location of a well. Furthermore we assume that the porous medium is isotropic, so that the flow is also rotational free. The asymptotic method we develop in section 6 is based on the assumption that the advective transport dominates the dispersive transport.

For the analysis in this study it is essential that the concentration c occurs linearly in the ADE. So, non-linear effects can not be incorporated. We come back to this issue in section 8.

2.3 The dispersion tensor

A commonly used expression for the (macro) dispersion tensor in an isotropic formation is

$$D_{ij} = a_T|v|\delta_{ij} + (a_L - a_T)\frac{v_i v_j}{|v|}, \qquad (i,j = 1...N) \qquad (2.2)$$

where a_L $[L]$ and a_T $[L]$ denote the longitudinal and transversal dispersivities, (Bear & Verruijt, 1987). In experiments it has been found that the longitudinal dispersivity is much larger than the transversal dispersivity. To allow for spatially varying dispersivities, we make the following decomposition:

$$a_L = \alpha_L f_L(y) \quad \text{and} \quad a_T = \alpha_T f_T(y), \qquad (2.3)$$

where α_L $[L]$ and α_T $[L]$ are (spatial) means of a_L and a_T and f_L and f_T are dimensionless functions accounting for the spatial variability.

Expression (2.2) is based on the assumption that the dispersion is proportional to the velocity. Decomposition (2.3) enables us to deal with problems where the dispersion depends non-linearly on the velocity. E.g. there exist situations in which f_L and f_T are functions of the Peclet number $Pe=l|v|/D_d$ and thus of the velocity. At laboratory scale l $[L]$ is a characteristic length of the pores and D_d $[L^2/T]$ is the coefficient of molecular diffusion (see e.g. Saffman, 1960, Bear and Bachmat, 1967). At field scale l is a length characterizing the heterogeneity of the aquifer and D_d is a pore-scale dispersion coefficient (Gelhar & Axness, 1983, Neumann et al., 1987). In such, cases f_L and f_T can be expressed as

$$f_L(y) = f_L(v(y)) \quad \text{and} \quad f_T(y) = f_T(v(y)), \qquad (2.4)$$

so that the dispersion tensor becomes a non-linear function of the velocity.

3. RANDOM WALK MODEL FOR SOLUTE SPREADING

Instead of analyzing the transport of a solute body we may also follow the path of a single particle in groundwater. Due to dispersion a single particle makes a random walk. The expected concentration of a solute can be interpreted as a probability density function for

the location of a particle some time after injection. So, the probability density function $p(y,t|x)$ for a particle with initial position x has to satisfy ADE (2.1), i.e.

$$\begin{aligned} &\frac{\partial p}{\partial t} = M_\lambda p \quad , \quad p(y,0|x) = \delta(x - y) \, , \\ &M_\lambda = -\frac{\partial}{\partial y_i}((v_i + \frac{\partial}{\partial y_j} D_{ij})\cdot) + \frac{\partial^2}{\partial y_i \partial y_j}(D_{ij}\cdot) - \lambda\cdot \quad . \end{aligned} \tag{3.1}$$

Setting

$$p = p_0 e^{-\lambda t} \, , \tag{3.2}$$

we find that p_0 has to satisfy the ADE for a conservative contaminant:

$$\frac{\partial p_0}{\partial t} = M_0 p_0 \, . \tag{3.3}$$

Equation (3.3) is the forward Kolmogorov or Fokker-Planck equation that corresponds with the diffusion process governed by the Ito stochastic differential equation

$$\partial y_i = (v_i + \frac{\partial}{\partial y_j} D_{ij})dt + F_{ij} dW_j \, , \tag{3.4}$$

The term $F_{ij}\, dW_j$ accounts for the stochastic displacement due to dispersion: W_j are independent Wiener processes (Gardiner, 1983, p. 66), F_{ij} is and amplitude tensor related to the dispersion tensor:

$$F_{ik} F_{jk} = 2D_{ij} \, , \tag{3.5}$$

Uffink (1989).

Because of linear irreversible adsorption and first order decay particles may be "killed". The term $e^{-\lambda t}$ in (3.2) may be interpreted as the probability that a particle has not been killed before time t. So, we can simulate the dispersive spread of pollution by a random walk process in which particles have an exponentially distributed life time.

4. THE BACKWARD KOLMOGOROV EQUATION AND EXIT PROBLEMS

Beside the forward Kolmogorov equation (3.3) p_0 also satisfies the backward Kolmogorov equation that describes how p_0 depends on the initial position x:

$$\begin{aligned} &\frac{\partial p_0}{\partial t} = L_0 p_0 \quad , \\ &L_\lambda = (v_i + \frac{\partial}{\partial x_j} D_{ij}) \frac{\partial \cdot}{\partial x_i} + D_{ij} \frac{\partial^2 \cdot}{\partial x_i \partial x_j} - \lambda\cdot = v_i \frac{\partial \cdot}{\partial x_i} + \frac{\partial}{\partial x_i}(D_{ij} \frac{\partial \cdot}{\partial x_j}) - \lambda\cdot \quad . \end{aligned} \tag{4.1}$$

(Gardiner, 1983, p. 143-170, Uffink, 1989). The backward operator L_λ is the formal

adjoint of the forward operator M_λ: $L_\lambda = M_\lambda^*$ (Garabedian, 1964, p. 185). The operator L_λ plays an important role in exit problems.

Let us consider a domain Ω in $\mathbb{R}^N$ (N = 1,2 or 3) with boundary $\partial\Omega$. The boundary $\partial\Omega$ is absorbing, i.e. $p(y,t|x)=0$ if $x\in\partial\Omega$. We wish to know the probability $u(x)$ that a particle with initial position $x\in\Omega$ is absorbed at a particular part $\partial\Omega_1$ of the boundary. The remainder of the boundary is called $\partial\Omega_0$ (figure 1).

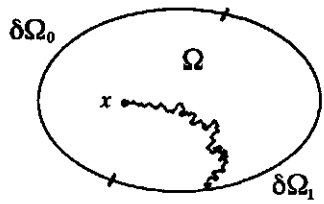

Figure 1. Example of the region Ω considered in section 4

The probability $u(x)$ of adsorption at $\partial\Omega_1$ is the solution of the boundary value problem

$$L_\lambda u = 0 \quad \text{in } \Omega\,, \qquad u = 0 \quad \text{at} \quad \partial\Omega_0 \quad , \quad u = 1 \quad \text{at} \quad \partial\Omega_1\,. \tag{4.2}$$

(For the case $\lambda = 0$, van Herwaarden, 1994, for the case $\lambda\neq 0$, see Van Kooten, 1994). The conditional *m'th* moments $T^{(m)}(n\geq 1)$ of the arrival time at $\partial\Omega_1$ is given by

$$T^{(m)}(x) = \frac{\bar{T}^{(m)}(x)}{u(x)}\,, \tag{4.3}$$

where $\bar{T}^{(1)}$ is the solution of

$$L_\lambda \bar{T}^{(1)}(x) = -u(x) \quad \text{in } \Omega\,, \qquad \bar{T}^{(1)} = 0 \quad \text{at} \quad \partial\Omega, \tag{4.4}$$

and for $m \geq 2$, $\bar{T}^{(m)}$ is the solution of

$$L_\lambda \bar{T}^{(m)}(x) = -m\,\bar{T}^{(m-1)}(x) \text{ in } \Omega\,, \qquad \bar{T}^{(m)} = 0 \quad \text{at} \quad \partial\Omega. \tag{4.5}$$

(For the case $\lambda = 0$, see Van Herwaarden, 1994, for the case $\lambda\neq 0$ see Van Kooten, 1994). The variance of the arrival time at $\partial\Omega_1$ is given by

$$\sigma^2 = T^{(2)} - (T^{(1)})^2\,. \tag{4.6}$$

5. DISPERSION IN ONE-DIMENSIONAL FLOW

The boundary value problems formulated in section 4 may be applied to various types of flow patterns. By way of introduction we show how these boundary value problems may

be applied to a simple, one-dimensional dispersion process. Let $\Omega = (-\infty,0)$, where $\partial\Omega_1=\{0\}$ is an absorbing boundary. The transport of a conservative solute which is injected in $x<0$, is described by

$$\frac{\partial c}{\partial t} = -v\frac{\partial c}{\partial y} + \frac{\partial}{\partial y}(D\frac{\partial c}{\partial y}) , \quad c(y,0) = \delta(x - y) , \quad c(0,t) = 0 , \tag{5.1}$$

where the advective flow rate $v>0$ is constant. The dispersion coefficient is given by

$$D = a_L v, \tag{5.2}$$

The dispersivity a_L is taken constant. The backward Kolmogorov operator for this example is

$$L_0 = v\frac{\partial \cdot}{\partial x} + \frac{\partial}{\partial x}(D\frac{\partial \cdot}{\partial x}) . \tag{5.3}$$

From boundary value problem (4.2) follows $u=1$: every particle will be absorbed sooner or later. From boundary value problems (4.4) and (4.5) we find for, respectively, the mean and variance of the arrival time at $\partial\Omega_1$

$$\mu = -\frac{x}{v} \quad \text{and} \quad \sigma^2 = -2D\frac{x}{v^3} = a_L\frac{x}{v^2} . \tag{5.4}$$

Note that μ equals the advective travelling time to $\partial\Omega_1$. The probability density function for absorption at $\partial\Omega_1$ at time τ is

$$\frac{-x}{\sqrt{4\pi D\tau^3}} \exp\{-\frac{(-x - v\tau)^2}{4D\tau}\} , \tag{5.5}$$

see Feller (1968, Ch.14). Using (5.4) we may also express (5.5) as

$$g(\mu,\sigma^2;\tau) = \frac{\mu^{3/2}}{\sqrt{2\pi\sigma^2\tau^3}} \exp\{-\frac{(\mu - \tau)^2\mu}{2\sigma^2\tau}\}. \tag{5.6}$$

So, the distribution for the arrival time τ at $\partial\Omega_1$ is completely determined by its first two moments. In section 7 expression (5.6) will be used to estimate the arrival time distribution of a contaminant at a pumping well.

6. TRANSPORT OF A CONSERVATIVE CONTAMINANT TOWARDS A WELL

The aim of this study is to provide a mathematical tool to control groundwater quality in pumping wells. Drinking water is often pumped up from a confined aquifer. A typical flow pattern around a pumping well is sketched in fig. 2. The region of advective flow towards the well, called the catchment area, is bounded by two separating streamlines ending in a stagnation point.

We start with studying the advective-dispersive transport of a conservative contaminant (λ=0). The aquifer is called $\Omega \subset \mathbb{R}^2$. The probability at which particles enter the well and the first two moments of the arrival time are the solutions of boundary value problems (4.2), (4.4) and (4.5) respectively, with $\partial\Omega_1$ being the position of the well. Assuming that advection dominates dispersion we solve these boundary value problems with the use of an asymptotic method. In particular we use that transversal dispersion only plays a significant role near a separating streamline. An outline of the method is given in section 6.1. In the sections 6.2, 6.3 and 6.4 the method is worked out in detail.

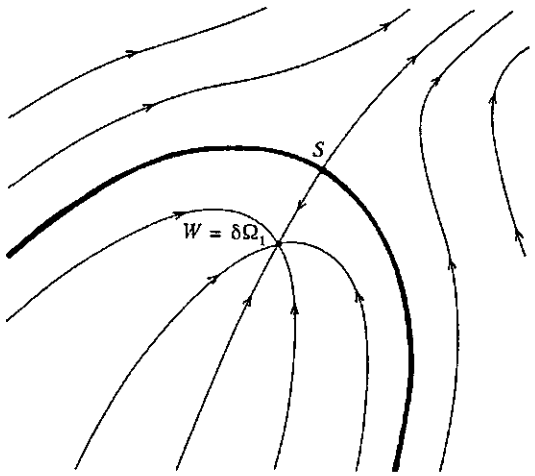

Figure 2. Example of a flow pattern with a well. The catchment area is bounded by two separating streamlines ending in the stagnation point S.

6.1 Outline of the asymptotic method

We consider spills of contaminant in three different regions of the aquifer. Firstly, we consider a spill in the point $x=(x_1,x_2)$ outside the catchment area, see fig. 3. The advective streamline through x does not end in the well. The point x is so far away from the separating streamline that transversal dispersion cannot deflect the path of a particle sufficiently to enter the well, so that the probability of entering the well is negligible. From boundary value problems (4.4) and (4.5) it follows that $u = 0$ implies that $\bar{T}^{(1)}$ and $\bar{T}^{(2)}$, which are related to the (conditional) first and second moment of the arrival time, are also 0. So, well outside the catchment area we approximately have

$$\bar{T}^{(1)} = 0 \quad \text{and} \quad \bar{T}^{(2)} = 0. \tag{6.1}$$

Secondly, we consider a spill of contaminant far inside the catchment area (fig. 4). Now, nearly all particles will reach the well: the probability of entering the well is close to 1. Again transversal dispersion has a negligible effect on the arrival rate. Because far inside the catchment area the travelling time along neighbouring streamline only varies slowly, the effect of transversal dispersion on the mean and variance of the arrival time is also negligible. Furthermore, the advective transport dominates the longitudinal dispersive transport, so that the first and second moment of the arrival time may be expanded in

asymptotic sequences in α_L. These expansions are called $T^{(1)}_{\text{catch}}$ and $T^{(2)}_{\text{catch}}$:

$$T^{(1)}_{\text{catch}} = T^{(1)}_{1,e} + \alpha_L T^{(1)}_{2,e} + O(\alpha_L^2), \tag{6.2a}$$

$$T^{(2)}_{\text{catch}} = T^{(2)}_{1,e} + \alpha_L T^{(2)}_{2,e} + O(\alpha_L^2). \tag{6.2b}$$

Remark that $u = 1$ implies that $T^{(1)}_{\text{catch}} = \bar{T}^{(1)}_{\text{catch}}$ and $T^{(2)}_{\text{catch}} = \bar{T}^{(2)}_{\text{catch}}$, see equation (4.3). The expansions are also valid in the vicinity of a well. In approaching the well $|v| \to \infty$ and thus $|D| \to \infty$. However α_L is a constant that is small in the entire region. In section 6.1 the terms of the expansions are determined.

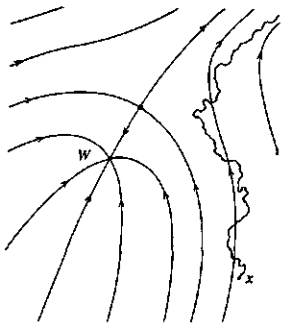

Figure 3 Spill outside the catchment area

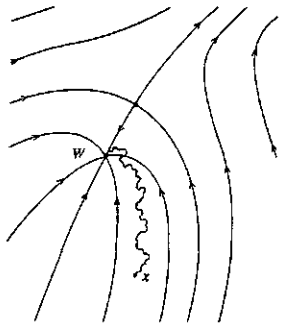

Figure 4 Spill inside the catchment area

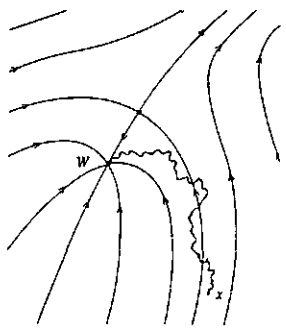

Figure 5 Spill near a separating streamline

Finally, we consider a spill of contaminant in the neighbourhood of a separating streamline (fig. 5). Near a separating streamline transversal dispersion may not be neglected. Due to transversal dispersion a particle released just outside the catchment area may cross the separating streamline and enter the well. Or in the opposite way: a particle released just inside the catchment area may cross the separating streamline, which would reduce the probability that the particle enters the well. So, near a separating streamline we have a boundary layer in which, due to transversal dispersion, the probability of entering the well changes rapidly from 1 to 0. This rapid change can be analyzed with the use of coordinate stretching techniques. In this way we derive an approximation for the probability of entering the well, which we denote by u_{bound}.

A similar approach results in approximations for the first two moments of the arrival time at the well for particles released in the boundary layer. Note that close to a separating streamline the advective travel time is large because the stagnation point is passed very closely. Therefore, in this region the advective travelling time may vary quickly among neighbouring streamlines. It follows that near a separating streamline transversal dispersion will have a non-negligible effect on the mean and variance of the arrival time. Let

$$T^{(1)}_{\text{bound}} = \frac{\bar{T}^{(1)}_{\text{bound}}}{u_{\text{bound}}} \quad \text{and} \quad T^{(2)}_{\text{bound}} = \frac{\bar{T}^{(2)}_{\text{bound}}}{u_{\text{bound}}} \tag{6.3}$$

be the first and second (conditional) moment of the arrival time at the well for a particle released inside the boundary layer. In analogy to (6.2) we expand u_{bound}, $\bar{T}^{(1)}_{\text{bound}}$ and $\bar{T}^{(2)}_{\text{bound}}$ in asymptotic sequences in α_L:

$$u_{\text{bound}} = u_{1,b} + \alpha_L u_{2,b} + O(\alpha_L^2), \tag{6.4a}$$

$$\bar{T}^{(1)}_{\text{bound}} = \bar{T}^{(1)}_{1,b} + \alpha_L \bar{T}^{(1)}_{2,b} + O(\alpha_L^2), \tag{6.4b}$$

$$\bar{T}^{(2)}_{\text{bound}} = \bar{T}^{(2)}_{1,b} + \alpha_L \bar{T}^{(2)}_{2,b} + O(\alpha_L^2). \tag{6.4c}$$

The difference with the expansions $T^{(1)}_{\text{catch}}$ and $T^{(2)}_{\text{catch}}$ is that the terms in the boundary layer expansions (6.4abc) depend on α_T. Outside the boundary layer the expansions (6.4abc) have to match the outer expansions, i.e. inside the catchment area u_{bound} must tend to 1 and the terms of $\bar{T}^{(1)}_{\text{bound}}$ and $\bar{T}^{(2)}_{\text{bound}}$ have to match the corresponding terms of $T^{(1)}_{\text{catch}}$ and $T^{(2)}_{\text{catch}}$, whereas outside the catchment area all terms tend to 0 (see eq. (6.1)). In section 6.3 expressions for the terms of the boundary layer expansions are derived.

The transition from a boundary layer to the outer regions is smooth, of course. Therefore, in section 6.4 the different types of approximations for the probability of entering the well and the mean and variance of the arrival time are melted together to smooth expansions valid in the entire aquifer, both inside and outside a boundary layer.

subscript	usage
catch	indicates an asymptotic expansion valid far inside catchment area
i,c	denotes *i'th* term of a 'catch'-expansion
bound	indicates an asymptotic expansion valid in boundary layer
i,b	denotes *i'th* term of a 'bound'-expansion
comp	indicates an expansion connecting the 'bound'- and 'catch'-expansions
sing	indicates an integral along streamlines close to a separating streamline
sep	indicates an expression for the 'catch'-expansions in (η,υ)-coordinates

Table 1 List of subscript used in the asymptotic approximations

6.2 Arrival at the well for particles released far inside the catchment area

Far inside the catchment area we may put $a_T = 0$, so that the backward Kolmogorov operator (4.1) for a conservative contaminant becomes

$$L_{\text{catch}} = v_1 \frac{\partial^*}{\partial x_1} + v_2 \frac{\partial^*}{\partial x_2} + \alpha_L \left(v_1 \frac{\partial}{\partial x_1} + v_2 \frac{\partial}{\partial x_2} \right) \left(\frac{f_L}{|v|} \left[v_1 \frac{\partial^*}{\partial x_1} + v_2 \frac{\partial^*}{\partial x_2} \right] \right). \tag{6.5}$$

(see Appendix A). The probability u of entering the well is approximately 1. Substituting the expansions $T^{(1)}_{\text{catch}}$ (6.2a) and $T^{(2)}_{\text{catch}}$ (6.2b) in the boundary value problems (4.4) and (4.5) (with $m = 2$) and collecting terms of equal power in α_L we obtain boundary value

problems for the terms of the expansions. These boundary value problems can be solved iteratively with the method of characteristics. In this way we have determined the expansions for the first and second moment of the arrival time up to the second terms:

$$T^{(1)}_{catch}(x) = T_{adv}(x) + \alpha_L \frac{f_L(x)}{|v(x)|}, \tag{6.6a}$$

$$T^{(2)}_{catch}(x) = T^2_{adv}(x) + 2\alpha_L (T_{adv} \frac{f_L(x)}{|v(x)|} + I(x)), \tag{6.6b}$$

where

$$T_{adv}(x) = \int_0^{\zeta} \frac{1}{v(\bar{\zeta})} d\bar{\zeta} \quad \text{and} \quad I(x) = \int_0^{\zeta} \frac{f_L(\bar{\zeta})}{v^2(\bar{\zeta})} d\bar{\zeta} . \tag{6.7}$$

The term T_{adv} is the advective travelling time to the well and ζ is a coordinate along the streamline through injection point x, see fig. 6. The corresponding approximation for the variance of the arrival time is

$$\sigma^2_{catch} = 2\ \alpha_L\ I(x) . \tag{6.8}$$

Note that $T^{(1)}_{catch}(x)$, $T^{(2)}_{catch}(x)$ and $\sigma^2_{catch}(x)$ only depend on the velocity and the longitudinal dispersivity along the streamline through x. Thus, for any flow pattern these approximations can easily be determined by particle tracking.

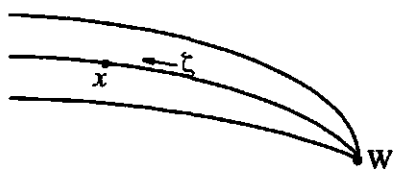

Figure 6 The coordinate ζ is taken along the streamline through the injection point x.

6.3 Arrival at the well of particles released near a separating streamline

Near a separating streamline transversal dispersion plays a crucial role. Its effect on the arrival of particles at the well can be analysed by introducing new (local) coordinates. These coordinates can be chosen in different ways. E.g. van der Hoek (1992) has taken the potential ϕ and the stream function ψ as new coordinate system. A drawback of this choice may be that, when the flow pattern is computed numerically, the streamfunction is not at hand. The coordinates we use are indicated in fig. 7: $\rho>0$ is a coordinate along the separating streamline and υ is a coordinate perpendicular to it. The stagnation point is in $(\rho,\upsilon) = (0,0)$. The velocity field in these new coordinates is given by

$$(v(\rho,\upsilon),\ w(\rho,\upsilon)). \tag{6.9}$$

Along a separating streamline a boundary layer of width $O(\sqrt{\alpha_T})$ is expected. To stretch

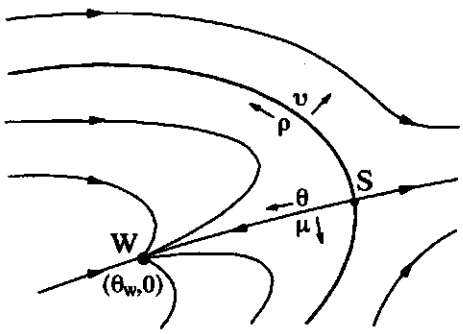

Figure 7. The coordinates ρ and υ are taken along and perpendicular to the separating streamline leading towards the stagnation point. The coordinates θ and μ are taken along and perpendicular to the separating streamline leading away from the stagnation point. The well is situated in $(\theta,\mu)=(\theta_w,0)$. The flow velocity in (θ,μ)-coordinates is given by $(r(\theta,\mu), s(\theta,\mu))$.

the boundary layer we introduce the coordinate

$$\eta = \upsilon/\sqrt{\alpha_T} . \tag{6.10}$$

Switching to (ρ,η)-coordinates we obtain (Appendix A) that for $\alpha_T \to 0$ the backward Kolmogorov operator asymptotically becomes

$$L_{\text{bound}} = v(\rho,0)\frac{\partial\cdot}{\partial\rho} + w_\upsilon(\rho,0)\eta\frac{\partial\cdot}{\partial\eta} - f_T(\rho,0)v(\rho,0)\frac{\partial^2\cdot}{\partial\eta^2}$$
$$- \alpha_L\Big(v(\rho,0)\frac{\partial}{\partial\rho} + w_\upsilon(\rho,0)\eta\frac{\partial}{\partial\eta}\Big)\Big(\frac{f_L(\rho,0)}{v(\rho,0)}\Big[v(\rho,0)\frac{\partial\cdot}{\partial\rho} + w_\upsilon(\rho,0)\eta\frac{\partial\cdot}{\partial\eta}\Big]\Big) . \tag{6.11}$$

The fact that the flow is divergence free implies that in (6.11) $w_\upsilon(\rho,0) = -v_\rho(\rho,0)$.

6.3.1 Boundary layer approximations without the effect of longitudinal dispersion

Boundary layer approximations for the probability and mean time of entering the well which do not take into account longitudinal dispersion have already been presented in Van Herwaarden & Grasman (1991), Van Herwaarden (1994) and van Kooten (1994). Putting $\alpha_L=0$ in (6.11) we find that the term $u_{1,b}$ in the expansion for the probability of arrival (6.4a) has to satisfy

$$v(\rho,0)\frac{\partial u_{1,b}}{\partial\rho} + w_\upsilon(\rho,0)\eta\frac{\partial u_{1,b}}{\partial\eta} - f_T(\rho,0)v(\rho,0)\frac{\partial^2 u_{1,b}}{\partial\eta^2} = 0 . \tag{6.12}$$

Outside the boundary layer $u_{1,b}$ must match with $u = 1$ and $u = 0$, i.e. for $\eta \gg 1$, $u_{1,b}$ must tend to 0 and for $\eta \ll -1$, $u_{1,b}$ must tend to 1. Grasman and Van Herwaarden (1991) have determined $u_{1,b}$ for the homogeneous case $f_T = 1$. Generalisation of their result to the heterogeneous case gives

$$u_{1,b}(\rho,\eta) = \frac{1}{\sqrt{2\pi}} \int_{\eta q(\rho)}^{-\infty} e^{-\frac{1}{2}t^2} dt \tag{6.13}$$

with

$$q(\rho) = \left(\frac{2}{\nu^2(\rho,0)} \int_0^{\rho} f_T(\bar{\rho},0)\nu^2(\bar{\rho},0)d\bar{\rho} \right)^{-1/2} . \tag{6.14}$$

Far outside the catchment area the terms $\bar{T}_{1,b}^{(1)}$ and $\bar{T}_{1,b}^{(2)}$ of the boundary layer expansions for the moments of the arrival time (6.4bc) must tend to 0 (see (6.1)). Far inside the catchment area $\bar{T}_{1,b}^{(1)}$ and $\bar{T}_{1,b}^{(2)}$ have to match $T_{1,c}^{(1)}=T_{adv}$ and $T_{1,c}^{(2)}=T_{adv}^2$, respectively (see (6.7)). So, for matching purposes an expression for T_{adv} in (ρ,υ)-coordinates is needed. For $\upsilon \uparrow 0$ T_{adv} will tend to infinity because a streamline near a separating streamline passes the stagnation point very closely. We say: for $\upsilon = 0$ T_{adv} has a singularity. Van Herwaarden (1994) has shown that for $-1<<\upsilon<0$

$$T_{adv}(\rho,\upsilon) \sim T_{sing}(\rho,\upsilon) \tag{6.15a}$$

where T_{sing} is the advective travelling time to the well along a characteristic ($\upsilon\nu(\rho,0)$=constant) of the differential operator L_{bound} (6.11) :

$$T_{sing}(\rho,\upsilon) = \frac{1}{\nu_\rho(0,0)} \ln\left(\frac{-\upsilon\nu(\rho,0)}{\rho\theta_w\nu_\rho(0,0)}\right) - \int_0^{\rho} \left(\frac{1}{\nu(\bar{\rho},0)} - \frac{1}{\nu_\rho(0,0)\bar{\rho}}\right) d\bar{\rho} + \int_0^{\theta_w} \left(\frac{1}{r(\theta,0)} - \frac{1}{r_\theta(0,0)\theta}\right) d\theta \tag{6.15b}$$

The coordinate $\theta>0$ is taken along the streamline leading away from the stagnation point, $r(\theta,0)$ is the velocity along this streamline, and θ_w is the distance of the stagnation point to the well along this streamline (see fig. 7).

The first term in the expansion for the mean arrival time (6.4b) has to satisfy

$$\begin{cases} \nu(\rho,0)\dfrac{\partial \bar{T}_{1,b}^{(1)}}{\partial \rho} + w_\upsilon(\rho,0)\eta\dfrac{\partial \bar{T}_{1,b}^{(1)}}{\partial \eta} - f_T(\rho,0)\nu(\rho,0)\dfrac{\partial^2 \bar{T}_{1,b}^{(1)}}{\partial \eta^2} = -u_{1,b} , \\ \bar{T}_{1,b}^{(1)} \to 0 \quad \text{for } \eta \to \infty , \\ \bar{T}_{1,b}^{(1)} \sim T_{sing} \quad \text{for } \eta << -1 . \end{cases} \tag{6.16}$$

With the symbol '$\sim$' we mean that $\bar{T}_{1,b}^{(1)}$ matches T_{sing} if η becomes more and more negative. The solution of (6.16) is a special case of a solution derived in van Kooten (1994):

$$\bar{T}_{1,b}^{(1)}(\rho,\upsilon) = \frac{1}{\sqrt{2\pi}} \int_{\eta q(\rho)}^{\infty} T_{sing}\left(\rho,\upsilon - \frac{t\sqrt{\alpha_T}}{q(\rho)}\right) e^{-\frac{1}{2}t^2} dt . \tag{6.17}$$

The first term in the expansion for the second moment of the arrival time (6.4c) is the solution of

$$\begin{cases} \nu(\rho,0)\dfrac{\partial \bar{T}^{(2)}_{1,b}}{\partial \rho} + w_v(\rho,0)\eta\dfrac{\partial \bar{T}^{(2)}_{1,b}}{\partial \eta} - f_T(\rho,0)\nu(\rho,0)\dfrac{\partial^2 \bar{T}^{(2)}_{1,b}}{\partial \eta^2} = -2\bar{T}^{(1)}_{1,b}\,, \\ \bar{T}^{(2)}_{1,b} \to 0 \quad \text{for } \eta \to \infty\,, \\ \bar{T}^{(2)}_{1,b} \sim T^2_{sing} \quad \text{for } \eta << -1\,. \end{cases} \tag{6.18}$$

Problem (6.18) can be solved with the same technique as problem (6.16). For a detailed description of this technique we refer to van Herwaarden (1994) or van Kooten (1994). The result is:

$$\bar{T}^{(2)}_{1,b}(\rho,\upsilon) = \frac{1}{\sqrt{2\pi}} \int_{\eta_0(\rho)}^{\infty} T^2_{sing}(\rho,\upsilon - \frac{t\sqrt{\alpha_T}}{q(\rho)})\, e^{-\frac{1}{2}t^2} dt\,. \tag{6.19}$$

6.3.2 Boundary layer approximations with the effect of longitudinal dispersion

The boundary layer terms $u_{1,b}$ (6.13), $\bar{T}^{(1)}_{1,b}$ (6.17) and $\bar{T}^{(2)}_{1,b}$ (6.19) only take into account the effect of transversal dispersion. The effect of longitudinal is accounted for by the terms $u_{2,b}$, $\bar{T}^{(1)}_{2,b}$ and $\bar{T}^{(2)}_{2,b}$ (see 6.4). Unfortunately, we have not succeeded in solving these terms from the boundary value problem (4.2), (4.3) and (4.5), where the backward Kolmogorov operator is given by (6.11). In this section we describe an alternative method to account for longitudinal dispersion in the boundary layer.

Longitudinal dispersion will mainly influence the shape of a contaminant plume: the plume will be stretched in time. The effect on the centre of mass of the plume will be much smaller. We therefore expect that in many cases the approximations for the probability and mean time of entering the well that do not take into account longitudinal dispersion will be quite good. This may also be concluded from simulation results presented in Van Herwaarden (1994) and Van Kooten (1994). However, longitudinal dispersion will have an important effect on the variance of the arrival time. In the remainder of this section we will mainly focus on the derivation of a boundary layer approximation for the variance of the arrival time which takes into account both the effect of longitudinal and transversal dispersion.

Note that the terms $u_{1,b}$ (6.13), $\bar{T}^{(1)}_{1,b}$ (6.17) and $\bar{T}^{(2)}_{1,b}$ (6.19) have the same structure. In order to clarify this structure, we rewrite $\bar{T}^{(1)}_{1,b}$ by substituting $\tilde{\upsilon} = \upsilon - \dfrac{t\sqrt{\alpha_T}}{q(\rho)}$:

$$\bar{T}^{(1)}_{1,b} = \frac{q(\rho)}{\sqrt{2\pi\alpha_T}} \int_{-\infty}^{0} T_{sing}(\rho,\tilde{\upsilon}) \exp\{\frac{-(\upsilon - \tilde{\upsilon})^2 q^2(\rho)}{2\alpha_T}\}\, d\tilde{\upsilon}\,. \tag{6.20}$$

The function

$$\frac{q(\rho)}{\sqrt{2\pi\alpha_T}} \exp\{\frac{-(\upsilon - \tilde{\upsilon})^2 q^2(\rho)}{2\alpha_T}\} \tag{6.21}$$

may be interpreted as the probability density function of a stochastic variable $\tilde{\upsilon}$, which

has a $N(\upsilon, \alpha_T/q^2(\rho))$ distribution. Due to transversal dispersion a particle that is released at distance υ from a separating streamline may jump to streamlines at distance $\tilde{\upsilon}$ from the separating streamline (see fig. 8). The most likely path of a particle is the streamline at which the particle is released. If the ρ-coordinate of a starting point increases, the probability of jumping to streamlines further away from the streamline on which the starting point lies, increases too. This phenomenon is understood from the fact that if ρ increases $q(\rho)$ (6.14) decreases so that the variance $\alpha_T/q^2(\rho)$ increases. So, if ρ increases the probability distribution becomes wider. The probability that a particle enters the well equals the probability that a particle follows a streamline at distance $\tilde{\upsilon}<0$ from the separating streamline, i.e. a streamline inside the catchment area (see fig. 8). The boundary layer approximation for the first moment of the arrival at the well (6.20) is the mean of the advective travelling time along all streamlines to which a particle may jump, as far as these streamlines end in the well. The approximation for the second moment of the arrival time (6.19) can be interpreted similarly.

Based on this interpretation we may improve the approximations for the first and second moment of the arrival time $\overline{T}^{(1)}_{1,b}$ (6.17) and $\overline{T}^{(2)}_{1,b}$ (6.19) with terms that account for the effect of longitudinal dispersion. In section 6.2 such terms have already been derived for the case in which transversal dispersion may be neglected. If $a_T = 0$ a "one-dimensional" dispersion process along a streamline of the advective flow remains. Comparison of (6.6) with (6.17) and (6.19) shows that the boundary layer approximations for the first and second moment of the arrival time are obtained by taking means of the first terms of the expansions that belong to these "one-dimensional" processes along the streamlines that end in the well. The idea is to do the same for the second terms, which account for the longitudinal dispersion. For that purpose the expansions $T^{(1)}_{\text{catch}}$ (6.6a) and $T^{(2)}_{\text{catch}}$ (6.6b) have to be expressed in (ρ,υ)-coordinates. Near a separating streamline, i.e. for $-1<<\upsilon<0$, we have

$$T^{(1)}_{\text{catch}} \sim T^{(1)}_{\text{sep}} \quad \text{and} \quad T^{(2)}_{\text{catch}} \sim T^{(2)}_{\text{sep}}, \tag{6.22}$$

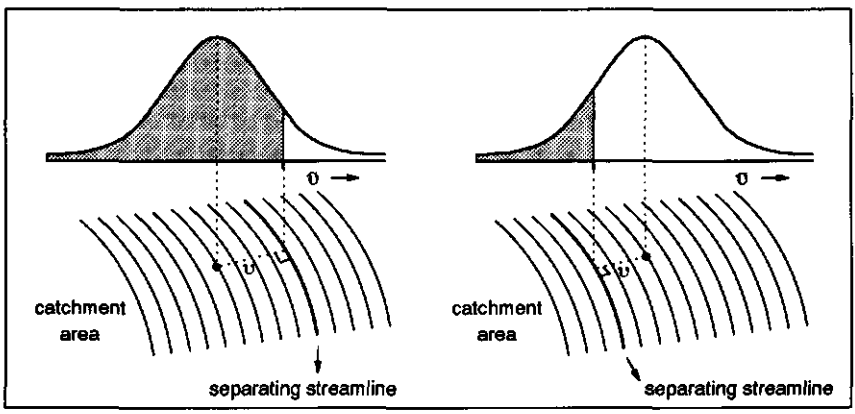

Figure 8. Examples of probability density functions for jumping to neighbouring streamlines for particles that were released inside ($\upsilon<0$, fig. a) and outside ($\upsilon>0$, fig. b) the catchment area. The probability of entering the well equals the area below the graph as far as it lies inside the catchment area.

where

$$T^{(1)}_{sep}(\rho,\upsilon) = T_{sing}(\rho,\upsilon) + \alpha_L \frac{f_L(\rho,0)}{|\nu(\rho,0)|} ,$$

$$T^{(2)}_{sep}(\rho,\upsilon) = T^2_{sing}(\rho,\upsilon) + 2\alpha_L \left(\frac{f_L(\rho,0)}{|\nu(\rho,0)|} T_{sing}(\rho,\upsilon) + I_{sing}(\rho,\upsilon)\right) , \tag{6.23}$$

with

$$I_{sing}(\rho,\upsilon) = \int_0^{\rho} \left(\frac{f_L(\bar{\rho},0)}{(\nu^4(\bar{\rho},0)+c^2\nu_\rho^2(\bar{\rho},0))^{1/2}} - \frac{f_L(0,0)}{(\nu_\rho^4(0,0)\bar{\rho}^4+c^2\nu_\rho^2(0,0))^{1/2}}\right) d\bar{\rho} + \tag{6.24}$$

$$\int_0^{\theta_w} \left(\frac{f_L(\theta,0)}{(r^4(\theta,0)+c^2 r_\theta^2(\theta,0))^{1/2}} - \frac{f_L(0,0)}{(r_\theta^4(0,0)\theta^4+c^2 r_\theta^2(0,0))^{1/2}}\right) d\theta + \int_{c/\theta_w}^{\rho} \frac{f_L(0,0)}{(\nu_\rho^4(0,0)\bar{\rho}^4+c^2\nu_\rho^2(0,0))^{1/2}} d\bar{\rho},$$

where $c = \upsilon\nu(\rho,0)$ and where θ, $r(\theta,0)$ and θ_w are again as indicated in figure 7, I_{sing} is the integral of $f_L/|\nu|^2$ along a characteristic of the operator L_{bound} (Appendix B).

In analogy to (6.17) and (6.19) we expect that the boundary layer approximations for $\bar{T}^{(1)}$ and $\bar{T}^{(2)}$ are given by:

$$\bar{T}^{(1)}_{bound}(\rho,\upsilon) = \frac{1}{\sqrt{2\pi}} \int_{\eta q(\rho)}^{\infty} T^{(1)}_{sep}(\rho,\upsilon - \frac{t\sqrt{\alpha_T}}{q(\rho)}) e^{-\frac{1}{2}t^2} dt$$

$$= \bar{T}^{(1)}_{1,b} + \alpha_L \frac{f_L(\rho,0)}{|\nu(\rho,0)|} u_{1,b} , \tag{6.25}$$

$$\bar{T}^{(2)}_{bound}(\rho,\upsilon) = \frac{1}{\sqrt{2\pi}} \int_{\eta q(\rho)}^{\infty} T^{(2)}_{sep}(\rho,\upsilon - \frac{t\sqrt{\alpha_T}}{q(\rho)}) e^{-\frac{1}{2}t^2} dt$$

$$= \bar{T}^{(2)}_{1,b} + 2\alpha_L \left(\frac{f_L(\rho,0)}{|\nu(\rho,0)|} \bar{T}^{(1)}_{1,b} + \frac{1}{\sqrt{2\pi}} \int_{\eta q(\rho)}^{\infty} I_{sing}(\rho,\upsilon - \frac{t\sqrt{\alpha_T}}{q(\rho)}) e^{-\frac{1}{2}t^2} dt\right) , \tag{6.26}$$

It can be shown that outside the boundary layer these approximations match the outer expansions, i.e.

$$\bar{T}^{(1)}_{bound} \to 0 \quad \text{and} \quad \bar{T}^{(2)}_{bound} \to 0 \quad \text{for } \eta \to \infty ,$$

$$\bar{T}^{(1)}_{bound} \sim T^{(1)}_{sep} \quad \text{and} \quad \bar{T}^{(2)}_{bound} \sim T^{(2)}_{sep} \quad \text{for } \eta << -1 . \tag{6.27}$$

Thus, boundary layer approximations for the (conditional) first and second moment of the arrival time which take into account the effect of both transversal and longitudinal dispersion are

$$T^{(1)}_{\text{bound}} = \frac{\bar{T}^{(1)}_{\text{bound}}}{u_{1,b}} \quad \text{and} \quad T^{(2)}_{\text{bound}} = \frac{\bar{T}^{(2)}_{\text{bound}}}{u_{1,b}}. \tag{6.28}$$

As approximation for the variance of the arrival time we find

$$\begin{aligned}\sigma^2_{\text{bound}} &= T^{(2)}_{\text{bound}} - \left(T^{(1)}_{\text{bound}}\right)^2 \\ &= \frac{\bar{T}^{(2)}_{1,b}}{u_{1,b}} - \left(\frac{\bar{T}^{(1)}_{1,b}}{u_{1,b}}\right)^2 + \frac{2\alpha_L}{u_{1,b}\sqrt{2\pi}} \int_{\eta\sqrt{q(\rho)}}^{\infty} I_{\text{sing}}\left(\rho, \upsilon - \frac{t\sqrt{\alpha_T}}{q(\rho)}\right) e^{-\frac{1}{2}t^2} dt \quad .\end{aligned} \tag{6.29}$$

From (6.23) and (6.27) it follows that outside the boundary layer

$$\sigma^2_{\text{bound}} \sim \sigma^2_{\text{sep}}, \tag{6.30a}$$

where

$$\sigma^2_{\text{sep}} = 2\alpha_L I_{\text{sing}}. \tag{6.30b}$$

Finally, we emphasize that the boundary layer approximations $u_{1,b}$ (6.13), $T^{(1)}_{\text{bound}}, T^{(2)}_{\text{bound}}$ (6.28) and σ^2_{bound} (6.29) are build up from functions that only use the velocity and dispersivities along a separating streamline.

6.4 Composite approximations

In section 6.2 we have derived approximations for the mean and variance of the arrival time, which are only valid far inside the catchment area. The approximations we have derived in section 6.3 are only valid inside a boundary layer along a separating streamline. As a final step we construct approximations which are valid in the entire region in which contaminant transport is studied.

Because $u_{1,b} = 1$ for $\eta << -1$ (i.e. $\upsilon << -\sqrt{\alpha_T}$) and $u_{1,b} = 0$ for $\eta >> 1$ (i.e. $\upsilon >> \sqrt{\alpha_T}$), $u_{1,b}$ may be used as approximation for the probability at which a particle enters the well which is valid in the entire region, both inside and outside the boundary layer.

Composite approximation for the mean and variance of the arrival time can be constructed as follows

$$T^{(1)}_{\text{comp}} = \begin{cases} T^{(1)}_{\text{catch}} - T^{(1)}_{\text{sep}} + T^{(1)}_{\text{bound}} & \text{if } \upsilon < 0 \\ T^{(1)}_{\text{bound}} & \text{if } \upsilon \geq 0 \end{cases} \tag{6.31}$$

and

$$\sigma^2_{\text{comp}} = \begin{cases} \sigma^2_{\text{catch}} - \sigma^2_{\text{sep}} + \sigma^2_{\text{bound}} & \text{if } \upsilon < 0 \\ \sigma^2_{\text{bound}} & \text{if } \upsilon \geq 0 \end{cases} \tag{6.32}$$

Inside the catchment area two situations may occur: outside the boundary layer the 'sep'-terms cancel the 'bound'-terms (see 6.27)), whereas inside the boundary layer the 'sep'-

terms cancel the 'catch'-terms (see (6.22)). Because particles released far outside the catchment area will not reach the well, the boundary layer approximations may be used in the entire region outside the catchment area. The composite approximations are continuous in υ. In the same way a composite approximation for the second moment of the arrival time may constructed.

7. BREAKTHROUGH OF A CONSERVATIVE CONTAMINANT AT A WELL

In section 6 we have derived approximations for the arrival rate and for the mean and variance of the arrival time of particles contaminant at a well. In applications one is not primarily interested in the mean and variance of the arrival time. Often one is mainly interested in breakthrough curves, which describe the arrival time distribution of the contaminant at a well.

7.1 Breakthrough of particles released far inside the catchment area

Far inside the catchment area transversal dispersion is negligible, so that a "one-dimensional" dispersion process along a streamline of the advective flow remains. In section 5 we have shown that the arrival time distribution of particles at the endpoint of a streamline in a uniform flow can be parameterized by the mean and variance of the arrival time. Although the flow velocity along a streamline ending in a well is not uniform, we use this parameterisation to estimate the breakthrough of a contaminant at a well; we expect that the distribution of the arrival time is still approximately of form (5.6), because the spatial variability of the velocity has already been taken into account in the approximations for the mean and variance of the arrival time $T^{(1)}_{catch}$ (6.6a) and σ^2_{catch} (6.9). So, for particles released at a point x far inside the catchment area the probability density function for entering the well at time τ is approximated by

$$g_{catch}(x;\tau) = g(T^{(1)}_{catch}(x),\sigma^2_{catch}(x);\tau), \tag{7.1}$$

where g is defined by (5.6). Consequently, the cumulative breakthrough curve, which gives the fraction of a contaminant which has entered the well before time τ, is approximated by

$$\int_0^{\tau} g_{catch}(x;\bar{\tau})\,d\bar{\tau}. \tag{7.2}$$

7.2 Breakthrough of particles released near a separating streamline

In section 6 we have shown that near a separating streamline the transfer of particles to neighbouring streamlines has an important effect on the probability of arrival and the moments of the arrival time at the well. In a boundary layer near a separating streamline the dispersion process is essentially 2-dimensional. In section 6.3 boundary layer approximations for the first and second moments of the travel time were obtained by taking the means of the first and second moments of the travel time along the streamlines to which a

particle may be transferred by transversal dispersion, as far as these streamlines end in the well (see fig. 8). Here we use this idea in a similar way: for particles released near a separating streamline the distribution of the arrival time at the well is the mean of the arrival time distributions that correspond with the "one-dimensional" processes along the streamlines to which a particle may be transferred by transversal dispersion, as far as these streamlines end in the well, i.e.

$$g_{bound}(\rho,\upsilon;\tau) = \frac{1}{\sqrt{2\pi}} \int_{\eta q(\rho)}^{\infty} g(T^{(1)}_{sep}(\rho,\upsilon - \frac{t\sqrt{\alpha_T}}{q(\rho)}),\ \sigma^2_{sep}(\rho,\upsilon - \frac{t\sqrt{\alpha_T}}{q(\rho)});\tau)\, e^{-\frac{1}{2}t^2} dt. \qquad (7.3)$$

The fraction of the contaminant that will eventually reach the well equals the integral of g_{bound} from $\tau=0$ to $\tau=\infty$. By changing the order of integration it can easily be seen that

$$\int_0^{\infty} g_{bound}(\rho,\upsilon;\bar{\tau})\, d\bar{\tau} = \frac{1}{\sqrt{2\pi}} \int_{\eta q(\rho)}^{\infty} e^{-\frac{1}{2}t^2} dt\ , \qquad (7.4)$$

which is consistent with (6.13). One can also easily check that the conditional mean and variance of the stochastic variable τ with p.d.f. g_{bound} (7.3), are equal to $T^{(1)}_{bound}$ (6.28) and σ^2_{bound} (6.29).

7.3 Composite approximation for the breakthrough curves

The p.d.f. g_{catch} (7.1) is only valid far inside the catchment area, whereas the p.d.f. g_{bound} (7.3) is only valid in a boundary layer near a separating streamline. To connect this two types of approximations to each other we construct a composite p.d.f. which is valid everywhere. This composite p.d.f. g_{comp} has to be constructed in such a way that the (conditional) mean and variance of the arrival time τ are equal to $T^{(1)}_{comp}$ (6.32) and σ^2_{comp} (6.33), respectively, i.e.

$$\int_0^{\infty} \tau\, g_{comp}\, d\tau/u_{1,b} = T^{(1)}_{comp} \qquad \text{and} \qquad \int_0^{\infty} (\tau - T^{(1)}_{comp})^2 g_{comp}\, d\tau/u_{1,b} = \sigma^2_{comp}\ . \qquad (7.5b)$$

Using (6.16), (6.23) and (6.25) we obtain that for $\upsilon \geq 0$, $T^{(1)}_{comp}$ (6.32) may be expressed as

$$\begin{aligned} T^{(1)}_{comp} &= \frac{1}{u_{1,b}\sqrt{2\pi}} \int_{\eta q(\rho)}^{\infty} (T^{(1)}_{catch}(x) - T^{(1)}_{sep}(\rho,\upsilon) + T^{(1)}_{sep}(\rho,\upsilon - \frac{t\sqrt{\alpha_T}}{q(\rho)}))e^{-\frac{1}{2}t^2} dt \\ &= \frac{1}{u_{1,b}\sqrt{2\pi}} \int_{\eta q(\rho)}^{\infty} (T^{(1)}_{catch}(x) + \frac{1}{\nu_\rho(0,0)} \ln(1 - \frac{t}{\eta q(\rho)}))e^{-\frac{1}{2}t^2} dt\ . \end{aligned} \qquad (7.6)$$

(Remark that for $\eta(=\upsilon/\sqrt{\alpha_T}) << -1$ the log-term in (7.6) may be neglected, which confirms that $T^{(1)}_{comp} \sim T^{(1)}_{catch}$ if $\eta << -1$). In analogy to expression (7.6) we define

$$g_{comp} = \frac{1}{\sqrt{2\pi}} \int_{\eta q(\rho)}^{\infty} g(\mu,\sigma^2,\tau) e^{-\frac{1}{2}t^2} dt \ , \tag{7.7a}$$

where

$$\mu = \begin{cases} T^{(1)}_{catch}(x) + \dfrac{1}{v_\rho(0,0)} \ln(11 - \dfrac{t}{\eta q(\rho)}) & \text{for } \upsilon<0 \ , \\ T_{sep}(\rho,\upsilon - \dfrac{t\sqrt{\alpha_T}}{q(\rho)}) & \text{for } \upsilon\geq 0 \ , \end{cases} \tag{7.7b}$$

$$\sigma^2 = \begin{cases} \sigma^2_{catch}(x) - \sigma^2_{sep}(\rho,\upsilon) + \sigma^2_{sep}(\rho,\upsilon - \dfrac{t\sqrt{\alpha_T}}{q(\rho)}) & \text{for } \upsilon<0 \ , \\ \sigma^2_{sep}(\rho,\upsilon - \dfrac{t\sqrt{\alpha_T}}{q(\rho)}) & \text{for } \upsilon\geq 0 \ . \end{cases} \tag{7.7c}$$

One can easily check that g_{comp} satisfies the conditions given by (7.5) and that

$$\begin{aligned} g_{comp} &\sim g_{bound} \quad \text{for } \upsilon = O(\sqrt{\alpha_T}) \ , \\ g_{comp} &\sim g_{catch} \quad \text{for } \upsilon/\sqrt{\alpha_T} << -1 \ , \end{aligned} \tag{7.8}$$

i.e. g_{comp} connects the arrival time distributions g_{catch} and g_{bound} to each other. So, g_{comp} may be used as approximation for the distribution of the arrival time at the well for a contaminant that was spilled in any point in the aquifer, both near and far away from a separating streamline.

8. BREAKTHROUGH OF A NON-CONSERVATIVE CONTAMINANT

8.1 Equilibrium adsorption

The arrival of a contaminant subject to linear equilibrium adsorption can be predicted by replacing the velocity v by the retarded velocity $v^R=v/R$ (section 2.1). Expression (2.2) implies that the dispersion tensor automatically transforms into its retarded form. The retardation only affects the arrival time at the well an not the ultimate arrival fraction (see (6.13) and (6.14)). The arrival time distribution is given by g_{comp} (7.7), where μ and σ^2 have to be replaced by their retarded values $\mu^R=\mu/R$ and $(\sigma^R)^2=(\sigma/R)^2$.

Non-linear equilibrium phenonema can not be taken into account. If the concentration c occurs non-linearly in the ADE the formal adjoint of the operator M_λ (3.1) does not exist, so that the boundary value problems for (4.2), (4.4) and (4.5) for the rate and time at which particle exit a region can not be derived.

8.2 First order decay

From (3.2) it follows that the probability density function for the arrival time τ for a particle of a linearly decaying contaminant that has been released in the point x equals

$$g_{comp}(x;\tau)e^{-\lambda\tau}. \tag{8.1}$$

In (8.1) $g_{comp}(x;\tau)$ is the p.d.f. for arrival at the well at time τ and $e^{-\lambda\tau}$ is the probability that a particle has not been "killed" before time τ. The breakthrough curve of the decaying contaminant is described by

$$\int_0^{\tau} g_{comp}(x;\bar{\tau})e^{-\lambda\bar{\tau}}d\bar{\tau}. \tag{8.2}$$

The fraction $u(x)$ of the particles contaminant that will reach the well can be computed from (8.2) by letting $\tau \to \infty$. In applications one may also be interested in the conditional mean of the arrival time which is given by

$$T^{(1)}(x) = \int_0^{\infty} \frac{\bar{\tau}\, g_{comp}(x;\bar{\tau})e^{-\lambda\bar{\tau}}d\bar{\tau}}{u(x)}. \tag{8.3}$$

The fraction u and the mean arrival time $T^{(1)}$ may also be obtained from the boundary value problems (4.2) and (4.4) (with $\lambda \neq 0$). These boundary value problems again can be solved with the asymptotic method described in section 6. Here, we do not work out this method in detail, because the asymptotic approximations for u and $T^{(1)}$ become rather complicated. Moreover, there is no need to know u and $T^{(1)}$ as accurately as possible, because the most important information concerning the arrival at the well is already contained in the arrival time distribution (8.1). Therefore, here we only give approximations for u and $T^{(1)}$ which do not take into account longitudinal dispersion.

Due to decay not all particles will reach the well, not even if they are released far inside the catchment area. When the effects of longitudinal and transversal dispersion are neglected, approximations for the probability and mean time at which a particle reaches the well are given by

$$u_{1,c}(x) = e^{-\lambda T_{adv}(x)}, \tag{8.4}$$

$$T^{(1)}_{1,c}(x) = T_{adv}(x). \tag{8.5}$$

Thus $u_{1,c}$ equals the probability that a particle has not been killed at time T_{adv}.

Along a separating streamline we again have a boundary layer in which transversal dispersion plays an important role. In van Kooten (1994) we have shown that boundary layer approximations for u and $T^{(1)}$ are

$$u_{1,b}(\rho,\upsilon) = \frac{1}{\sqrt{2\pi}} \int_{\eta q(\rho)}^{\infty} u_{sing}\left(\rho,\upsilon - \frac{t\sqrt{\alpha_T}}{q(\rho)}\right)e^{-\frac{1}{2}t^2}dt, \tag{8.6}$$

$$T^{(1)}_{1,b}(\rho,\upsilon) = \frac{\bar{T}^{(1)}_{1,b}(\rho,\upsilon)}{u_{1,b}(\rho,\upsilon)}, \tag{8.7}$$

with

$$u_{sing}(\rho,\upsilon) = e^{-\lambda T_{sing}(\rho,\upsilon)} , \tag{8.8}$$

$$\bar{T}^{(1)}_{1,b}(\rho,\upsilon) = \frac{1}{\sqrt{2\pi}} \int_{\eta_0(\rho)}^{\infty} T_{sing}(\rho,\upsilon - \frac{t\sqrt{\alpha_T}}{q(\rho)}) u_{sing}(\rho,\upsilon - \frac{t\sqrt{\alpha_T}}{q(\rho)}) e^{-\frac{1}{2}t^2} dt . \tag{8.9}$$

where T_{sing} again is given by (6.15). Note that for $\lambda = 0$, $u_{1,b}$ (8.6) and $\bar{T}_{1,b}$ (8.7) are identical to the expressions (6.13) and (6.17). In fact (6.13) and (6.17) are special cases of (8.6) and (8.7). The boundary layer approximation $u_{1,b}$ (8.6) can be interpreted as the mean of the probability of reaching the well along all streamlines to which a particle may be transferred by transversal dispersion, as far as these streamlines end in the well. $\bar{T}^{(1)}_{1,b}$ may be interpreted similarly.

Composite approximations for the rate and mean time of arrival which are valid both inside and outside the boundary layer are

$$u_{comp} = \begin{cases} u_{1,c} - u_{sing} + u_{1,b} & \text{for } \upsilon<0 \\ u_{1,b} & \text{for } \upsilon\geq 0 , \end{cases} \tag{8.10}$$

$$T^{(1)}_{1,comp} = \begin{cases} T_{adv} - T_{sing} + T^{(1)}_{1,b} & \text{for } \upsilon<0 \\ T_{1,b} & \text{for } \upsilon\geq 0 . \end{cases} \tag{8.11}$$

Note that for $\lambda = 0$, u_{comp} equals $u_{1,b}$ for both $\upsilon<0$ and $\upsilon\geq 0$ (see also section 6.4) and $T^{(1)}_{1,comp}$ is equal to the $O(1)$ terms in $T^{(1)}_{comp}$ (6.31). From simulation results in van Kooten (1994) it may be concluded that in many cases the approximations u_{comp} and $T^{(1)}_{1,comp}$ will be quite satisfactory.

9. EXAMPLE: CONTAMINATION OF A WELL IN A UNIFORM BACKGROUND FLOW

As an example we show how the asymptotic approximations for the arrival rate and for the mean and variance of the arrival time as well as for the breakthrough curves may be applied to a well in a uniform background flow. We assume that the background flow is parallel to the x-axis and that the well is situated in (0,0). The complex potential for the flow field is

$$\omega(z) = z - \ln(z) , \qquad z = x + iy. \tag{9.1}$$

The corresponding velocity field is given by

$$v_1(x,y) = 1 - \frac{x}{x^2 + y^2} , \quad v_2(x,y) = \frac{-y}{x^2 + y^2} . \tag{9.2}$$

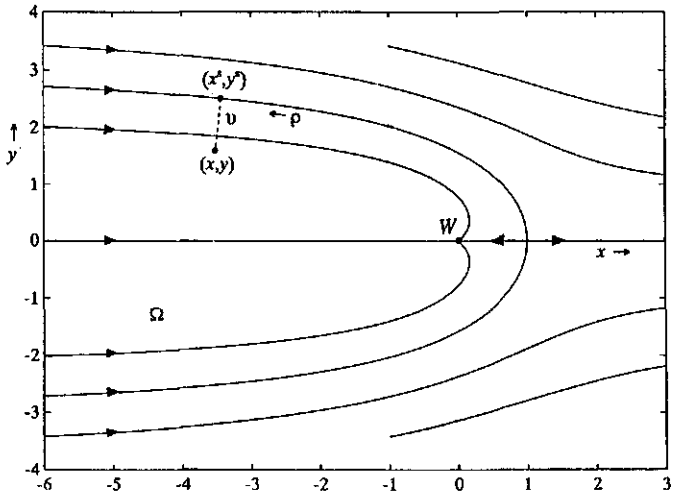

Figure 9 Stream pattern for a well in a uniform background flow

Along a streamline the streamfunction $\psi = \mathrm{Im}(\omega)$ is constant, so that the streamlines are described by

$$x = y/\tan(y-\psi) \ . \tag{9.3}$$

For $\psi = 0$ (9.3) describes the separating streamlines which end in the stagnation point (1,0). The advective travelling time to the well from a point inside the catchment area is

$$T_{adv}(x,y) = \ln(\frac{y}{\sin y}) - \ln(\frac{y}{\tan y} - x) - x \ , \tag{9.4}$$

see van der Hoek (1992). From (6.6a) we obtain as approximation for the mean arrival time of a conservative contaminant released far inside the catchment area

$$T^{(1)}_{catch}(x,y) = T_{adv}(x,y) + a_L(x,y)\frac{x^2 + y^2}{(x-1)^2 + y^2} \ . \tag{9.5}$$

The variance of the arrival time σ^2_{catch} can be computed numerically from (6.7) and (6.8).

In order to predict the arrival of a contaminant that is released near a separating streamline we first have to carry out some preliminary coordinate transformations. The (ρ,υ)-coordinates of a point (x,y) near a separating streamline are given by

$$\rho = \int_0^{y^s} w(y)dy \ , \quad \upsilon = \sqrt{(x-x^s)^2 + (y-y^s)^2} \ , \tag{9.6a}$$

with

$$w(y) = \left\{1 + (\frac{1}{\tan y} - \frac{y}{\sin^2 y})^2\right\}^{\frac{1}{2}} \tag{9.6b}$$

and where (x^s, y^s) is a point on the separating streamline so that the vector $(x-x^s, y-y^s)^T$ is perpendicular to the separating streamline (figure 9).

The flow velocity $v(\rho,0)$ along the separating streamline is

$$v(\rho,0) = -\sin(y^s)\sqrt{1 + (\frac{1}{\tan y^s} - \frac{1}{y^s})^2} \quad . \tag{9.7}$$

Furthermore, $\theta = 1 - x$ is a coordinate along the separating streamline leading from the stagnation point to the well. The velocity $r(\theta,0)$ along this streamline is given by

$$r(\theta,0) = \frac{\theta}{1 - \theta} . \tag{9.9}$$

From (6.16) we obtain that near a separating streamline the advective travelling time to the well may be expressed as

$$T_{sing}(\rho,\upsilon) = -\ln(-\upsilon) - \frac{1}{2}\ln(1 + (\frac{1}{\tan y^s} - \frac{1}{y^s})^2) - x^s . \tag{9.10}$$

With the above information one can compute the boundary layer and composite approximations for the arrival of a contaminant at the well which we have derived in sections 6, 7 and 8.

We have tested the accuracy of the asymptotic approximations by comparing them with results of random walk simulation. The stochastic motion of particles is described by the stochastic differential equation (3.4). In discretised form in two dimensions it reads:

$$\begin{aligned} \Delta X &= (v_1 + \frac{\partial}{\partial x}D_{11} + \frac{\partial}{\partial y}D_{12})\Delta t + \sqrt{2a_L|v|}\frac{v_1}{|v|}Z_L\sqrt{\Delta t} + \sqrt{2a_T|v|}\frac{v_2}{|v|}Z_T\sqrt{\Delta t} \quad , \\ \Delta Y &= (v_2 + \frac{\partial}{\partial x}D_{21} + \frac{\partial}{\partial y}D_{22})\Delta t + \sqrt{2a_L|v|}\frac{v_2}{|v|}Z_L\sqrt{\Delta t} - \sqrt{2a_T|v|}\frac{v_1}{|v|}Z_T\sqrt{\Delta t} \quad , \end{aligned} \tag{9.11}$$

where Z_L and Z_T are random deviates from a uniform distribution with mean 0 and variance 1 (see also Kinzelbach, 1988). On the separating streamline we took the point D with coordinates $(\rho,\upsilon) = (5.445, 0)$, corresponding with $(x,y) = (-3.347, 2.50)$. From several points on a line through D perpendicular to the separating streamline we carried out random walk simulations. From the points inside the catchment area ($\upsilon \le 0$) 15.000 particles were released. From the points outside the catchment area ($\upsilon > 0$) 30.000 particles were released. In these simulations the dispersivities were taken constant: a_L=0.01 and a_T=0.001. In fig. 10 arrival rates and means and deviations of arrival times obtained from simulations with a conservative contaminant are compared with the asymptotic approximations $u_{1,b}$ (6.13), $T^{(1)}_{comp}$ (6.31) and σ_{comp} (6.32), respectively. Some arrival time distributions and breakthrough curves as obtained from the simulations and as computed from (7.7) are displayed in fig. 11. From the figures we may conclude that the approximations are surprisingly accurate for this example. The figures confirm the boundary layer behaviour of the contaminant transport: near a separating streamline the small transversal dispersivity has a large impact on the arrival of a contaminant at the well, whereas far away from a separating streamline its effect may be neglected. Because particles released at the separating streamline pass the stagnation point very closely, in fig. 11e a kind of "tailing" can be observed.

To check the accuracy of the asymptotic approximations for the arrival of a linearly decaying contaminant, we also carried out random walk simulations in which particles were "killed" at exponentially distributed times (see section 3). The decay coefficient λ was taken 0.1. In figure 12 we compare a simulated arrival time distribution and breakthrough curve with the asymptotic approximations (8.1) and (8.2). In fig. 12b the asymptotic approximation for the arrival rate (8.4) is indicated, too. Again we observe a good resemblance between simulation results and asymptotic approximations.

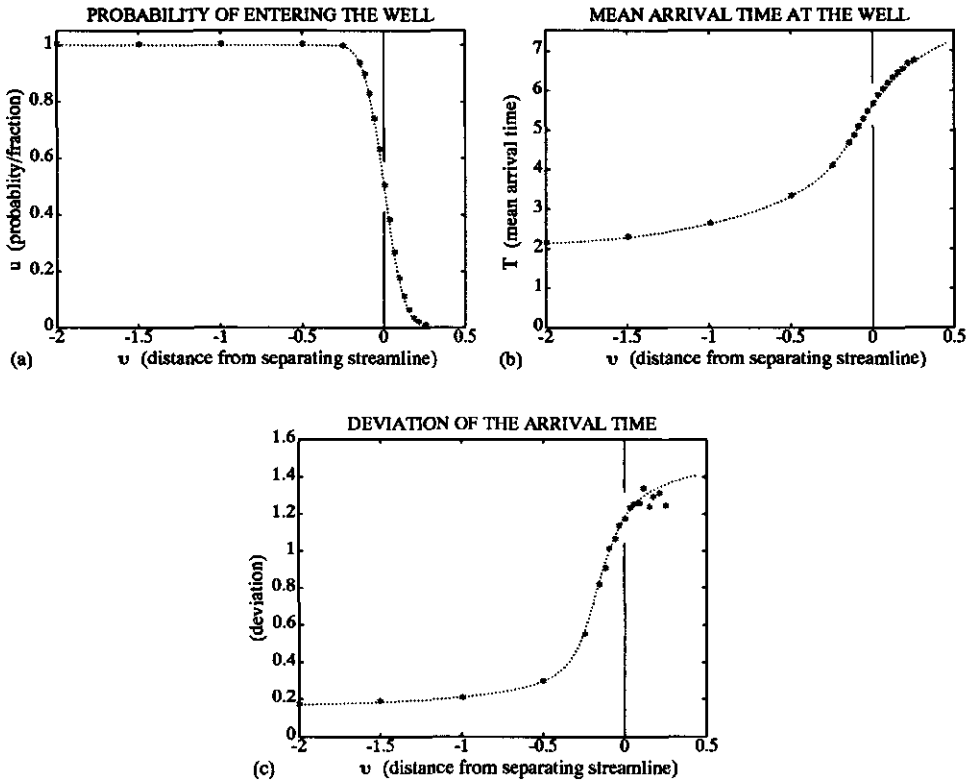

Figure 10 Simulation results (*) for particles of a conservative contaminant released in points (ρ,υ) with ρ = 5.445 and υ between −2.0 and 0.5. In fig. 10a the fraction of the particles that entered the well is compared with the asymptotic approximation (6.13). In fig. 10b the mean arrival time of the particles is compared with the asymptotic approximation (6.31). In fig. 10c deviation, i.e. the square root of the variance, of the arrival time is compared with the asymptotic approximation (6.32).

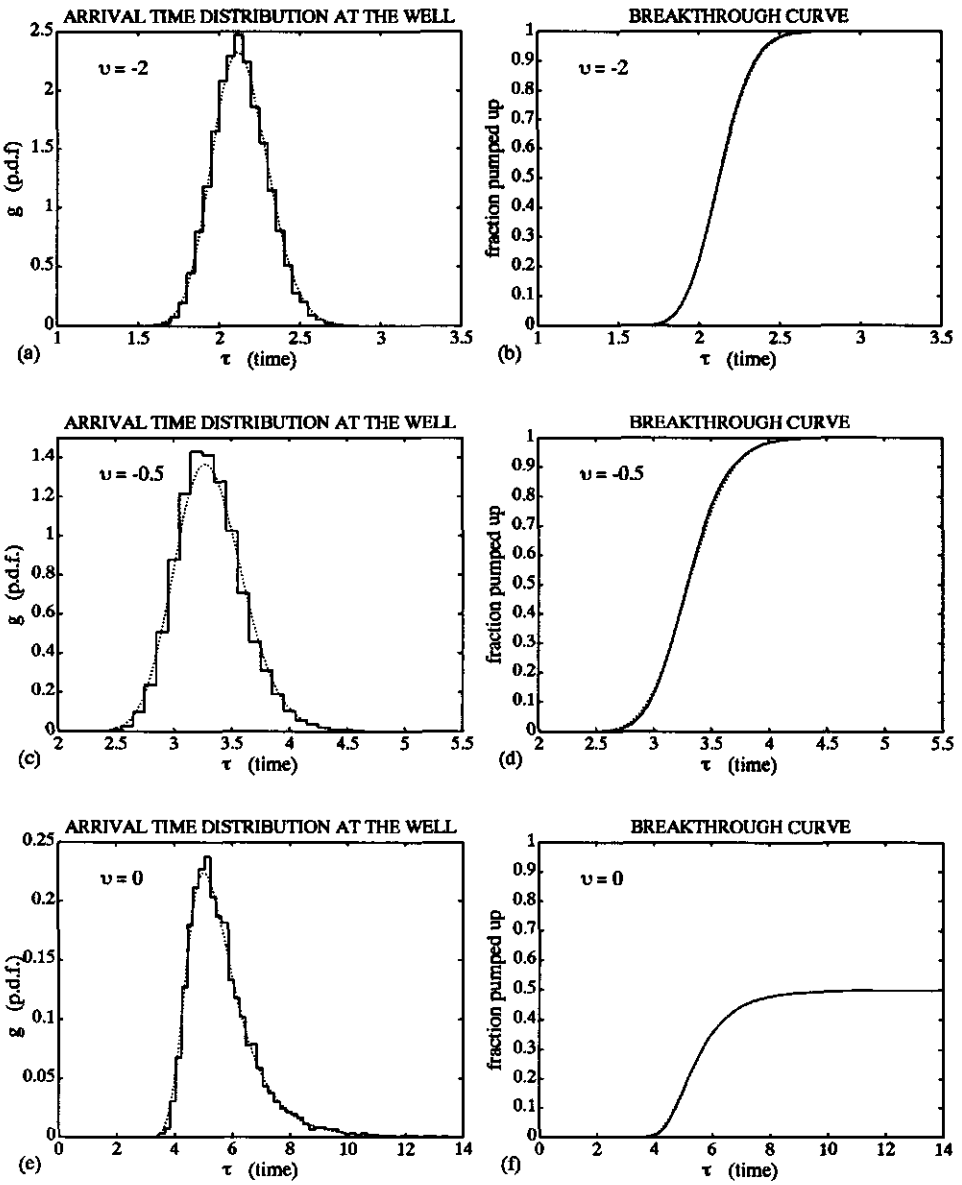

Figure 11 Arrival time distributions and breakthrough curves for particles of a conservative contaminant released in the points (ρ,υ) with ρ=5.445 and υ=−2.0 (fig. a,b), υ = -0.5 (fig. c,d) and υ=0 (fig. e,f). The solid lines in fig. a, c and e denote the arrival time distributions obtained from random walk simulations. The dotted lines denote the asymptotic approximations for the arrival time distributions computed from (7.7). The breakthrough curves are obtained by integration of the corresponding arrival time distributions.

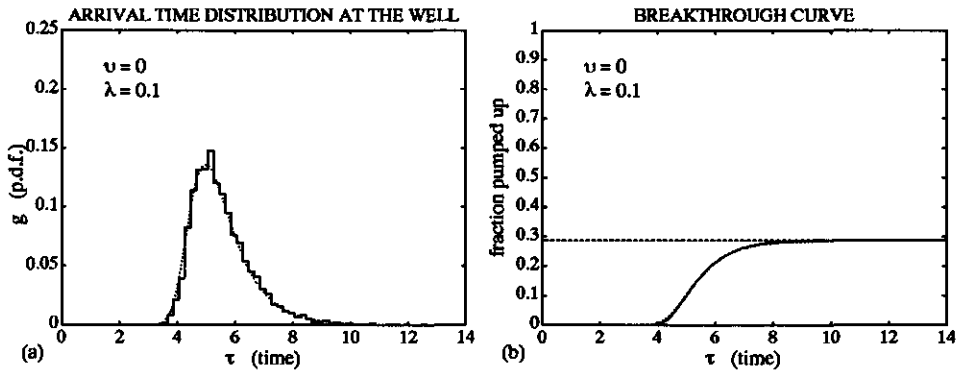

Figure 12 Arrival time distribution (fig. a) and breakthrough curve (fig. b) for a linearly decaying contaminant (λ=0.1) released in the point D (ρ,υ) = (5.554,0) on the separating streamline. The solid lines denote random walk results. The dotted lines denote the asymptotic approximations (8.1) (fig. a) and (8.2) (fig. b). The dashed line in fig. b denotes the approximation for the arrival rate (8.11).

10. IMPLEMENTATION OF THE METHOD

The method described in this paper has been implemented in the software package ECOWELL (Buse & van Kooten, 1995). ECOWELL must be used in connection with a finite difference or finite element code for the simulation of groundwater flow. With such code a numerical hydraulic head field can be generated for an aquifer in which one or more wells are operating. Together with the corresponding discretization, the conductivity and the porosity, this head field serves as input for our computer program. Using Darcy's law the program computes a velocity field.

First, the program searches for the stagnation points in the flow. The separating streamlines are determined by backward tracking with a Runga-Kutta method. Next, from any point in the domain the arrival of a contaminant at a certain well can be predicted. The approximations $T^{(1)}_{catch}$ (6.6a) and σ^2_{catch} (6.8) that only take into account longitudinal dispersion are computed with particle tracking. To incorporate the effect of transversal dispersion the program determines the (ρ,υ)-coordinates of a point with respect to each relevant separating streamline. The boundary layer approximations for the arrival rate and for the mean and variance of the arrival time only depend on the velocity and the dispersivities along a separating streamline. The expressions for $u_{\perp,b}$ (6.13), $T^{(1)}_{bound}$ (6.28) and σ^2_{bound} (6.29) can be evaluated with numerical integration. The arrival time distribution can be determined accordingly.

CONCLUDING REMARKS

To control groundwater quality in pumping wells it is not sufficient to model contaminant transport by advection only. Even when advection is the dominating transport mechanism, longitudinal and transversal dispersion may have an important effect on the arrival of a contaminant at a well. In this study we present a method to predict the advective-dispersive transport of a contaminant to a well in a confined aquifer. We allow the dispersion to be a non-linear function of the velocity. Using perturbation techniques we have constructed analytical expressions for the fraction of a contaminant that enters the well, for the mean and variance of the arrival time and for the breakthrough curves. Near the boundary of the catchment area special attention should be paid to transversal dispersion, even when it is very small. The accuracy of the asymptotic approximations increases when the ratio between advection and dispersion increases. As an example we considered the special case of a well in a uniform background flow. The approximations were shown to be in good agreement with the results of random walk simulations.
The asymptotic method has the following features and advantages:

- The method is nearly as accurate as random walk simulation, whereas the costs are much lower: the time needed to compute the asymptotic approximations is of the same order as the time needed to carry out a few random walks. In the example of a well in a uniform background flow it took several hours CPU-time to carry out the random walk simulations, whereas the asymptotic approximations could be computed in a few seconds.
- The advantage of the asymptotic method above solving the advection-dispersion equation numerically is considerable. The latter method is very time and memory consuming and is subject to numerical dispersion, especially at high Peclet numbers, i.e. if the ratio between advection and dispersion is large.
- The method can be applied to any given flow pattern. Once an analytical or numerical flow field is given, the separating streamlines can be determined by particle tracking or from the stream function. Next, the transformation to local coordinates ρ and υ (fig. 7) can be carried out, so that the boundary layer approximations can computed. We note that the coordinate υ may also so be taken along an equipotential line, so that it is perpendicular to both a separating streamline and the neighbouring streamlines.
- The effects of linear equilibrium adsorption and first order decay can be incorporated. In the meantime we have also extended the results for a kinetically adsorbing contaminant (van Kooten, 1995).
- The method can also be used to predict the arrival at a well of a pollution that is distributed over a certain area Ω. Let $c(x)$ be the initial concentration of the pollution, then the breakthrough at the well is described by

  $$\int_{\Omega} c(x) g_{comp}(x;\tau) e^{-\lambda\tau} dx \ ,$$

  where $g_{comp}(x)$ (7.7) the arrival time distribution of a contaminant released in the point x. So, the method may be a useful tool to design aquifer cleanup strategies.

The approximations $T^{(1)}_{catch}(x)$ (6.6a) and $\sigma^2_{catch}(x)$ (6.8) that only take into account longitudinal dispersion, are completely determined by the velocity and dispersivity along the streamline through the injection point x. Therefore, these approximations and the corresponding approximation for the arrival time distribution $g_{catch}(x)$ (7.1) may also be aplied to three dimensionsal flow patterns.

ACKNOWLEDGEMENTS

I am grateful to Johan Grasman and Maarten de Gee for the stimulating discussions and the valuable suggestions concerning the subject treated in this paper. I also thank Pieter Raats for reading the text critically. The work was funded by NWO (Nederlandse Organisatie voor Wetenschappelijk Onderzoek/Dutch Organisation for Scientific Research).

Appendix A: The backward Kolmogorov equation in (x_1,x_2) and (ρ,υ)-coordinates

Using that the flow is divergence and rotational free we obtain that in two dimenstions the backward Kolmogorov equation (4.1) can be written as:

$$L_{\text{catch}} = v_1\frac{\partial^*}{\partial x_1} + v_2\frac{\partial^*}{\partial x_2} + \alpha_L(v_1\frac{\partial}{\partial x_1} + v_2\frac{\partial}{\partial x_2})(\frac{f_L}{|v|}[v_1\frac{\partial^*}{\partial x_1} + v_2\frac{\partial^*}{\partial x_2}]\,) \\ \alpha_T(v_2\frac{\partial}{\partial x_1} - v_1\frac{\partial}{\partial x_2})(\frac{f_T}{|v|}[v_2\frac{\partial^*}{\partial x_1} - v_1\frac{\partial^*}{\partial x_2}]\,). \qquad \text{(A1)}$$

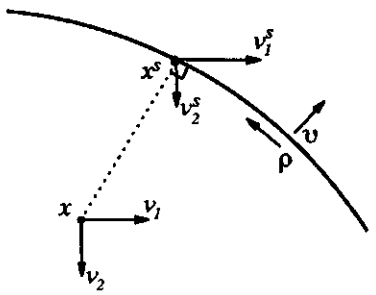

Figure 13 Orhogonal projection of x at a separating streamline.

Let $x^s=(x_1^s,x_2^s)$ be the orthogonal projection of $x=(x_1,x_2)$ at a separating streamline. The velocity vector in x^s we denote by $v^s=(v_1^s,v_2^s)^T$ (fig. 13). The derivatives of the coordinates ρ and υ with respect to x_1 and x_2 are

$$\frac{\partial\rho}{\partial x_1} = -\frac{v_1^s}{|v^s|}, \qquad \frac{\partial\rho}{\partial x_2} = -\frac{v_2^s}{|v^s|}, \\ \frac{\partial\upsilon}{\partial x_1} = \frac{v_2^s}{|v^s|}, \qquad \frac{\partial\upsilon}{\partial x_2} = -\frac{v_1^s}{|v^s|}. \qquad \text{(A2)}$$

Furthermore, the velocities $v(\rho,\upsilon)$ and $w(\rho,\upsilon)$ can be expressed as

$$v(\rho,\upsilon) = \frac{\langle v,-v^s\rangle}{|v^s|} = -\frac{v_1v_1^s + v_2v_2^s}{|v^s|}, \\ w(\rho,\upsilon) = \frac{\langle v,(v^s)^\perp\rangle}{|v^s|} = \frac{v_1v_2^s - v_2v_1^s}{|v^s|}, \qquad \text{(A3)}$$

where $\langle\cdot,\cdot\rangle$ denotes an inner-produkt of two vectors. Using (A2) and (A3) we obtain that the operator (A1) in (ρ,υ)-coordinates reads

$$L_{catch} = v(\rho,\upsilon)\frac{\partial^*}{\partial\rho} + w(\rho,\upsilon)\frac{\partial^*}{\partial\upsilon} + \alpha_L\left(v(\rho,\upsilon)\frac{\partial}{\partial\rho} + w(\rho,\upsilon)\frac{\partial}{\partial\upsilon}\right)\left(\frac{f_L}{|v|}\left[v(\rho,\upsilon)\frac{\partial^*}{\partial\rho} + w(\rho,\upsilon)\frac{\partial^*}{\partial\upsilon}\right]\right)$$
$$+ \alpha_T\left(w(\rho,\upsilon)\frac{\partial}{\partial\rho} - v(\rho,\upsilon)\frac{\partial}{\partial\upsilon}\right)\left(\frac{f_T}{|v|}\left[w(\rho,\upsilon)\frac{\partial^*}{\partial\rho} - v(\rho,\upsilon)\frac{\partial^*}{\partial\upsilon}\right]\right). \qquad (A4)$$

To stretch the boundary layer near a separating streamline we have introduced the coordinate $\eta=\upsilon/\sqrt{\alpha_T}$ (6.10). Because

$$\frac{\partial}{\partial\upsilon} = \frac{1}{\sqrt{\alpha_T}}\frac{\partial}{\partial\eta} \quad \text{and} \quad \lim_{\alpha_T\to 0}\frac{w(\rho,\eta\sqrt{\alpha_T})}{\sqrt{\alpha_T}} = \lim_{\alpha_T\to 0}\eta\frac{w(\rho,\eta\sqrt{\alpha_T})}{\eta\sqrt{\alpha_T}} = \eta\, w_\upsilon(\rho,0)\,, \qquad (A5)$$

we arrive for $\alpha_T \to 0$ at expression (6.11).

Appendix B: Derivation of an expression for I in (ρ,υ)-coordinates near a separating streamline

The function I (6.7) is the integral of $f_L/|v|^2$ along a streamline of the advective flow. In mathematical terms I is an integral along a characteristic of the operator L_{catch} (6.5). To obtain an expression for I in (ρ,υ)-coordinates near a separating streamline, we decompose I into three parts (see fig. 14 and fig. 7): I_1 is the contribution to I close along the separating streamline, I_2 is the contribution in an (δ,ε)-neighbourhood of the stagnation point, and I_3 is the contribution to I close along the streamline leading away from the stagnation point.

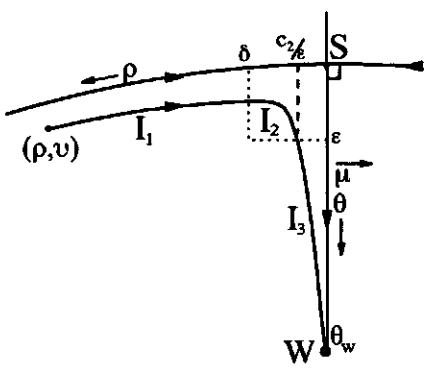

Figure 14 Decomposition of the integral I into the parts I_1, I_2 and I_3 for small υ, δ and ε.

The characteristics of the operator L_{bound} (6.11) are described by $\eta v(\rho,0)$ = constant, or, in (ρ,υ)-coordinates, $\upsilon v(\rho,0) = c_1$ (constant). The product $\upsilon v(\rho,0)$ may be interpreted as the

increment of the streamfunction, which describes the flux between the separating streamline and an adjacent streamline. The integral I_1 along the characteristic $\upsilon\nu(\rho,0) = c_1$ ($\Leftrightarrow$ $\upsilon=c_1/\nu(\rho,0)$) may be expressed as

$$I_1 = \int_0^{\rho} \frac{f_L(\bar{\rho},0)(1+(\partial\upsilon/\partial\rho)^2)^{1/2}}{\nu^2(\bar{\rho},0)+\upsilon^2\nu_\rho^2(\bar{\rho},0)}\,d\bar{\rho} = \int_0^{\rho} \frac{f_L(\bar{\rho},0)}{(\nu^4(\bar{\rho},0) + c_1^2\nu_\rho^2(\bar{\rho},0))^{1/2}}\,d\bar{\rho}\ . \tag{B1}$$

Near a stagnation point $\nu(\rho,0) \sim \nu_\rho(0,0)\rho$, so that near the stagnation point the streamline is described by $\upsilon\rho = c_2$, where $c_2 = c_1/\nu_\rho(0,0)$. It follows that I_2 may be expressed as

$$I_2 = \int_{c_2/\varepsilon}^{\delta} \frac{f_L(0,0)(1+(\partial\upsilon/\partial\rho)^2)^{1/2}}{\nu_\rho^2(0,0)\bar{\rho}^2 + \upsilon^2\nu_\rho^2(0,0)}\,d\bar{\rho} = \int_{c_2/\varepsilon}^{\delta} \frac{f_L(0,0)}{(\nu_\rho^4(0,0)\bar{\rho}^4 + c_1^2\nu_\rho^2(0,0))^{1/2}}\,d\bar{\rho}\ . \tag{B2}$$

Since the flow is rotational free the separating streamlines leading towards and leading away from the stagnation point are perpendicular. Streamlines close to the streamline leading away from the stagnation point are described by $\mu\, r(\theta,0) = c_3$. Because the flow is divergence free $\nu_\rho(0,0) = r_\theta(0,0)$, so that for $c_3 = c_1$ such a streamline connects with the streamline originating in (ρ,υ). For the integral I_3, we find

$$I_3 = \int_{\varepsilon}^{\theta_\infty} \frac{f_L(\theta,0)(1+(\partial\mu/\partial\theta)^2)^{1/2}}{r^2(\theta,0) + \mu^2 r_\theta^2(\theta,0)}\,d\theta = \int_{\varepsilon}^{\theta_\infty} \frac{f_L(\theta,0)}{(r^4(\theta,0) + c_1^2 r_\theta^2(\theta,0))^{1/2}}\,d\theta \tag{B3}$$

So, for small υ the function I can be approximated by

$$I_{sing} = I_1 + I_2 + I_3 \tag{B4}$$

Remark that for $\upsilon = 0$ the term I_2 has a singularity. In order to remove δ and ε we rewrite I_{sing} as follows:

$$I_{sing} = \int_0^{\rho} \left(\frac{f_L(\bar{\rho},0)}{(\nu^4(\bar{\rho},0) + c_1^2\nu_\rho^2(\bar{\rho},0))^{1/2}} - \frac{f_L(0,0)}{(\nu_\rho^4(0,0)\bar{\rho}^4 + c_1^2\nu_\rho^2(0,0))^{1/2}}\right)d\bar{\rho} + \tag{B5}$$

$$\int_{c_1/\theta_\infty}^{\rho} \frac{f_L(0,0)}{(\nu_\rho^4(0,0)\bar{\rho}^4+c_1^2\nu_\rho^2(0,0))^{1/2}}\,d\bar{\rho} + \int_{\varepsilon}^{\theta_\infty}\left(\frac{f_L(\theta,0)}{(r^4(\theta,0)+c_1^2 r_\theta^2(\theta,0))^{1/2}} - \frac{f_L(0,0)}{(r_\theta^4(0,0)\theta^4+c_1^2 r_\theta^2(0,0))^{1/2}}\right)d\theta$$

Letting ε, $\delta \to 0$ we arrive at expression (6.24).

REFERENCES

Bear, J. and A. Verruijt, Modelling Groundwater Flow and Pollution, Dordrecht, Reidel, 1987.

Bear, J. and Y. Bachmat, Introduction to transport phenomena in porous media, Dordrecht, Reidel, 1990.

Buse, O.A. and J.J.A van Kooten, ECOWELL: A program to Estimate the Contamination at Wells, User Manual, Department of Mathematics, Wageningen Agricultural University, 1995.

Dagan, G., Solute transport in heterogeneous porous formations, J. Fluid Mech., 145, 151-177, 1984.

Dagan, G., Flow and transport in Porous Formations. Berlin, Heidelberg, Springer, 1989.

Feller, W., An introducion to probability theory and and its applications, Volume I, third edition, John Wiley, New York, 1968.

Gardiner, C.W., Handbook of stochastic methods for physics, chemistry and natural sciences, Berlin Heidelberg, Springer, 1983.

Garabedian, P.R., Partial Differential Equations, New York, John Wiley, 1964.

Gelhar, L.W. and C.L. Axness, Three dimensional stochastic analysis of macro dispersion in aquifers. Water Resour. Res. 19(1), 161-180, 1983.

van der Hoek, C.J., Contamination of a well in a uniform background flow. Stochastic Hydrol. Hydraul. 6, 191-208, 1992.

van Herwaarden, O.A. and J. Grasman, Dispersive groundwater flow and pollution. Math. Mod. and Meth in Appl. Sci. 1, 61-81, 1991.

van Herwaarden, O.A., Spread of pollution by dispersive groundwater flow. SIAM J. of Appl. Math. 54(1), 26-41, 1994

Javandel I. and C-F. Tsang, Capture-zone type curves: a tool for aquifer cleanup, Groundwater, 24(5), 616-625 , 1986.

van Kooten, J.J.A., Groundwater contaminant transport including adsorption and first order decay, Stochastic Hydrol. Hydraulics 8, 185-205, 1994.

van Kooten, J.J.A., A method to solve the advection-dispersion equation with kinetic adsorption, Technical Report TN 95-02, Department of Mathematics, Wageningen Agricultural University, 1995 (Submitted for publication).

Kabala, Z.J. and G. Sposito, A stochastic model of reactive solute transport with time-varying velocity in a heterogeneous aquifer. Water Resour. Res. 27(3), 341-350, 1991.

Kinzelbach,W., The random walk method in pollutant transport simulation. In: Custodio E. et al. (eds.), Groundwater Flow and Quality Modeling, 227-245, Reidel, Dordrecht, 1988.

Neumann, S.P., C.L. Winter and C.M. Newman, Stochastic theory of field-scale Fickian dispersion in anisotropic porous media, Water Resour. Res. 23, 453-466, 1987.

Roberts, P.V., M.N. Goltz and D.M. Mackay, A natural gradient experiment in a sand aquifer, 3, Retardation estimates and mass balances for organic solutes, Water Resour. Res. 22, 2047-2058, 1986.

Saffman, P.G., Dispersion due to molecular diffusion and macroscopic mixing in flow through a network of capillaries, Journ. Fluid Mech. 7(2), 194-208, 1960.

Schafer-Perini, A.L. and J.L. Wilson, Efficient and accurate front tracking for two-dimensional groundwater flow models, Water Resour. Res. 27(7), 1471-1485, 1991.

Strack, O.D.L., Groundwater Mechanics, New Yersey, Prentice Hall, 1989.

Sudicky, E.A., A natural-gradient experiment on solute transport in a sand aquifer: spatial variability of hydraulic conductivity and its role in the dispersion process, Water Resour. Res. 22, 2069-2082, 1986.

Uffink, G.J.M., Application of Kolmogorov's backward equation in random walk simulation of groundwater contaminant transport. In: Contaminant Transport in Groundwater, Kobus and Kinzelbach (eds.), pp. 283-289, Balkema, Rotterdam, 1989.

CHAPTER 3

A METHOD TO SOLVE THE ADVECTION-DISPERSION EQUATION WITH KINETIC ADSORPTION

(by J.J.A. van Kooten, in revised form accepted for publication in Advances in Water Resources)

Abstract: This study deals with a method to solve the transport equations for a kinetically adsorbing solute in a porous medium with spatially varying velocity field and dispersion coefficients. Making use of the stochastic nature of a first order kinetic process, we show that the advection-dispersion equation and the adsorption isotherm can be decoupled. Once the solution for a non-adsorbing solute is known, the method provides an exact solution for the kinetically adsorbing solute. The method is worked out in three examples. In particular we demonstrate how the method can be applied simultaneously with a numerical transport code: the advective-dispersive transport is computed numerically, whereas kinetic effects are incorporated analytically. The proposed approach may be useful in field scale applications with complex flow patterns.

1. INTRODUCTION

Solute transport in groundwater may be highly affected by interactions between the solute and the solid. Therefore transport models should contain equilibrium or non-equilibrium isotherms that account for these interactions. The most simple model is obtained by applying the linear equilibrium isotherm. Linear equilibrium adsorption only retards the transport of a solute. The local equilibrium assumption (LEA) may be valid if the rate of mass change due to the adsorption process is much faster than that due to the flow process (Valocchi, 1985). If the LEA is not valid a kinetic model may give a better description of the solute transport. An equilibrium approach is often preferred above a kinetic approach; the retardation factor in the equilibrium model can be estimated more easily from experimental data than the kinetic reaction rates. Moreover, a kinetic model requires more complicated mathematics than the equilibrium model. One of the aims of this study is to show that the mathematics can be understood from the physics of the kinetic process. In this way the practical applicability of the kinetic model may be enlarged.

The conventional advection-dispersion model for a solute subject to first order reversible kinetics is

$$\frac{\partial C}{\partial t} + \frac{\partial S}{\partial t} = - \frac{\partial}{\partial x_i}(v_i C) + \frac{\partial}{\partial x_i}(D_{ij}\frac{\partial C}{\partial x_j}) + \gamma(x) \,, \tag{1a}$$

$$\frac{\partial S}{\partial t} = k_1 C - k_2 S \,, \tag{1b}$$

where x is the vector of space coordinates, $C(x,t)$ (M/L^3) is the concentration of the solute in the free phase, $S(x,t)$ (M/L^3) is the concentration in the adsorbed phase, v (L/T) is the

fluid velocity vector, D_{ij} (L^2/T) is the dispersion tensor, $\gamma(x)$ (M/L^3T) is the rate of zero-order production in the point x and k_1 (T^{-1}) and k_2 (T^{-1}) are the forward and backward reaction rate, respectively. With respect to the indices we use the Einstein summation convention.

Model (1) is mathematically equivalent with a dual porosity model, i.e. a model for transport in a medium in which two zones can be distinguished: a mobile zone in which flow and transport take place and an immobile zone (e.g. dead end pores) in which the water is nearly stagnant (Van Genuchten & Wierenga, 1976).

In literature analytical solutions of (1) are available for various initial and boundary conditions. Lindstrom & Narasimham (1973) have presented a one-dimensional solution for a previously distributed contaminant. Solutions for migration through a semi-infinite column with different types of solute input at the inlet have been obtained by Ogata (1964), Cameron & Klute (1977), Van Genuchten & Wierenga (1976) and De Smedt & Wierenga (1979). Three-dimensional solutions for a point spill of pollution in an infinite domain have been derived by Carnahan & Remer (1984) and Goltz & Roberts (1987). Lassey (1988) has derived solutions for arbitrary solute input after t=0. Recently also solutions have been derived with zero-order production ($\gamma \neq 0$); Torido et al. (1993) have presented a wide class one-dimensional solutions assuming arbitrary input concentration, initial conditions and production functions. In all papers the velocity field was assumed to be uniform and one-dimensional. The dispersion coefficients were taken constant. At field scale these conditions will often not be satisfied. All solutions were obtained with the Laplace transform method. From mathematical point of view this method may be quite powerful. However, it does not always give insight in the relation between the structure of a solution and the underlying physical processes. Moreover, the Laplace method fails if model parameters are space dependent.

The objective of this study is to develop a method to solve model (1) in a multi-dimensional system with spatially varying v, D and γ. The sorption rates k_1 and k_2 are assumed to be constant. All coefficients are assumed to be time-independent. We interpret the adsorption kinetics as a stochastic process in which a particle is alternately free or sorbed (section 2). Keller & Giddings (1960) have presented four conditional distributions for the residence time in the free phase during a time interval t. We use these distributions to solve the set of partial differential equation (1). For arbitrary initial and boundary conditions we show that the solution of (1) is a convolution of solutions of the classical ADE (1a) without adsorption term and a combination of these distributions (section 3). So, in fact we show that the advection-dispersion equation (1a) and the reaction equation (1b) can be decoupled. Analytical solutions of the classical ADE have been derived for numerous initial and boundary conditions (e.g. Leij et al. 1990, 1991). Now, for all these problems we also have the solution for a kinetically adsorbing contaminant. Some examples are considered in section 4. Furthermore, we demonstrate how the method may be applied simultaneously with a numerical transport model. The transport equation is solved numerically, whereas the kinetic adsorption is incorporated analytically.

2. RESIDENCE TIME DISTRIBUTIONS IN THE FREE PHASE

The kinetic adsorption process described by equation (1b) can be considered as a stochastic process in which particles are alternately in the free and sorbed phase. Between transitions the residence times in the free (f) and sorbed (s) phase are exponentially distributed with mean $1/k_1$ and $1/k_2$ respectively. During a time interval t a particle may

make several transitions from the one state to the other. Assuming that at least one transition has taken place, Keller & Giddings (1960) have presented probability density functions for the time fraction χ ($0 \le \chi \le 1$) that a particle has spent in the free phase (see also Giddings & Eyring, 1955). These distributions depend on the initial and final state of a particle. For the purpose of this study we rewrite these distributions in terms of τ (= χt), the residence time in the fluid phase during a time interval t:

$$h_{ff}(\tau,t) = \sum_{n=1}^{\infty} \frac{(k_1k_2\tau)^n(t-\tau)^{n-1}}{n!\,(n-1)!}\, e^{-(k_1-k_2)\tau-k_2t} = \left(\frac{k_1k_2\tau}{t-\tau}\right)^{1/2} e^{-(k_1-k_2)\tau-k_2t}\, I_1\left(2\sqrt{k_1k_2\tau(t-\tau)}\right), \quad (2)$$

$$h_{fs}(\tau,t) = k_1 \sum_{n=0}^{\infty} \frac{(k_1k_2\tau)^n(t-\tau)^n}{(n!)^2}\, e^{-(k_1-k_2)\tau-k_2t} = k_1 e^{-(k_1-k_2)\tau-k_2t}\, I_0\left(2\sqrt{k_1k_2\tau(t-\tau)}\right), \quad (3)$$

$$h_{sf}(\tau,t) = \frac{k_2}{k_1}\, h_{fs}(\tau,t), \quad (4)$$

$$h_{ss}(\tau,t) = \frac{t-\tau}{\tau}\, h_{ff}(\tau,t), \quad (5)$$

where the first and second subscript of the functions h denote the initial and final state of a particle, respectively. In (2) and (3) I_0 and I_1 denote modified Bessel functions. For the distributions h_{fs} and h_{sf} the condition that at least one transition has taken place is satisfied automatically. In the two other cases there is also the possibility that a particle remains in the initial state all the time; the probabilities that a particle spends time t in the free or sorbed phase are $\exp(-k_1t)$ or $\exp(-k_2t)$, respectively. Some integration and differentiation properties of the distributions are given in the Appendix A.

In general, only the expressions in terms of the modified Bessel functions are given (see e.g. Valocchi & Quinodoz, 1989). The reason that we have also given the summation representation is twofold: Firstly, it is closer to the underlying physical process: e.g. the counter n is the number of times a particle has returned to the initial state. Secondly, this representation automatically gives power expansions for the distributions which are valid for each t and τ. This fact may be helpful when programming the distributions on the computer.

3. DECOUPLING OF TRANSPORT AND REACTION EQUATION

The residence time distributions (2)-(5) can be used to decouple the transport equation (1a) and the reaction equation (1b). In this section we show that the solutions C and S can be expressed as an integral of a proper combination of the h-distributions and $\tilde{C}$, the concentration of a non-adsorbing contaminant satisfying

$$\frac{\partial \tilde{C}}{\partial t} = M_{AD}\tilde{C} + \gamma(x) \qquad \text{with} \qquad M_{AD} = -\frac{\partial}{\partial x_i}(v_i\,\cdot) + \frac{\partial}{\partial x_i}\left(D_{ij}\frac{\partial\,\cdot}{\partial x_j}\right). \quad (6)$$

In the sequel we refer to M_{AD} as the advection-dispersion operator.

Let Ω ($\Omega \subset R^N$, N=1,2 or 3) be the region in which contaminant transport is studied. The boundary $\partial\Omega$ may consist of two disjunct parts. At the part $\partial\Omega_D$ the concentration is prescribed. At the part $\partial\Omega_N$ the mass flux is prescribed. In mathematical terms $\partial\Omega_D$ is a Dirichlet boundary and $\partial\Omega_N$ is a Neumann boundary.

A method to solve the kinetic model (1) for arbitrary initial and boundary conditions is developed in three steps. First we consider the case of non-zero initial conditions and zero boundary conditions. Next, we consider the opposite case: zero initial conditions

and non-zero boundary conditions. Finally, the solution for arbitrary initial and boundary conditions is obtained by superposition of the two former cases. We also give a physical interpretation of the solutions.

3.1 Transport of a contaminant distributed at or before t=0

In this section we consider the transport of a contaminant which has been distributed at or before t=0. It is assumed that the distributions of both C and S at t=0 are known:

$$C(x,0) = C_{init}(x) \quad \text{and} \quad S(x,0) = S_{init}(x) \; . \tag{7}$$

Furthermore, we assume that no contaminant is added to or extracted from the system so that γ=0 and the boundary conditions are

$$\begin{cases} C(x,t) = 0 & \text{at } \partial\Omega_D \; , \\ n_i \cdot (v_i - D_{ij}\dfrac{\partial}{\partial x_j})C = 0 & \text{at } \partial\Omega_N \; , \end{cases} \tag{8}$$

where n is the outward normal vector on $\partial\Omega$.

An expression for the solution of model (1) subject to these initial and boundary conditions can be found with physical arguments. We first give this expression. Next, we explain how it is obtained.

$$C(x,t) = \bar{C}_f(x,t)e^{-k_1 t} + \int_0^t (\bar{C}_f(x,\tau)h_{ff}(\tau,t) + \bar{C}_s(x,\tau)h_{sf}(\tau,t))d\tau, \tag{9a}$$

$$S(x,t) = S_{init}(x)e^{-k_2 t} + \int_0^t (\bar{C}_f(x,\tau)h_{fs}(\tau,t) + \bar{C}_s(x,\tau)h_{ss}(\tau,t))d\tau, \tag{9b}$$

where both $\bar{C}_f$ and $\bar{C}_s$ are solution of ADE (6) (with γ=0) subject to the initial conditions

$$\bar{C}_f(x,0) = C_{init}(x) \quad \text{and} \quad \bar{C}_s(x,0) = S_{init}(x) \tag{10}$$

and zero boundary conditions.

The physical reasoning behind expression (9) is as follows. During the time that particles are in the free phase their transport is governed by the classical ADE (6). In the sorbed phase particles are immobile. The residence time in the free phase τ is stochastic. With the help of the residence time distributions h_{ff}, h_{fs}, h_{sf} and h_{ss} the expected advective-dispersive displacement can be computed. The free phase transport of the contaminant with initial state 'f' is described by $\bar{C}_f$ and the free phase transport of the contaminant with initial state 's' is described by $\bar{C}_s$. To compute the concentration C in the free phase at time t the distributions with final state 'f' should be used and to compute the concentration S the distributions with final state 's' should be used. The term $\exp(-k_1 t)$ in (9a) represents the probability that particles have remained in the free phase continuously. The term $\exp(-k_2 t)$ in (9b) represents the probability that a particle has not moved at all.
The mathematical verification is given in Appendix B.

It is often possible to simplify expression (9). For example, if all contaminant is injected instantaneously at t=0 (see section 4.1) then S=0, so that $\bar{C}_s$=0. In many applications it is assumed the initial distributions C and S are in equilibrium, which implies that $\bar{C}_s=(k_1/k_2)\bar{C}_f$ so that only $\bar{C}_f$ has to be determined. A one dimensional example of the latter case is discussed in Lindstrom & Narasimham (1973).

3.2 Transport of continuously injected contaminant

If a domain is uncontaminated at t=0, the initial conditions are

$$C(x,0) = 0 \quad \text{and} \quad S(x,0) = 0 \ . \tag{11}$$

We assume that from t=0 there is a constant input and output of contaminant. The input/output may take place at the boundary of the domain and inside the domain, e.g. at an injection or withdrawal well. Contaminant input/output at the boundary is described by

$$\begin{cases} C(x,t) = C_b(x) & \text{at } \partial\Omega_D \ , \\ n_i(v_i C - D_{ij}\dfrac{\partial C}{\partial x_j}) = F(x) & \text{at } \partial\Omega_N \ . \end{cases} \tag{12}$$

Production/withdrawal inside the domain is described by the term γ in (1). The functions C_b, F and γ may vary in space.

One-dimensional examples of this case with γ=0 are discussed in Ogata (1964), Cameron & Klute (1977), Van Genuchten & Wierenga (1976) and De Smedt & Wierenga (1979). We have rewritten their solutions in terms of the residence time distributions h_{ff}, h_{fs}, h_{sf} and h_{ss}. For the solutions that are expressed in terms of the Goldstein J-function (Goldstein, 1953) we have applied relation A3 and A4 of Appendix A. All solutions turned out to have the same structure. Generalizing the result to multi-dimensional systems with spatially varying velocity fields and dispersion coefficients and $\gamma \neq 0$ we have found that the solution of (1) with zero initial conditions and boundary conditions (12) can be expressed as

$$C(x,t) = \tilde{C}_0(x,t)e^{-k_1 t} + \int_0^t \tilde{C}_0(x,\tau)\{h_{ff}(\tau,t) + \frac{k_1}{k_2}h_{sf}(\tau,t)\}d\tau \ , \tag{13a}$$

$$S(x,t) = \int_0^t \tilde{C}_0(x,\tau)\{h_{fs}(\tau,t) + \frac{k_1}{k_2}h_{ss}(\tau,t)\}d\tau \ , \tag{13b}$$

where $\tilde{C}_0$ is the concentration of a non-adsorbing contaminant satisfying ADE (6) with zero initial condition and boundary conditions given by (12). The mathematical verification is sketched in Appendix B.

Because contamination is constantly entering and leaving the porous medium the physical interpretation of expression (13) is less straightforward than that of (9). However, using the differentiation properties of Appendix A one may check that the time derivatives of (13) can be written as

$$\frac{\partial C(x,t)}{\partial t} = \frac{\partial \tilde{C}_0(x,t)}{\partial t}e^{-k_1 t} + \int_0^t \frac{\partial \tilde{C}_0(x,\tau)}{\partial \tau}h_{ff}(\tau,t)d\tau \ , \tag{14a}$$

$$\frac{\partial S(x,t)}{\partial t} = \int_0^t \frac{\partial \tilde{C}_0(x,\tau)}{\partial \tau}h_{fs}(\tau,t)d\tau \ . \tag{14b}$$

The physical interpretation of (14) is straightforward. When particles are in the free phase the change in the concentration is described by equation (6). Because the residence time in the free phase is stochastic, this change should be weighted with the proper residence time distribution. Because particles enter or leave the medium in the free phase, only the distributions with initial state (f) are relevant. The term $\exp(-k_1 t)$ in (13a) and (14a) again represents the probability that particles have remained in the free phase continuously.

3.3 Arbitrary initial and boundary conditions

The solution of model (1) (with $\gamma \neq 0$) subject to non-zero initial conditions

$$C(x,0) = C_{init}(x) \quad \text{and} \quad S(x,0) = S_{init}(x) \tag{15}$$

and non-zero boundary conditions

$$\begin{cases} C(x,t) = C_b(x) & \text{at } \partial\Omega_D \ , \\ n_i \cdot (v_i - D_{ij}\dfrac{\partial}{\partial x_j})C = F(x) & \text{at } \partial\Omega_N \ , \end{cases} \tag{16}$$

is the superposition of (9) and (13). This superposition can be written as

$$C(x,t) = \tilde{C}_1(x,t)e^{-k_f t} + \int_0^t (\tilde{C}_1(x,\tau)h_{ff}(\tau,t) + \tilde{C}_2(x,\tau)\frac{k_1}{k_2}h_{sf}(\tau,t))d\tau, \tag{17a}$$

$$S(x,t) = S_{init}(x)e^{-k_f t} + \int_0^t (\tilde{C}_1(x,\tau)h_{fs}(\tau,t) + \tilde{C}_2(x,\tau)h_{ss}(\tau,t))d\tau, \tag{17b}$$

where $\tilde{C}_1 = \tilde{C}_f + \tilde{C}_0$ and $\tilde{C}_2 = \tilde{C}_s + (k_1/k_2)\tilde{C}_0$, so that $\tilde{C}_1$ and $\tilde{C}_2$ are concentrations of a non-adsorbing contaminant satisfying equation (6) with the initial and boundary conditions respectively given by

$$\tilde{C}_1(x,0) = C_{init}(x) \ , \qquad \begin{cases} \tilde{C}_1(x,t) = C_b(x) & \text{at } \partial\Omega_D \ , \\ n_i \cdot (v_i - D_{ij}\dfrac{\partial}{\partial x_j})\tilde{C}_1 = F(x) & \text{at } \partial\Omega_N \ , \end{cases} \tag{18}$$

$$\tilde{C}_2(x,0) = S_{init}(x) \ , \qquad \begin{cases} \tilde{C}_2(x,t) = (k_1/k_2)C_b(x) & \text{at } \partial\Omega_D \ , \\ n_i \cdot (v_i - D_{ij}\dfrac{\partial}{\partial x_j})\tilde{C}_2 = (k_1/k_2)F(x) & \text{at } \partial\Omega_N \ . \end{cases} \tag{19}$$

A considerable simplification is achieved if it may be assumed that the initial concentration distributions are in equilibrium, i.e.

$$S_{init} = (k_1/k_2)C_{init}, \tag{20}$$

which implies that $\tilde{C}_1 = (k_1/k_2)\tilde{C}_2$ so that only $\tilde{C}_1$ has to be determined.

3.4 Further generalisations

If contaminant input only takes place during time T_{in}, i.e. for $t \leq T_{in}$ the boundary conditions and/or γ are not equal to 0 and for $t > T$ they are 0, then the solution of model (1) is

$$\begin{aligned} C_T(x,t) &= C(x,t) && \text{and} \quad S_T(x,t) = S(x,t) && \text{for } t \leq T_{in}, \\ C_T(x,t) &= C(x,t) - C(x,t-T_{in}) && \text{and} \quad S_T(x,t) = S(x,t) - S(x,t-T_{in}) && \text{for } t > T_{in}, \end{aligned} \tag{21}$$

where C and S are given by (17).

ERRATUM

Equation (17) at p. 68 should be

$$C(x,t) = \bar{C}_1(x,t)e^{-k_1 t} + \int_0^t (\bar{C}_1(x,\tau)h_{f0}(\tau,t) + \bar{C}_2(x,\tau)h_{s0}(\tau,t))\,d\tau \ , \qquad (17a)$$

$$S(x,t) = S_{init}(x)e^{-k_2 t} + \int_0^t (\bar{C}_1(x,\tau)h_{f0}(\tau,t) + \bar{C}_2(x,\tau)h_{s0}(\tau,t))\,d\tau \ , \qquad (17b)$$

where $\bar{C}_1$ and $\bar{C}_2$ satisfy equation (6) with $\gamma_1=\gamma(x)$ and $\gamma_2=(k_1/k_2)\gamma(x)$, respectively. The initial and boundary conditions are given by (18) and (19).

It is well known that for large k_1 and k_2 a kinetic model approximately predicts the same transport as the linear equilibrium model

$$R\frac{\partial C}{\partial t} + \frac{\partial S}{\partial t} = -\frac{\partial}{\partial x_i}(v_i C) + \frac{\partial}{\partial x_i}(D_{ij}\frac{\partial C}{\partial x_j}) + \gamma(x) ,$$
$$S = \frac{k_1}{k_2} C \qquad (22)$$

where $R=1+(k_1/k_2)$ is the retardation factor. On the other hand, it may occur that neither the kinetic nor the equilibrium model describe the transport of a solute satisfactorily (Cameron&Klute, 1977). A combined equilibrium and kinetic approach may be required:

$$R\frac{\partial C}{\partial t} + \frac{\partial S}{\partial t} = -\frac{\partial}{\partial x_i}(v_i C) + \frac{\partial}{\partial x_i}(D_{ij}\frac{\partial C}{\partial x_j}) + \gamma(x) ,$$
$$\frac{\partial S}{\partial t} = k_3 C - k_4 S , \qquad (23)$$

where k_3 (T^{-1}) and k_4 (T^{-1}) again denote a forward and backward sorption rate, respectively. After introduction of the retarded parameters $v_i^R=v_i/R$, $D_{ij}^R=D_{ij}/R$, $\gamma^R=\gamma/R$, $S^R=S/R$ and $k_3^R=k_3/R$ model (23) transforms into a model equivalent to (1), so that the method presented in this study also applies to the combined model.

4 SOME EXAMPLES

In section 3 we have shown that once the transport of a non-adsorbing solute is known, also the transport of a kinetically adsorbing solute can be determined. In this section the theory is worked out in some examples. In the first example we show how a solution of a kinetic model presented by Carnaham&Remer (1984) and Goltz&Roberts (1986) can be obtained as a special case of the method described in this study. In the second example the method is applied to predict the breakthrough of a contaminant at a well. We extend the results for the breakthrough of a non-adsorbing contaminant obtained in previous publications (Van Herwaarden, 1994, van Kooten 1994, 1995). In example 3 we demonstrate how the method can be combined with a numerical transport model.

In all examples we assume that the dispersion tensor is given by

$$D_{ij} = a_T|v|\delta_{ij} + (a_L - a_T)\frac{v_i v_j}{|v|} , \qquad (24)$$

where a_L and a_T denote the longitudinal and transversal dispersivities (Bear&Verruyt, 1987). In example 2 we allow a_L and a_T to vary in space.

4.1 example 1: 3D transport of instantaneously injected solute

In three dimensions the kinetic model for transport in an isotropic formation with uniform flow in the x_1-direction reads

$$\begin{cases} \dfrac{\partial C}{\partial t} + \dfrac{\partial S}{\partial t} = -v_1 \dfrac{\partial C}{\partial x_1} + D_{11}\dfrac{\partial^2 C}{\partial x_1^2} + D_{22}\dfrac{\partial^2 C}{\partial x_2^2} + D_{33}\dfrac{\partial^2 C}{\partial x_3^2}, \\ \dfrac{\partial S}{\partial t} = k_1 C - k_2 S. \end{cases} \tag{25a}$$

At t=0 an amount Q (M) of solute is injected in the origin (x_1,x_2,x_3)=(0,0,0), so that the following initial conditions apply to (25a).

$$C(x,0) = Q\delta(x) \qquad \text{and} \qquad S(x,0) = 0 . \tag{25b}$$

where $\delta(x)$ denotes the Dirac delta function. As boundary condition we require that C vanishes at infinity. The concentration of a non-adsorbing solute, i.e. k_1=k_2=0 in (25), is given by

$$\tilde{C}_f(x,t) = \frac{Q}{\sqrt{\pi^3 t^3 D_{11} D_{22} D_{33}}} \exp\{-\frac{1}{4t}(\frac{(x_1 - v_1 t)^2}{D_{11}} + \frac{x_2^2}{D_{22}} + \frac{x_3^2}{D_{33}})\} \tag{26}$$

(see e.g. Carnaham & Remer, 1984). Now, from (9) we directly obtain the concentrations of the kinetically adsorbing solute in the free and sorbed phase:

$$\begin{aligned} C(x,t) &= \tilde{C}_f(x,t)e^{-k_1 t} + \int_0^t \tilde{C}_f(x,\tau) h_{ff}(\tau,t)\, d\tau , \\ S(x,t) &= \int_0^t \tilde{C}_f(x,\tau) h_{fs}(\tau,t)\, d\tau. \end{aligned} \tag{27}$$

(Note that in this example $\tilde{C}_s$=0, because S=0 at t=0). Solutions equivalent to (27) were presented by Carnaham & Remer (1984) and Goltz & Roberts (1986). However, they obtained the solutions after lengthy Laplace transforms. Here, the solutions simply follow with a more general theory which, moreover, is closer to the underlying physical process.

In fig. 1 a comparison is made between the evolution of the concentration profiles $\tilde{C}_f$, C and S along the x_1-axis (x_2=x_3=0). For small t the concentration profiles of C and S have a strong non-Gaussian shape. This can be explained from the fact that shortly after the injection the solute concentration close to the origin is high so that a large amount of solute will be adsorbed. The adsorbed amount is released slowly. Furthermore the figures clearly illustrate the enhanced longitudinal spreading and tailing due to kinetic adsorption.

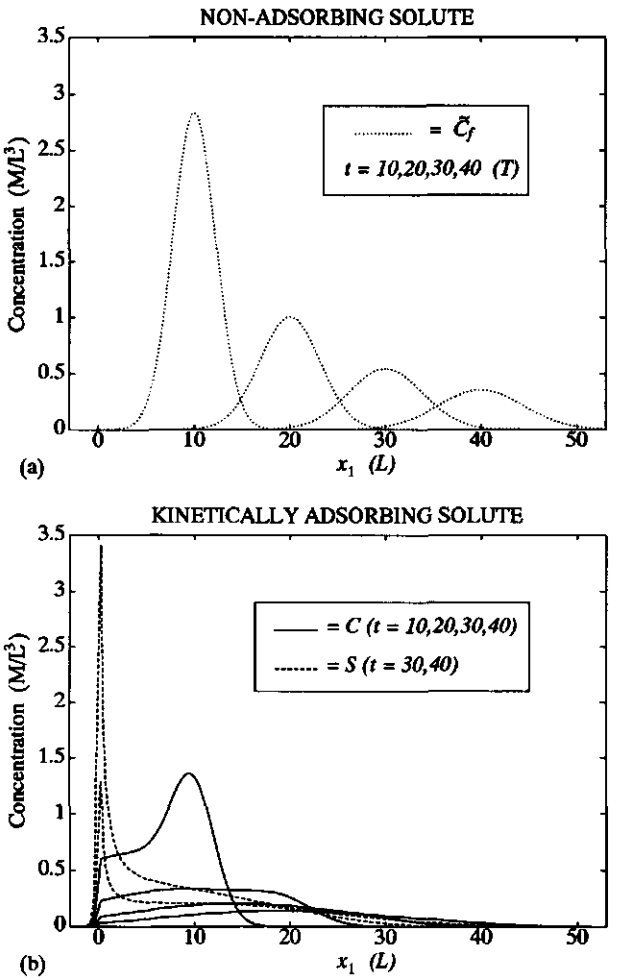

Fig. 1 Evolution in time of the concentration profiles $\bar{C}_f$ (eq. 26), C and S (eq. 27) along the x_1-axis. (Q=100 (M), v_1=1 (M/L), D_{11}=0.25 (L^2/T), D_{22}=D_{33}=0.05 (L^2/T), k_1=k_2=0.1 (T^{-1})).

4.2 Example 2: Contamination of a pumping well

In previous publications we have studied the arrival of conservative or linearly decaying contaminants at a well in a confined aquifer (e.g. Van Herwaarden & Grasman, 1991, Van Herwaarden, 1994, Van Kooten, 1994, 1995). A typical flow pattern for groundwater discharge is shown in fig. 3. Van Herwaarden and Grasman have analyzed the effect of the transversal dispersion on the arrival rate. If a contaminant is subject to first order kinetics, then during intervals a particle is adsorbed and not displaced in the transversal direction. Thus, kinetic adsorption only affects the time at which particles pass a certain point and not the ultimate transversal spreading. Therefore, the approximation for the fraction of a contaminant that reaches the well presented by van Herwaarden (1994, eq.(4.5)), may also be used for a kinetically adsorbing contaminant.

In van Kooten (1995) we have derived approximations for the arrival time distribution at a well. E.g. for particles released in the point x far inside the catchment area, where the effect of the transversal dispersion is negligible, the arrival time distribution can be approximated by

$$\tilde{g}(x,t) = \frac{\mu^{3/2}}{\sqrt{2\pi\sigma^2\tau^3}} \exp\{-\frac{(\mu-\tau)^2\mu}{2\sigma^2\tau}\}, \tag{28a}$$

where μ and σ^2 are asymptotic approximations for the mean and variance of the arrival time:

$$\mu(x) = T_{adv}(x) + \frac{a_L(x)}{|v(x)|} \quad \text{and} \quad \sigma^2(x) = 2\int_0^{\zeta} \frac{a_L(\bar{\zeta})}{v^2(\bar{\zeta})}\, d\bar{\zeta} \tag{28b}$$

In (28b) T_{adv} is the advective travelling time to the well and ζ is a coordinate along the streamline through x, see fig. 2. Note that for any flow pattern μ and σ^2 can easily be determined by particle tracking. For a detailed description of how to take into account transversal dispersion we refer to van Kooten (1995).

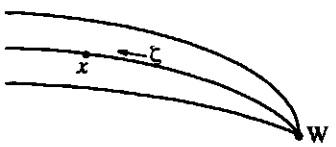

Figure 2 The coordinate ζ is taken along the streamline through the point x.

With the residence time distributions of section 2 kinetic adsorption can be incorporated without making any further approximation. It is assumed that in an aquifer Ω at t=0 the concentrations of the contaminant in the free and sorbed phase are given by $C_{init}(x)$ and $S_{init}(x)$. The arrival time distributions of the corresponding conservative cases are

$$\tilde{g}_f(t) = \int_\Omega C_{init}(x)\tilde{g}(x,t)\,dx \quad \text{and} \quad \tilde{g}_s(t) = \int_\Omega S_{init}(x)\tilde{g}(x,t)\,dx, \tag{29}$$

and, thus, the arrival time distribution for a kinetically adsorbing contaminant is

$$g(t) = \tilde{g}_f(t)e^{-k_1 t} + \int_0^t (\tilde{g}_f(\tau)h_{ff}(\tau,t) + \tilde{g}_s(\tau)h_{sf}(\tau,t))\,d\tau. \tag{30}$$

For an instantaneous spill in the point x (30) reduces to

$$g(x,t) = \tilde{g}(x,t)e^{-k_1 t} + \int_0^t \tilde{g}(x,\tau)h_{ff}(\tau,t)\,d\tau. \tag{31}$$

We have worked out the above for the special case of a well in a uniform background flow (fig. 3). The corresponding velocity field is given by

$$v_1(x_1,x_2) = 1 - \frac{x_1}{x_1^2+x_2^2}, \qquad v_2(x_1,x_2) = \frac{-x_2}{x_1^2+x_2^2}. \tag{32}$$

We assume that at t=0 in the point (x_1,x_2)=(-4,1) an instantaneous spill of contaminant takes place. For various values of k_1 and k_2 the approximation for the arrival time distribution (31) at the well is displayed in fig. 4. The dispersivities are a_L=0.1 and a_T=0.01. The figures show that the tail due to kinetic effects becomes more pronounced if k_1 increases and/or k_2.

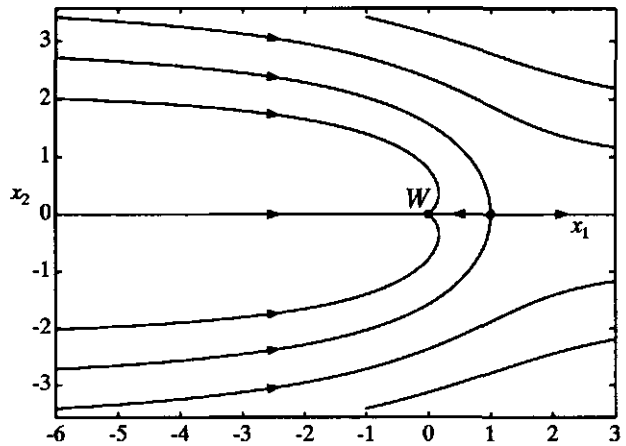

Figure 3 Flow pattern for a well in a uniform background flow.

decreases, i.e. if the expected time of one stay in the fluid phase ($1/k_1$) decreases and/or the expected time of one stay ($1/k_2$) in the fluid phase increases.

To assess the accuracy of the approximations we have made a comparison with the results of random walk simulations. There exist various random walk algorithms that take into account kinetic adsorption (Valocchi&Quinodoz, 1989, Andricevic& Foufoula-Georgiou, 1991). Here, it suffices to select the most natural and straightforward method (method 1 of Valocchi&Quinodoz, 1989).

In the free phase the stochastic displacement of a particle is governed by

$$\begin{aligned}\Delta X &= (v_1 + \frac{\partial}{\partial x}D_{11} + \frac{\partial}{\partial y}D_{12})\Delta t + \sqrt{2a_L|v|}\frac{v_1}{|v|}Z_L\sqrt{\Delta t} + \sqrt{2a_T|v|}\frac{v_2}{|v|}Z_T\sqrt{\Delta t} \\ \Delta Y &= (v_2 + \frac{\partial}{\partial x}D_{21} + \frac{\partial}{\partial y}D_{22})\Delta t + \sqrt{2\alpha_L|v|}\frac{v_2}{|v|}Z_L\sqrt{\Delta t} - \sqrt{2\alpha_T|v|}\frac{v_1}{|v|}Z_T\sqrt{\Delta t}\end{aligned} \quad (33)$$

where Δt is the time step and Z_L and Z_T are random deviates from a uniform distribution with mean 0 and variance 1 (see van Kooten, 1994). First the time τ_f of one stay in the fluid phase is generated from an exponential distribution. During time τ_f a particle is advected-dispersed according to (34). Next, from an exponential distribution the time τ_s that a particle stays in the adsorbed phase is generated. The time τ_s is added to t, the total time elapsed from the beginning of the simulation. This process is repeated, until the particle enters the well.

From the point (-4,1) we carried out 15000 random walks with k_1=0.5 (T^{-1}) and k_2=0.2 (T^{-1}). The time step Δt was chosen 0.001 except if τ_f would be exceeded. In the latter case Δt was taken equal to the difference between τ_f and the time that has been spend in the fluid phase yet. From fig. 5 we may conclude that approximation (31) agrees quite well with the arrival time distribution obtained from the simulations. The small differences are caused mainly by the irregular behaviour of the simulations, and it is to be expected that the agreement will still become better if the number of random walks is increased.

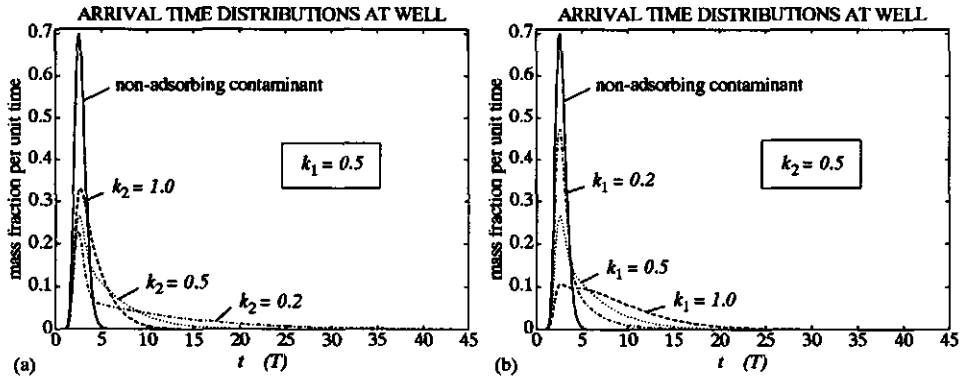

Figure 4 Some arrival time distributions at the well for a contaminant spilled in (-4,1). In (a) the adsorption rate k_1 is kept fixed. In (b) the desorption rate k_2 is kept fixed.

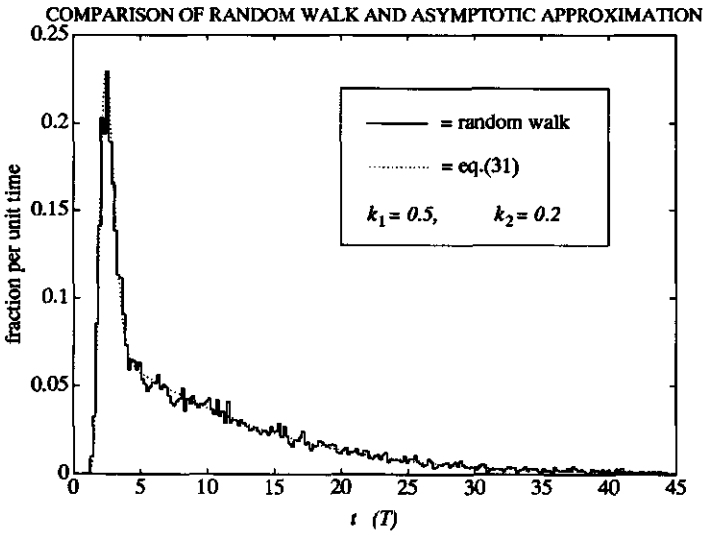

Figure 5 Comparison of the arrival time distributions obtained with the random walk simulation and computed from eq. (31).

4.3 Example 3: Simultaneous application with a numerical transport model

Currently, there exist many finite element (FE) and finite difference (FD) codes to solve the ADE for a conservative contaminant. The aim of this example is to demonstrate how the theory of section 3 can be used simultaneously with such a code. Once the transport of a conservative contaminant has been computed numerically, with some post processing the transport of a kinetically adsorbing contaminant can be computed. In this example the numerical computation were carried out with the FE code METROPOL, which has been developed by the National Institute of Public Health and Environmental Protection in the Netherlands.

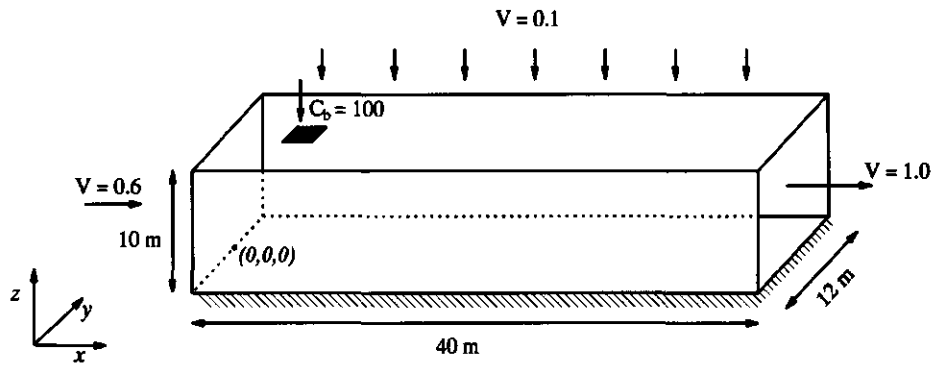

Figure 6 Sketch of the aquifer considered in section 4.3

We consider contaminant transport in an aquifer which is recharged at the top (figure 6). From below the formation is confined by an impervious layer. The effective velocities (m/day) of the incoming and outgoing flow are indicated in the figure. In the y-direction no flow takes place. Initially the aquifer is unpolluted. From t=0 at the top of the aquifer for x between 7 and 10 m and y between -1 and 1 m contaminated water constantly leaches into the aquifer. The concentration of the contaminant in the incoming water is C_b=100 $\mu g/m^3$. At the remainder of the top surface C_b=0. Because of the symmetry in y-direction it suffices to solve the transport problem in only one half of the aquifer, with a no flux condition at the surface y=0. At the downstream boundary x=40 we impose a zero concentration condition. The surfaces x=0, y=0 and z=0 are no flux boundaries. The aquifer was covered by 40x20x12=9600 cubic elements. Because of the zero initial conditions the theory for simulating the transport of a kinetically adsorbing contaminant is described in section 3.2.

With the METROPOL code the concentration profile $\tilde{C}_0$ of a non-adsorbing contaminant was computed from t=0 to t=20 days with time step Δt = 0.2 days and dispersivities a_L=0.6 m and a_T=0.3 m. The computation time at a Sun3 workstation was about 6 hours. In fig. 7a the flow pattern and the concentration contours in the y=0 plane at t=20 are shown. For each nodal point the time profile of $\tilde{C}_0$ was stored in a data file. The time profiles were post processed by substitution in eq.(13). In between partition point $t_i=i\Delta t$ the concentration was again determined by linear interpolation. The concentration contours for a kinetically adsorbing contaminant with k_1=0.1 and k_2=0.1 (days^{-1}) are displayed in fig. 7b. The post processing could be carried out in about 2 minutes, so that the cost of the post processing are almost negligible compared to the cost of solving the ADE numerically.

In fig. 7c we have drawn the concentration contours resulting from an equilibrium model with retardation factor $R=1+(k_1/k_2)=2$. The solution of the equilibrium model was obtained from the METROPOL output by replacing the time t by the retarded time $t^R=t/R$. Compared to the kinetic model the downstream spreading is clearly underestimated. The "kinetic" profile is more flat than the "equilibrium" profile. So, the application of a kinetic or equilibrium model may have large consequences on, for example, the delineation of the polluted region for remediation purposes. In fig. 8 various "kinetic" profiles along the z-axis through x=20 m are compared with an "equilibrium" profile. The figure confirms that for increasing sorption rates the kinetic model approaches the equilibrium model.

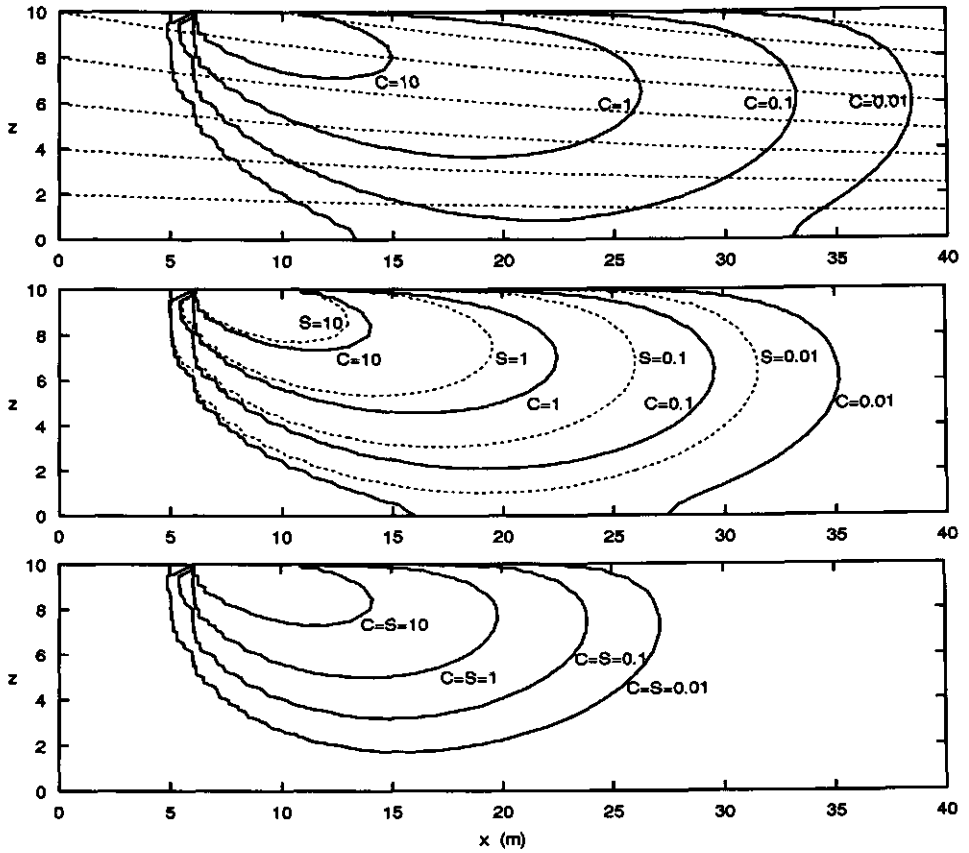

Figure 7 Flow pattern and concentration contours in the y=0 plane at t=20 (days).
(a) Non-adsorbing contaminant
(b) Kinetically adsorbing contaminant with k_1=0.1 and k_2=0.1 (days^{-1}).
(c) Contaminant subject to linear equilibrium adsorption with R=2.

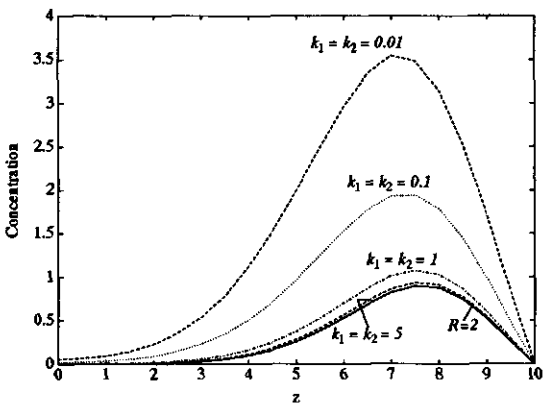

Figure 8 Comparison of various kinetic profiles (k_1/k_2=1) with an equilibrium profile (R=2) at t=20 (days) along the z-axis through x=20 m.

5. CONCLUDING REMARKS

In this paper a transport model is studied for a kinetically adsorbing solute in a porous medium with homogeneous adsorption properties. We allow the velocity field and the dispersivities to vary in space, so that the medium may be heterogeneous with respect to the hydro-geological properties. Furthermore, solute may be added to or extracted from the system.

We have presented a method to decouple the advection-dispersion equation and the adsorption isotherm. This method is directly based on the stochastic nature of the first order kinetic process. Therefore it may contribute to a better understanding of the solutions for the kinetic model presented here and in other papers. The four conditional distributions for the residence time of particles in the free phase of Keller&Giddings (1960) play an important role. For arbitrary initial and boundary conditions we have shown that once the transport of non-adsorbing solutes has been computed, the transport of a kinetically adsorbing can be determined with the aid of these distributions.

Often an analytical solution for a non-adsorbing contaminant is already quite complicated (see e.g. Leij et al. 1991) or is even not at all at hand. Therefore, the method will probably find its major application when it is used simultaneously with a numerical transport model. With such model the transport of a non-adsorbing contaminant is computed first. Next, by substitution of the output in expression (9), (13) or (17) the effect of the kinetic adsorption can be incorporated analytically. An example is given in section 4.3. The proposed approach may be useful in field scale applications with complex flow fields. The advantages above solving the complete model (1) numerically are:

- If the values of the reaction rates k_1 and k_2 are changed, no new run with the numerical code has to be performed. Only the post-processing has to be repeated. This feature may be very cost-saving when model output has to be fitted with experimental data.
- The approach is computational more efficient. The costs of solving one differential equation numerically are lower than the costs of solving two coupled equation.

Although in the mixed numerical-analytical approach no additional errors are introduced due to discretization of the reaction eq. (1b), recent simulations have revealed that a full numerical solution and a mixed solution have the same order of accuracy. The dominating error appears to be caused by the space-time discretization of the parabolic ADE (1a).

A disadvantage of the approach may be that the time profiles of the concentrations in the nodal points have to be stored, so that for large grids much computer memory is required. In practice this disadvantage is not too large, because one is often only interested in the breakthrough of a contaminant at some particular points. In this case, just as for a traditional numerical method, only in the breakthrough points the time profiles need to be stored.

ACKNOWLEDGEMENTS

The author thanks M. de Gee, J. Grasman, P.A.C. Raats and S.E.A.T.M. van der Zee for the valuable discussions and for reading the paper critically. I am grateful to O.A. Buse for his help with drawing the figures. I also thank the Institute of Public Health and Environmental Protection (in particular A. Leynse) for their permission to use the METROPOL code. The work was funded by the Nederlandse Organisatie voor Wetenschappelijk Onderzoek (Dutch Organisation for Scientific Research).

APPENDIX A: Some mathematical properties of the distributions h_{ff}, h_{fs}, h_{sf} and h_{ss}

1. Differentiation properties

By differentiation of (2),(3),(4) and (5) we obtain

$$\frac{\partial h_{ff}}{\partial t} = -\frac{\partial h_{ff}}{\partial \tau} - \frac{\partial h_{fs}}{\partial t} \quad \text{and} \quad \frac{\partial h_{sf}}{\partial t} = -\frac{\partial h_{sf}}{\partial \tau} - \frac{\partial h_{ss}}{\partial t}, \tag{A1}$$

$$\frac{\partial h_{fs}}{\partial t} = k_1 h_{ff} - k_2 h_{fs} \quad \text{and} \quad \frac{\partial h_{ss}}{\partial t} = k_1 h_{sf} - k_2 h_{ss}. \tag{A2}$$

2. Integration properties

In the analytical solutions of the kinetic model (1) presented in literature, frequently the Goldstein J function appears (Goldstein, 1953). The J function and the distributions h_{ff}, h_{fs}, h_{sf} and h_{ss} are related as follows:

$$-\frac{\partial}{\partial \tau} J(k_1\tau, k_2(t-\tau)) = h_{ff}(\tau,t) + h_{fs}(\tau,t), \tag{A3}$$

$$\frac{\partial}{\partial \tau} J(k_2(t-\tau), k_1\tau) = h_{sf}(\tau,t) + h_{ss}(\tau,t), \tag{A4}$$

(see also De Smedt & Wierenga, 1979). Using that $J(a,0) = e^{-a}$ and $J(0,b) = 1$ we find

$$\exp(-k_1 t) + \int_0^t h_{ff}(\tau,t)\,d\tau + \int_0^t h_{fs}(\tau,t)\,d\tau = 1, \tag{A5}$$

$$\exp(-k_2 t) + \int_0^t h_{ss}(\tau,t)\,d\tau + \int_0^t h_{sf}(\tau,t)\,d\tau = 1. \tag{A6}$$

The determination of the integral of only a single h-function is less straightforward. Let

$$H(t) = \int_0^t h_{ff}(\tau,t)\,d\tau \tag{A7}$$

Using (A1) and (A5) we find that H satisfies the differential equation

$$\frac{d}{dt} H = -(k_1 + k_2)H + k_2(1 - e^{-k_1 t}). \tag{A8}$$

The solution of (A8) is

$$\int_0^t h_{ff}(\tau,t)\,d\tau = \frac{k_2}{k_1 + k_2} + \frac{k_1}{k_1 + k_2} e^{-(k_1+k_2)t} - e^{-k_1 t}. \tag{A9}$$

From A5 it follows that

$$\int_0^t h_{fs}(\tau,t)\,d\tau = \frac{k_1}{k_1 + k_2}(1 - e^{-(k_1+k_2)t}). \tag{A10}$$

In a similar way it can be shown that

$$\int_0^t h_{ss}(\tau,t)\,d\tau = \frac{k_1}{k_1 + k_2} + \frac{k_2}{k_1 + k_2} e^{-(k_1+k_2)t} - e^{-k_2 t}, \tag{A11}$$

$$\int_0^t h_{sf}(\tau,t)\,d\tau = \frac{k_2}{k_1 + k_2}(1 - e^{-(k_1+k_2)t}). \tag{A12}$$

APPENDIX B: Mathematical verification of the solutions of the kinetic model

1. *Verification of the solution presented in section 3.1*

It is obvious that C (9a) and S (9b) satisfy the initial conditions (7). Because $\tilde{C}_f$ and $\tilde{C}_s$ have zero boundary conditions, C and S have zero boundary conditions too.

To check whether the differential equations (1a) and (1b) are fulfilled we start with differentiating S to t:

$$\frac{\partial S}{\partial t} = -k_2 S_{init} e^{-k_2 t} + k_1 \tilde{C}_f e^{-k_1 t} + \int_0^t \{\tilde{C}_f(x,\tau)\frac{\partial h_{fs}}{\partial t}(\tau,t) + \tilde{C}_s(x,\tau)\frac{\partial h_{ss}}{\partial t}(\tau,t)\}\, d\tau. \quad \text{(B1)}$$

In (B1) we used that $h_{fs}(t,t) = k_1 \exp(-k_1 t)$ and $h_{ss}(t,t) = 0$. Applying differentiation property (A2) and ordering the terms that belong to C and S, one can see that (B1) is equivalent with equation (1b).

For C we have on the one hand

$$\frac{\partial C}{\partial t} = \frac{\partial \tilde{C}_f}{\partial t} e^{-k_1 t} - k_1 \tilde{C}_f e^{-k_1 t} + \tilde{C}_f h_{ff}(t,t) + \tilde{C}_s h_{sf}(t,t) + \int_0^t \{\tilde{C}_f(x,\tau)\frac{\partial h_{ff}}{\partial t}(\tau,t) + \tilde{C}_s(x,\tau)\frac{\partial h_{sf}}{\partial t}(\tau,t)\}\, d\tau \,. \quad \text{(B2)}$$

Since $\tilde{C}_f$ and $\tilde{C}_s$ are solutions of ADE (6) with $\gamma \neq 0$ we have on the other hand

$$\begin{aligned} M_{AD} C &= M_{AD}\tilde{C}_f e^{-k_1 t} + \int_0^t \{M_{AD}\tilde{C}_f(x,\tau)h_{ff}(\tau,t) + M_{AD}C_s(x,\tau)h_{sf}(\tau,t)\}\, d\tau \\ &\quad \frac{\partial \tilde{C}_f}{\partial t} e^{-k_1 t} + \int_0^t \{\frac{\partial \tilde{C}_f}{\partial \tau}(x,\tau)h_{ff}(\tau,t) + \frac{\partial \tilde{C}_s}{\partial \tau}(x,\tau)h_{sf}(\tau,t)\}\, d\tau \end{aligned} \quad \text{(B3)}$$

Applying partial integration we find

$$\begin{aligned} M_{AD} C &= \frac{\partial \tilde{C}_f}{\partial t} e^{-k_1 t} + \tilde{C}_f(x,t)h_{ff}(t,t) + \tilde{C}_s(x,t)h_{sf}(t,t) - \tilde{C}_f(x,0)h_{ff}(0,t) - \tilde{C}_s(x,0)h_{sf}(0,t) \\ &\quad - \int_0^t \{\tilde{C}_f(x,\tau)\frac{\partial h_{ff}}{\partial \tau}(\tau,t) + \tilde{C}_s(x,\tau)\frac{\partial h_{sf}}{\partial \tau}(\tau,t)\}\, d\tau \,. \end{aligned} \quad \text{(B4)}$$

Note that $h_{ff}(0,t) = 0$ and $\tilde{C}_s(x,0)h_{sf}(0,t) = k_2 S_{init}(x) e^{-k_2 t}$. Substituting integration property (A1) in (B2) we obtain that (B2) + (B1) = (B4), so that equation (1a) is satisfied too.

2. *Verification of the solution presented in section 3.2*

If $x \in \partial\Omega_N$ then for any t, $\tilde{C}_0(x,t)=C_b(x)$, so that (13) reduces to

$$C(x,t) = C_b(x)\exp(-k_1 t) + C_b(x)\{\int_0^t h_{ff}(\tau,t)d\tau + \int_0^t h_{fs}(\tau,t)d\tau\}.$$

Since $(k_1/k_2)h_{sf}=h_{fs}$ it follows from integration property (A5) that $\tilde{C}(x,t)=C_b(x)$, so that at $\partial\Omega_N$ C satisfied the right boundary condition. In a similar way it can be shown that at $\partial\Omega_D$ the solute flux equals $F(x)$.

To verify that C and S satisfy the differential equations of the kinetic model the steps of *B1* can be repeated with $\tilde{C}_f$ replaced by $\tilde{C}_0$ and $\tilde{C}_s$ by $(k_1/k_2)\tilde{C}_0$. To include the effect of the production term γ, integration property (A5) must be applied in step (B3).

REFERENCES

Andricevic, R. and E. Foufoula-Georgiou: Modeling kinetic non-equilibrium using the first two moments of the residence time distributions, Stoch. Hydrol. Hydraul. (5), 155-171, 1991.

Bear, J. and A. Verruyt: Modelling Groundwater Flow and Pollution, Dordrecht, Reidel, 1987.

Cameron, D.R., and A. Klute: Convective dispersive solute transport with a combined equilibrium and kinetic adsorption model, Water Resour. Res., 13, 183-188, 1977.

Carnahan, C.L. and J.S. Remer: Nonequilibrium and equilibrium sorption with a linear sorption isotherm during mass transport through an infinite porous medium: some analytical solutions, J. Hydrology, 73, 227-258, 1984.

van Genuchten, M.Th. and P.J. Wierenga: Mass transfer studies in sorbing porous media, 1, Analytical solutions, Soil Sci. Soc. Am. J. 40, 473-480, 1976.

Giddings, J.C. and H. Eyring, A molecular dynamic theory of chromatography, J. Phys. Chem., 59, 416-421, 1995.

Goldstein, S.: On the mathematics of exchange processes in fixed columns, 1. Mathematical solutions and asymptotic expansions, Proc. Roy. Soc. London, Ser. A. 219, 151-171, 1953.

Goltz, M.N., P.V. Roberts: Three-dimensional solutions for solute transport in an infinite medium with mobile and immobile zones, Water Resour. Res. 22 (7), 1986.

van Herwaarden, O.A. and J. Grasman: Dispersive groundwater flow and pollution, Math. Mod. and Meth. in Appl. Sci. 1, 61-81, 1991.

van Herwaarden, O.A. : Spread of Pollution by Dispersive Groundwater Flow. SIAM J. of Appl. Math. 54(1), 26-41, 1994.

van der Hoek, C.J.: Contamination of a well in a uniform background flow, Stochastic Hydrol. Hydraul. 6: 191-208, 1992.

Keller, R.A. and J.C. Giddings: Multiple zones and spots in chromatography, J. Chromatog. 3, 205-220, 1960.

van Kooten, J.J.A.: Groundwater contaminant transport including adsorption and first order decay, Stoch. Hydrol. Hydraulics 8, 185-205, 1994.

van Kooten, J.J.A.: An asymptotic method to predict the contamination of a pumping well, Advances in Water Resources, 18 (5), 295-313, 1995.

Lassey, K.R.: Unidimensional solute transport incorporating equilibrium and rate-limited isotherms with first-order loss, 1. Model conceptualizations and analytical solutions, Water Resour. Res. 24 (3), 343-350, 1988.

Leij, F.J., T.H. Skags, M.Th. van Genuchten, Analytical solutions for transport in three-dimensional semi-infinite porous media, Water Resour. Res, 27, 2719-2734, 1991.

Leij, F.J. and J.H. Dane, Analytical solutions of the one dimensional advection equation and two- or three-dimensional dispersion equation, Water Resour. Res., 26, 1475-1482, 1990.

Lindstrom, F.T., and M.N.L. Narasimham: Mathematical theory of a kinetic model for dispersion of previously distributed chemicals in a sorbing porous medium, SIAM J. of Appl. Math. 24, 496-510, 1973.

Ogata, A.: Mathematics of dispersion with linear adsorption isotherm, U.S. Geol. Surv. Prof. Pap, 411-H, 9 pp, 1964.

Smedt, F. de and P.J. Wierenga: A Generalized solution for solute flow in soils with mobile and immobile water, Water Resour. Res., 15 (5), 1137-1141, 1979.

Torido, N., F.J. Leij and M.T. van Genuchten: A comprehensive set of analytical solutions for nonequilibrium solute transport with first-order decay and zero-order production, Water Resour. Res., 29, 2167-2182, 1993.

Valocchi, A.J.: Validity of the local equilibrium assumption for modeling sorbing solute through homogeneous soils. Water Resour. Res. 6, 808-820, 1985.

Valocchi, A.J. and H.A.M. Quinodoz: Application of the random walk method to simulate the transport of kinetically adsorbing solutes, In: Abriola, L.M. (eds), Groundwater Contamination: Proceedings of the Third Scientific Assembly of the IAHS, 35-42, Baltimore, 1989.

CHAPTER 4

ECOWELL, A PROGRAM TO ESTIMATE THE CONTAMINATION OF WELLS: *TECHNICAL DOCUMENTATION*

CONTENTS

		Page
1	**Introduction**	82
2	**Basic equations**	83
3	**Discretization**	
	3.1 Triangular elements	84
	3.2 Barycentric coordinates and element width	84
	3.3 Neighbour elements	85
	3.4 Boundary points	85
4	**The head and velocity field**	86
5	**The stagnation points and separating streamlines**	
	5.1 Searching the stagnation points	88
	5.2 Separating streamlines leading towards a stagnation point	89
	5.3 Separating streamlines leading away from a stagnation point	91
	5.4 Evaluation of the integral $q_T(\rho)$	92
6	**Arrival at a well with only the effect of longitudinal dispersion included**	93
7	**Incorporation of transversal dispersion**	
	7.1 Transition to (ρ,v)*-coordinates*	94
	7.2 The boundary layer approximations	95
	7.3 Evaluation of the integrals Iu, $IT^{(1)}$ *and* $IT^{(2)}$	96
	7.4 The travelling time T_{sing}	97
	7.5 Evaluation of σ^2_{sep}	97
8	**The arrival time distribution**	98
9	**Incorporation of adsorption and decay**	
	9.1 Linear equilibrium adsorption	99
	9.2 First order decay	99
	9.3 Linear kinetic adsorption	100
	9.4 Combined effects	103
10	**Contour lines for** *h*, *u* **and arrival times**	
	10.1 Equipotential lines	104
	10.2 Contour lines for u and arrival times using a grid	104
	10.3 Contour lines for u if $\lambda = 0$.	105
Appendices		
A:	**Approximations for** *Iu,* $IT^{(1)}$ **and** $IT^{(2)}$ **near the endpoint singularity**	106
B:	**Bounds for the amount of pollution pumped up before or after a certain time**	
	B1 Non-adsorbing contaminant	107
	B2 Kinetically adsorbing contaminant	107

1. INTRODUCTION

In various papers researchers of the Department of Mathematics of the Wageningen Agricultural University have developed an analytical approximation method to predict the advective-dispersive transport of a contaminant towards a pumping well in a confined aquifer (Grasman & van Herwaarden (1991), van Herwaarden (1994), van Kooten (1994, 1995a and 1995b)). In this report we give a technical description of the implementation of the method in the computer program ECOWELL. For the run instructions and the visualization of the results we refer to the User Manual (Buse & van Kooten, 1995). We do not repeat the formula's that arise in the asymptotic method; when necessary we refer to a formula in the literature. Most formula's can be found in van Kooten (1995a). For easy reference a formula of that paper is marked with the superscript ^{K} , e.g. $(xx)^{K}$. Each section of this report describes one or more algorithms that have been used in ECOWELL.

The computer package ECOWELL must be used in connection with a finite element- or finite difference package for simulating groundwater flow. With such package a numerical head field can be generated for 2D-flow in an aquifer in which one or more withdrawal and injection wells are operating. Together with the corresponding discretization (section 3), the conductivities and porosity this head field is input for ECOWELL. With respect to the hydraulic conductivity the aquifer may be heterogeneous. Using Darcy's law the program computes a velocity field (section 4). In order to apply the asymptotic method ECOWELL first searches the stagnation points in the flow. The separating streamlines which bound the region of advective flow to a well are determined by backward integration from the stagnation points (section 5). Next from any point in the aquifer the effects of longitudinal and transversal dispersion on the transport of a contaminant towards a well can be analyzed. Analytical approximations are computed for

- the arrival fraction of a contaminant at a well,
- the mean and variance of the arrival time,
- the arrival time distribution and breakthrough curve.

ECOWELL can generate contours of equal arrival rates and arrival times, which may provide useful information for delineating a protection zone or for designing a remediation strategy. The program may also be used for standard facilities, such as the computation of streamlines and equipotential lines, or to carry out random walk simulations.

2. BASIC EQUATIONS

The method is based on the assumption that the flow in the aquifer is approximately 2-dimensional, steady state and divergence free (except at the location of a well). Furthermore the aquifer should be isotropic. The transport of a contaminant takes place by advection and longitudinal and transversal dispersion. The advective displacement should dominate the dispersive displacement. The effects of linear equilibrium adsorption, kinetic adsorption and first order decay can be incorporated. In the papers mentioned in the introduction the method has been developed stepwise. The transport model in which all aforementioned effects are included and combined is

$$\begin{cases} R\dfrac{\partial C}{\partial t} = -\nabla(vC) + \nabla(D\nabla\cdot C) - R\lambda C - k_f C + k_b S \,, \\ \dfrac{\partial S}{\partial t} = k_f C - k_b S - \lambda S \,, \end{cases} \tag{1}$$

where

C = concentration of the contaminant in the free phase (M/L^3),
S = concentration in the immobile phase (due to kinetic adsorption) (M/L^3),
v = the effective fluid velocity vector (L/T),
R = retardation factor (due to equilibrium adsorption) (-),
λ = first order decay rate (T^{-1}),
k_f = forward kinetic adsorption rate (T^{-1}),
k_b = backward kinetic adsorption rate (T^{-1})

The adsorption/reaction parameters R, λ, k_f and k_b should be constant.
Physically spoken, it is assumed that decay takes place in all phases and that the equilibrium and kinetic adsorption mechanisms are independent, i.e. they do not interact. A pore wall may consist of several chemical and biological compounds. A solute particle moving through the pore may interact at different rates with different consistuents. The retardation factor R account for fast ("instantaneous" equilibrium) interactions. The kinetic isotherm accounts for the slow interactions (see Cameron & Klute, 1979).
The entries of the dispersion tensor D (L^2/T) are in the classical way given by

$$D_{ij} = a_T|v|\delta_{ij} + (a_L - a_T)\frac{v_i v_j}{|v|} \,, \tag{2}$$

where

a_L = longitudinal dispersivity (L),
a_T = transversal dispersivity (L).

The dispersivities are allowed to vary in space.

3. THE DISCRETIZATION

3.1 Triangular elements

A numerical head field for 2D-groundwater flow can be generated with a finite element or finite difference method. Because a finite element method has a greater flexibility in handling complex geometries, it is often preferred to the finite difference method. A finite element method can be based on triangular or quadrangular elements. Triangular elements easier allow for local refinement, which for example may be necessary in the vicinity of a well. Because popular flow models, as Micro-FEM and AQUA, use triangular elements, we have chosen this type of flow models as starting point for ECOWELL. The triangularization that has been used by the flow model, is input for ECOWELL. The network may be highly irregular. It should be specified in two files. The first file contains the coordinates of the nodal points. The second file describes which nodal points are connected in an element (Figure 1).

Of course ECOWELL may also run in connection with a flow model based on a finite element method with quadrangular elements or a finite difference method. In this case the user should first specify a selfmade network of triangles.

Nodal point file (File 1)

1849	(=*number of nodal points*)	
1	-50.0	-50.0
2	-45.0	-49.0
3	-40.0	-48.0
...	...	...
...	...	...
k	*x*	*y*
...	...	...

k = nodal point number

Network file (File 2)

3050	(= *number of elements*)		
1	1	2	67
2	2	67	68
3	2	68	69
..	..	..	..
..	..	..	..
elem	k_1	k_2	k_3
..	..	..	..

elem = element number
k_i = *nodal point number*

Fig. 1 Example of input files describing the triangularization. File 1 gives the (x,y)-coordinates of the nodal points. File 2 specifies the network of triangles.

3.2 Barycentric coordinates and element width

To facilitate computations with irregular shaped triangular elements we use barycentric (or area) coordinates. For the concept of barycentric coordinates we refer to Lapidus & Pinder (1982, p. 109-116). The barycentric coordinates $(\beta_1,\beta_2,\beta_3)$ of a point (x,y) with respect to an element with nodal points (x_1,y_1), (x_2,y_2) and (x_3,y_3) (fig. 2.) are given by

$$\beta_1 = \frac{1}{2A}[(y_2-y_3)x + (x_3-x_2)y + (x_2y_3-x_3y_2)] ,$$

$$\beta_2 = \frac{1}{2A}[(y_3-y_1)x + (x_1-x_3)y + (x_3y_1-x_1y_3)] , \qquad (3)$$

$$\beta_3 = 1 - \beta_1 - \beta_2 ,$$

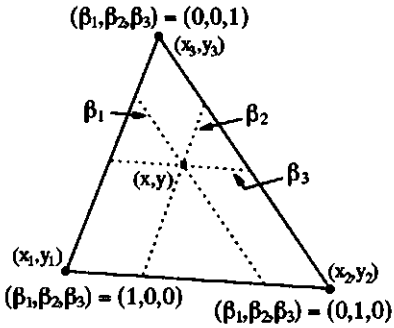

Fig. 2 Barycentric coordinates.

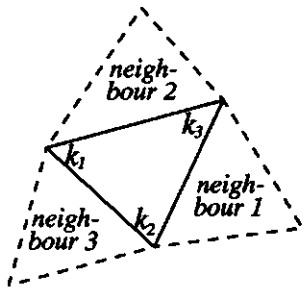

Fig. 3 Ordering of neighbour elements.

where A is the area of the element:

$$A = \frac{1}{2}[(x_1-x_3)(y_2-y_3) - (x_2-x_3)(y_1-y_3)] \,. \tag{4}$$

The point (x,y) is located inside the triangle if and only if $\beta_1>0$, $\beta_2>0$ and $\beta_3>0$. So, we have a simple criterium to decide whether a point is inside or outside a triangle. Furthermore, barycentric coordinates are of great use for linear interpolation in elements (eq. (6)).

For particle tracking purposes we introduce the width l of an element, which we define as the mean of the distances of the three nodal points to an opposite edge:

$$l = \frac{A}{3}\left[\frac{1}{\sqrt{(x_1-x_2)^2+(y_1-y_2)^2}} + \frac{1}{\sqrt{(x_2-x_3)^2+(y_2-y_3)^2}} + \frac{1}{\sqrt{(x_1-x_3)^2+(y_1-y_3)^2}}\right] . \tag{5}$$

3.3 Neighbour elements

To enhance the computational efficiency ECOWELL builds a list of neighbour elements. Two elements are called neighbours if they have a common edge, i.e. if they have two nodal points in common (fig. 3). So, an element that is not located at the boundary of a domain has three neighbours. The neighbour opposite to nodal point k_i (i= 1,2,3) (see also fig. 1, file 2) is called neighbour i. An element at the boundary of the domain has only one or two neighbours. The missing neighbour is set to -1.

3.4 Boundary points

The user does not have to specify which nodal points are at the boundary of the domain. From the Neighbour list ECOWELL itself builds a list of boundary points. For example, if in an element with nodal point numbers k_1, k_2 and k_3 neighbour 1 has been set to -1, k_2 and k_3 are boundary points. First ECOWELL searches for all boundary points. Next, with a linear sort algorithm, the points are sorted in such a way that, if they are connected, a closed line is formed.

4 THE HEAD AND VELOCITY FIELD

The hydraulic head in the grid points of the finite element or finite difference discretization are input for ECOWELL. Inside a triangular element the head field is determined by linear interpolation. Let h_1, h_2 and h_3 be the hydraulic heads in the nodal points of an element, then the head in a point (x,y) inside the element is

$$h = \beta_1 h_1 + \beta_2 h_2 + \beta_3 h_3 \quad . \tag{6}$$

where the barycentric coordinates β_1, β_2 and β_3 are defined by (3). Furthermore, a file should be given with the positions and discharges of sinks and sources and the thickness B of the aquifer at the position of sinks and sources (fig.4). It is assumed that sinks and sources are always located in a nodal point of the mesh.

In groundwater modelling theory the velocity field $v=(Vx,Vy)$ is computed from the head field with Darcy's law (Bear & Verruijt, 1987)

$$v = \frac{K}{n} \nabla h \quad . \tag{7}$$

where K (>0)is the hydraulic conductivity and n is the porosity. If the formation is hetero-

Head file (File 3)

1	10.44
2	10.12
3	9.87
...	...
...	...
k	*h*
...	...

k = nodal point number
h = hydraulic head

Well file (File 4)

3	1	(= *number of sources and sinks, resp.*)
456	-12.34	10.2
671	-25.00	11.12
898	-13.1	10.54
544	16.5	10.4
k	*Q*	*B*

k = nodal point number
Q = discharge (<0 for sink, >0 for source)
B = thickness of the layer at the well

Conductivity file (File 5)

1	0.14
2	0.15
3	0.134
...	...
...	...
k/e	*K*
...	...

k/e = nodal point/element number
K = conductivity

Fig. 4 Example of input files describing the flow in the aquifer. File 3 gives the head values in the nodal points. File 4 contains information on the sinks and sources. File 5 specifies the conductivities either in the nodal points or in the elements.

geneous, ECOWELL expects a file in which the conductivities are specified either element or nodal point wise (File 5). From the number of rows in the file the program itself detects how the conductivities are specified.

Because inside an element the head field is linear, the gradient of h is constant inside an element and discontinuous across interelement boundaries. From (3) and (6) it follows that it is given by

$$\nabla h = \begin{pmatrix} (y_2 - y_3)h_1 + (y_3 - y_1)h_2 + (y_1 - y_2)h_3 \\ (x_3 - x_2)h_1 + (x_1 - x_3)h_2 + (x_2 - x_1)h_3 \end{pmatrix} . \tag{8}$$

In the asymptotic method for predicting the contamination of a well the stagnation points in the flow play a crucial role. The velocity field that results from straightforward application of (7) and (8) will not contain stagnation points. At most it may contain a stagnation element, i.e. an element in which $\partial h/\partial x = \partial h/\partial y = 0$ ($\Leftrightarrow h_1 = h_2 = h_3$). Therefore, this velocity field can not be used in the asymptotic method.

In several papers methods have been proposed to obtain a velocity field that is continuous in the sense that it is mass-conservative. The mixed finite element method (see e.g. Ewing et al., 1985) produces piecewise polynomial approximations for both the head and velocity field. The lowest order mixed method has been discussed in detail by Kaasschieter et al. (1992, 1995). The mixed method can not be applied in connection with a standard finite element flow model. A method that does not have this drawback is proposed by Cordes & Kinzelbach (1992). They subdivide each triangle into four subtriangle. By fully utilizing that at each nodal point is divergence free in the weak sense, they construct a velocity field in which the flux across interelement boundaries is continuous. However, both the lowest order mixed method and the method of Cordes & Kinzelbach result in a velocity field that inside a (sub)element is constant, so that it is still impossible to find a stagnation point. Moreover, the asymptotic method uses the derivative of the flow velocity at the stagnation point (see e.g. (32) and (34)). With the aforementioned methods this derivative would be zero.

To obtain a velocity field that is continuous and (almost everywhere) differentiable, we apply the following "smoothing procedure". First, in each element the flow velocity is computed from (7) and (8). Next, in each nodal point we define the velocity as the mean of the velocity in the surrounding elements, i.e. the elements of which the nodal point is part. From now on the velocity inside elements is computed by linear interpolation of the velocity in the nodal points, so that a continuous velocity field results. Let (Vx_1, Vy_1), (Vx_2, Vy_2) and (Vx_3, Vy_3) be the mean velocities in the nodal point of an element, then the velocity in a point with barycentric coordinates $(\beta_1, \beta_2, \beta_3)$ equals

$$\begin{aligned} Vx &= \beta_1 Vx_1 + \beta_2 Vx_2 + \beta_3 Vx_3 , \\ Vy &= \beta_1 Vy_1 + \beta_2 Vy_2 + \beta_3 Vy_3 . \end{aligned} \tag{9}$$

In the smoothing procedure an exception is made for the nodal points in which a well is located. In a well we have an essential discontinuity; in the elements near a well the velocity field is pointing toward the well so that all streamlines end into the well. The smoothing procedure would disturb this important characteristic. Inside an element that

contains a well the approach is quasi-analytical: we assume that the velocity field can be approximated by the velocity field for radial flow towards a well of discharge Q

$$Vx = \frac{Q}{2\pi B}\frac{x-x_w}{(x-x_w)^2+(y-y_w)^2} \quad \text{and} \quad Vy = \frac{Q}{2\pi B}\frac{y-y_w}{(x-x_w)^2+(y-y_w)^2}\ , \tag{10}$$

where (x_w,y_w) is the position of the well.

5. THE STAGNATION POINTS AND SEPARATING STREAMLINES

The separating streamlines, that bound the region of advective flow towards a well, play a crucial role in the asymptotic method. Near a separating streamline we have a boundary layer in which transversal dispersion has an important effect on contaminant transport. This effect has been analyzed by introducing the local coordinates ρ and υ (fig. 7)[K] (see also fig. 6 of this report). To carry out the coordinate transformation rapidly ECOWELL stores the coordinates of the separating streamlines in an array. In this section we describe how the stagnation points and the corresponding separating streamlines are determined.

5.1 Searching the stagnation points

For each element that does not contain a well the program checks if it contains a stagnation point. Because inside such element the velocity is determined by linear interpolation, barycentric coordinates are a helpful tool for searching the stagnation points. Solving Vx=0 and Vy=0 (9) we find that the barycentric coordinates of a stagnation point should be given by

$$\begin{aligned}
\beta_1^s &= \frac{Vx_3Vy_2 - Vx_2Vy_3}{(Vx_2-Vx_3)(Vy_1-Vy_3) - (Vx_1-Vx_3)(Vy_2-vy_3)}\ ,\\
\beta_2^s &= \frac{Vx_1Vy_3 - Vx_3Vy_1}{(Vx_2-Vx_3)(Vy_1-Vy_3) - (Vx_1-Vx_3)(Vy_2-Vy_3)}\ ,\\
\beta_3^s &= 1 - \beta_1^s - \beta_2^s\ .
\end{aligned} \tag{11}$$

If $\beta_1^s \geq 0$, $\beta_2^s \geq 0$ and $\beta_3^s \geq 0$ we may conclude that the element contains a stagnation point, which in cartesian-coordinates is given by

$$\begin{aligned}
x_{STAG} &= \beta_1^s x_1 + \beta_2^s x_2 + \beta_3^s x_3\ ,\\
y_{STAG} &= \beta_1^s y_1 + \beta_2^s y_2 + \beta_3^s y_3\ .
\end{aligned} \tag{12}$$

The asymptotic method assumes that with each sink at least one stagnation point is connected. Therefore, if the program finds less stagnation points then sources and sinks the user should check his flow pattern. If for a sink no stagnation point - and thus no (complete) catchment area - is found, the asymptotic method may give unreliable results for that sink. The user may have to refine the discretization or to enlarge the domain.

5.2 The separating streamlines leading toward a stagnation point

The separating streamlines that bound the region of advective flow towards a well are determined by back-tracking from a stagnation point. In a stagnation point, however, the flow velocity is zero, so that a stagnation point is not suitable as starting point for the tracking method. Therefore, first we analyze the flow pattern near the stagnation point.

From (3),(9),(11) and (12) we obtain that the velocity field in an element that contains a stagnation point can be expressed as

$$\begin{aligned} Vx &= (\beta_1-\beta_1^s)Vx_1+(\beta_2-\beta_2^s)Vx_2+(\beta_3-\beta_3^s)Vx_3 = m_{11}(x-x_{STAG})+m_{12}(y-y_{STAG}),\\ Vy &= (\beta_1-\beta_1^s)Vy_1+(\beta_2-\beta_2^s)Vy_2+(\beta_3-\beta_3^s)Vy_3 = m_{21}(x-x_{STAG})+m_{22}(y-y_{STAG}), \end{aligned} \tag{13a}$$

where

$$\begin{aligned} m_{11} &= \frac{\partial Vx}{\partial x} = [(y_2-y_3)Vx_1 + (y_3-y_1)Vx_2 + (y_1-y_2)Vx_3]/2A\ ,\\ m_{12} &= \frac{\partial Vx}{\partial y} = [(x_3-x_2)Vx_1 + (x_1-x_3)Vx_2 + (x_2-x_1)Vx_3]/2A\ ,\\ m_{21} &= \frac{\partial Vy}{\partial x} = [(y_2-y_3)Vy_1 + (y_3-y_1)Vy_2 + (y_1-y_2)Vy_3]/2A\ ,\\ m_{22} &= \frac{\partial Vy}{\partial y} = [(x_3-x_2)Vy_1 + (x_1-x_3)Vy_2 + (x_2-x_1)Vy_3]/2A\ . \end{aligned} \tag{13b}$$

It follows that the set of equations for movement along a streamline reads

$$\begin{pmatrix} \partial x/\partial t \\ \partial y/\partial t \end{pmatrix} = \begin{pmatrix} Vx \\ Vy \end{pmatrix} = \begin{pmatrix} m_{11} & m_{12} \\ m_{21} & m_{22} \end{pmatrix} \begin{pmatrix} x-x_{STAG} \\ y-y_{STAG} \end{pmatrix} = M \begin{pmatrix} x-x_{STAG} \\ y-y_{STAG} \end{pmatrix}\ . \tag{14}$$

The eigenvalues and eigenvectors of the matrix M are given by

$$\lambda_i = \frac{m_{11}+m_{22}+(-1)^i\sqrt{(m_{11}+m_{22})^2-4(m_{11}m_{22}-m_{12}m_{21})}}{2} \qquad (i=1,2),$$

$$e_1 = \begin{pmatrix} \lambda_1-m_{22} \\ m_{21} \end{pmatrix} \quad \text{and} \quad e_2 = \begin{pmatrix} m_{12} \\ \lambda_2-m_{11} \end{pmatrix}\ . \tag{15}$$

Because the stagnation point should be a saddle point (fig. 5), λ_1 must be negative and λ_2 must be positive. If not, the stagnation point is a (negative) attractor, and in fact it acts as a (hidden) sink or source. In this case the user should check whether all sinks and sources have been specified or if the head field has been generated with a too coarse mesh.

The general solution of (14) is a linear combination of the eigenvectors of M:

$$\begin{pmatrix} x(t)-x_{STAG} \\ y(t)-y_{STAG} \end{pmatrix} = C_1 e_1 \exp(\lambda_1 t) + C_2 e_2 \exp(\lambda_2 t) , \tag{16}$$

where the constants C_1 and C_2 follow from the initial conditions. The separating streamline leading towards and leading away from the stagnation point are described by (14) with C_2=0 and C_1=0, respectively. Eliminating the time variable t we find an (x,y)-representation for the separating streamlines towards the stagnation point:

$$(\lambda_1 - m_{22})(y - y_{STAG}) = m_{21}(x - x_{STAG}) \tag{17}$$

From (17) the intersection points $(x^{(1)},y^{(1)})$ and $(x^{(2)},y^{(2)})$ of the separating streamlines with the boundary of an element can be calculated (fig. 5a). In very special cases - e.g. if the mesh is regular and the natural background flow is parallel to the x- or y-axis - it may happen that the stagnation point itself is located at the boundary of an element, an expression similar to (17) must be derived for the neighbour element that contains the stagnation point too (fig. 5b).

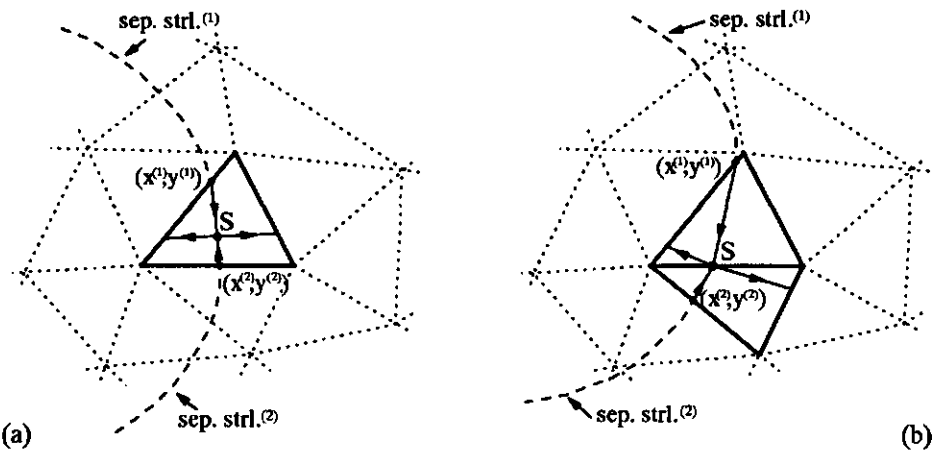

Fig. 5 The intersection points of the separating streamlines with the boundary of the element that contains the stagnation point S are determined from eq. (17). Fig. (b) illustrates the special case that the stagnation point itself is located at an interelement boundary.

We note that in the elements that do not contain a stagnation point the streamlines are described by expressions similar to (16). In these cases (x_{STAG},y_{STAG}) is a fictive point outside the element, of which the barycentric coordinates are still given by (11) with $\beta_1<0$, $\beta_2<0$ or $\beta_3<0$. So, element by element parts of a (separating) streamline can be determined analytically. To obtain a smooth streamline, for each element C_1 and C_2 have to be chosen

in such a way that the various parts connect to each other. However, in general it is impossible to eliminate t from (16), so that this procedure becomes quite complicated. Therefore, this procedure has not been worked out in ECOWELL.

Starting from, respectively, $(x_1,y_1)=(x^{(1)},y^{(1)})$ and $(x_1,y_1)=(x^{(2)},y^{(2)})$, ECOWELL determines the remainder of the two separating streamlines by integrating the (smoothed) velocity field backward in time with a Runga-Kutta method,

$$x_{i+1} = x_i + Vx(x_h,y_h)\Delta t \quad \text{and} \quad y_{i+1} = y_i + Vy(x_h,y_h)\Delta t \ ,$$

with (18)

$$x_h = x_i + Vx(x_i,y_i)\Delta t/2 \quad \text{and} \quad y_h = y_i + Vy(x_i,y_i)\Delta t/2 \ ,$$

The time step Δt is chosen in such a way that in each element approximately four steps are made:

$$\Delta t = -\frac{l_i}{4v_i} \ , \tag{19}$$

where l_i (5) is the width of the element in which (x_i,y_i) is situated and v_i is the absolute value of the velocity in (x_i,y_i). So, in the parts of the region where the grid has been refined, the streamlines are determined more accurately than in the parts with a coarser grid. The coordinates (x_i,y_i) are stored in an array. The Runga-Kutta method terminates if the separating streamline has crossed the boundary of the domain or if it has approached a source up to a distance less than $l_i/4$.

5.3 The separating streamlines leading away from a stagnation point

Putting $C_1=0$ in (16) and eliminating the time variable t we find an (x,y)-representation for the separating streamlines leading away from a stagnation point:

$$m_{12}(y-y_{STAG}) = (\lambda_2 - m_{11})(x-x_{STAG}) \ . \tag{20}$$

From (20) the two intersection points of the separating streamlines leading away from a stagnation point with the boundary of the element that contains the stagnation point are determined (fig. 5). By forward integration with the Runga-Kutta method (18) we determine the sinks with which the stagnation point are connected, i.e. the sink in which the separating streamlines end. E.g. in figure 6 stagnation point 1 is connected with sinks (or wells) *W1* and *W2*, stagnation point 2 is only connected with well *W2*, etc.

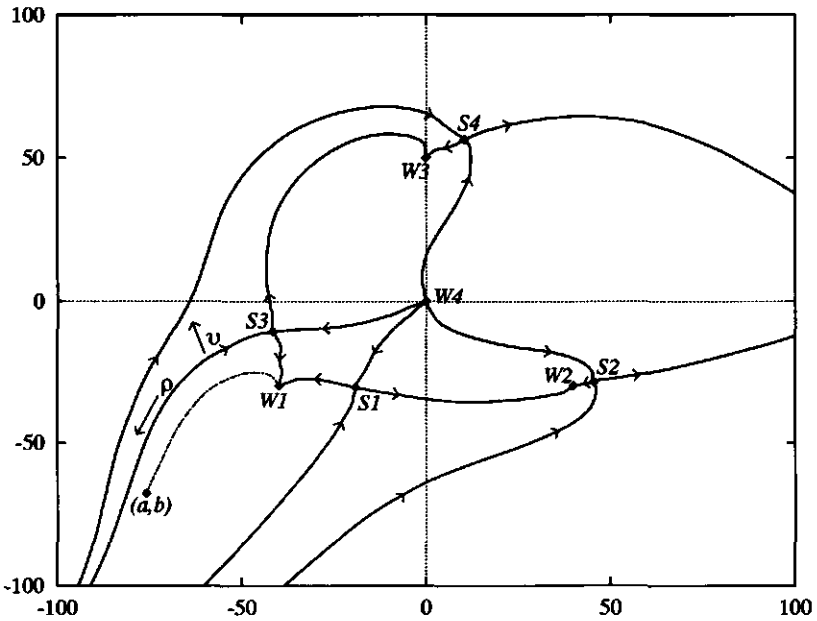

Fig. 6. Example of flow pattern: *W1*, *W2* and *W3* are sinks, *W4* is a source, *S1* to *S4* are stagnation points. To predict the transport of a contaminant from (a,b) to *W1* (or *W3*), we introduce (ρ,υ)-coordinates along the separating streamline ending in stagnation point *S3*.

5.4 Evaluation of the integral $q_T(\rho)$ along a separating streamline

In the boundary layer approximations for the arrival rate and for the moments of the arrival time an important term is

$$q_T(\rho) = \left(\frac{2}{\nu^2(\rho,0)}\tilde{q}(\rho)\right)^{-1/2} \qquad \text{with} \qquad \tilde{q}(\rho) = \int_0^\rho \alpha_T(\bar{\rho},0)\nu^2(\bar{\rho},0)\,d\bar{\rho}\ , \qquad (21)$$

where $v(\rho,0)$ and $\alpha_T(\rho,0)$ denote the velocity and transversal dispersivity along the separating streamline, respectively. (Note that $q_T(\rho) = \sqrt{\alpha_T}q(\rho)$, where $q(\rho)$ is defined by $(6.14)^K$ and α_T is a (spatial) mean of a_T $(2.3)^K$). To avoid that in one run of ECOWELL the integral $q_T(\rho)$ has to be evaluated repeatedly, it is evaluated during the calculation of the separating streamlines. Let ρ_i be the distance along the separating streamline from the stagnation point to the point (x_i,y_i). We denote the velocity and transversal dispersivity in (x_i,y_i) by v_i and $\alpha_{T,i}$, respectively. We assume that between two successive points (x_{i-1},y_{i-1}) and (x_i,y_i) the velocity and dispersivity vary linearly. Because the velocity in the stagnation point is zero it follows that

$$\tilde{q}_1 = \int_0^{\rho_1} a_T(\rho,0)v^2(\rho,0)d\rho = \int_0^{\rho_1} [a_{T,STAG} + (a_{T,1}-a_{T,STAG})(\frac{\rho}{\rho_1})](\frac{\rho}{\rho_1}v_1)^2 d\rho$$
$$= \rho_1(\frac{1}{12}a_{T,STAG} + \frac{1}{4}a_{T,1})v_1^2 \quad . \tag{22}$$

For $i \geq 2$ we have

$$\tilde{q}_i = \int_0^{\rho_i} a_T(\rho,0)v^2(\rho,0)d\rho \tag{23}$$
$$= q_{i-1} + \int_{\rho_{i-1}}^{\rho_i} \{a_{T,i-1} + (a_{T,i}-a_{T,i-1})(\frac{\rho-\rho_{i-1}}{\rho_i-\rho_{i-1}})\}(v_{i-1} + (v_i - v_{i-1})(\frac{\rho-\rho_{i-1}}{\rho_i-\rho_{i-1}}))^2 d\rho$$
$$= q_{i-1} + (\rho_i-\rho_{i-1})[(\tfrac{1}{4}a_{T,i-1} + \tfrac{1}{12}a_{T,i})v_{i-1}^2 + (\tfrac{1}{6}a_{T,i-1} + \tfrac{1}{6}a_{T,i})v_{i-1}v_i + (\tfrac{1}{12}a_{T,i-1} + \tfrac{1}{4}a_{T,i})v_i^2] \quad .$$

The values

$$q_i = v_i(2\tilde{q}_i)^{-1/2} \tag{24}$$

are stored in an array.

Furthermore, the asymptotic method also uses the derivative of the flow velocity in a stagnation point, which is given by

$$v_\rho(0,0) = v_1/\rho_1 \quad . \tag{25}$$

6. ARRIVAL AT A WELL WITH ONLY THE EFFECT OF LONGITUDINAL DISPERSION INCORPORATED

The asymptotic method first incorporates the effect of longitudinal dispersion. In this section we describe how the corresponding approximations for the mean $(6.6a)^K$ and variance $(6.8)^K$ of the arrival time are computed.

By forward tracking with the Runga-Kutta method (18) we determine the advective travelling time T_{adv} along the streamline through the injection point (a,b). The timestep is the absolute value of (19). The tracking terminates if a streamline crosses the boundary of the domain or if the streamline has approached a certain well up to a distance less than $l_i/4$, where l_i (5) is the width of the element in which the well and (x_i,y_i) are situated. The approximation for the variance σ^2_{catch} consists of an integral of a_L/v^2 along the streamline. During the tracking this integral is evaluated with a trapezium rule.

If the streamline ends in a well the mean and variance of the arrival time are used in an approximation for the arrival time distribution at the well (eq.$(7.1)^K$). If not, the mean and variance of the arrival time are meaningless.

7. INCORPORATION OF THE EFFECT OF TRANSVERSAL DISPERSION

7.1 Transition to (ρ,υ)-coordinates

The asymptotic method is based on the assumption that the effect of transversal dispersion is most crucial near the separating streamlines in the flow. This effect can be analyzed by introducing (ρ,υ)-coordinates along the nearest "*relevant*" separating streamline. A separating streamline is called "*relevant*" if it bounds the catchment area of the well of which we wish to estimate the contamination. To carry out the coordinate transformation, first the orthogonal projection of the initial point (a,b) on a separating streamline should be determined.

As example we again consider the flow pattern of fig. 6. At $t=0$ in (a,b) a contaminant is released. To predict the arrival of the contaminant at well *W1* we have to determine the orthogonal projection of (a,b) with respect to the separating streamlines ending in stagnation point *S1* and *S3*. We call the separating streamlines ending in stagnation point *S2* and *S4* *non-relevant* for this case because they do not bound the catchment area of *W1*: the stagnation points *S2* and *S4* are not connected with well *W1*.

The algorithm to determine the orthogonal projection on a separating streamline is as follows. Let (x_{i-1},y_{i-1}) and (x_i,y_i) denote two successive points on a separating streamline that have been determined with the Runga-Kutta method (section 5.2). A vector representation for a line through the two points is:

$$s_i : \begin{pmatrix} x \\ y \end{pmatrix} = \begin{pmatrix} x_{i-1} \\ y_{i-1} \end{pmatrix} + \mu_i \begin{pmatrix} x_i - x_{i-1} \\ y_i - y_{i-1} \end{pmatrix} \quad . \tag{26}$$

A vector representation for the line through (a,b) perpendicular to s_i is

$$\begin{pmatrix} x \\ y \end{pmatrix} = \begin{pmatrix} a \\ b \end{pmatrix} + \lambda_i \begin{pmatrix} y_{i-1} - y_i \\ x_i - x_{i-1} \end{pmatrix} \quad . \tag{27}$$

In the intersection point of the two lines we have

$$\mu_i = \frac{(a - x_{i-1})(x_i - x_{i-1}) + (b - y_{i-1})(y_i - y_{i-1})}{(x_i - x_{i-1})^2 + (y_i - y_{i-1})^2} \quad . \tag{28}$$

Let *Npoint* be the number of points on a separating streamline that have been calculated with the Runga-Kutta method. Starting from i=1 we make the following steps to determine the projection point (a_p,b_p):

1. From (28) we compute μ_i.
2. - If $0 \le \mu_i \le 1$ the projection of (a,b) on the line s_i is in between (x_{i-1},y_{i-1}) and (x_i,y_i), so that this projection is on the separating streamline (fig. 7a). The corresponding projection point is $(\bar{a}_p,\bar{b}_p)=(x_{i-1} + \mu_i(x_i - x_{i-1}),\ y_{i-1} + \mu_i(y_i - y_{i-1}))$.
   - If $\mu_i<0$ and $\mu_{i-1}>1$ (a,b) lies inside the shaded domain in fig. 7b. In this case we

define the projection by $(\bar{a}_p,\bar{b}_p)=(x_{i-1},y_{i-1})$.

- In all others case (a,b) can not be projected on the line piece between (x_{i-1},y_{i-1}) and (x_i,y_i). The program continuous with step 4.

3. If the distance from (a,b) to $(\bar{a}_p,\bar{b}_p)$ is less than the distance to projection points determined in previous steps (smaller i's), then the projection point (a_p,b_p) is replaced by $(\bar{a}_p,\bar{b}_p)$, i.e. we put $(a_p,b_p)=(\bar{a}_p,\bar{b}_p)$.
4. If i<*Npoint* the steps are repeated with i:=i+1.

The above algorithm is carried out for all relevant separating streamlines. For certain separating streamlines no projection point (a_p,b_p) will be found because the perpendicular projection does not exist. E.g in fig. 6 (a,b) can not be projected on the separating streamline between *S3* and *W4*. From all found projection points, we can determine the separating streamlines to which (a,b) is most close. Along this separating streamline we introduce (ρ,υ)-coordinates. In particular we determine the distance υ from (a,b) to (a_p,b_p) and the value of the integral $q_T(\rho)$ (21): if (a_p,b_p) is in between the points (x_{i-1},y_{i-1}) and (x_i,y_i) then $q_T(\rho)=q_{i-1} + \mu_i(q_i - q_{i-1})$, where q_i and μ_i are given by (24) and (28) respectively.

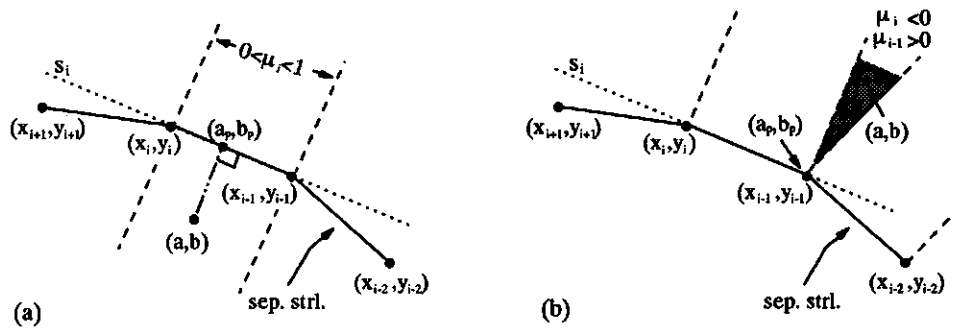

Fig. 7. Examples of projections of a point (a,b) on (a piece of) a separating streamline.

7.2 The boundary layer approximations

Once we have determined υ and $q_T(\rho)$ we can compute the asymptotic approximations for the arrival rate, the mean and variance of the arrival time and the arrival time distribution at a well that have been presented in van Kooten (1995). To facilitate computations the approximations are slightly rewritten in this report. We first indicate how the approximations are rewritten.

From $(2.3)^K$, $(6.13)^K$ and $(6.14)^K$ it follows that the asymptotic approximation for the arrival rate u can be expressed as

$$u(\rho,\upsilon) = \frac{1}{\sqrt{2\pi}} Iu \tag{29}$$

The integral Iu is defined in Table I, where $\kappa = 0$, $A = \upsilon q_T(\rho)$ and q_T is given by (21).

In the asymptotic approximations for the mean travelling time use is made of T_{sing} $(6.15)^K$ which is an approximation for the advective travelling time to a well in (ρ,υ)-

coordinates. In section 7.4 we pay more attention to T_{sing}. Using that

$$T_{sing}(\rho,\upsilon) = \frac{1}{\nu_\rho(0,0)}\ln(-\upsilon) + T_{sing}(\rho,-1) \quad , \tag{30}$$

we obtain that the composite approximation for the mean arrival time $(6.31)^K$ can be written as

$$T^{(1)}_{comp} = \begin{cases} T^{(1)}_{catch} + \dfrac{1}{\nu_\rho(0,0)}\left[-\ln(-A) + \dfrac{IT^{(1)}}{Iu}\right] & \text{if } \upsilon<0 \ , \\ T_{sing}(\rho,-1) + \dfrac{1}{\nu_\rho(0,0)}\left[-\ln(q_T(\rho)) + \dfrac{IT^{(1)}}{Iu}\right] + \dfrac{a_L(\rho,0)}{|\nu(\rho,0)|} & \text{if } \upsilon\geq 0 \ . \end{cases} \tag{31}$$

The integral and $IT^{(1)}$ is defined in Table I. From $(6.17)^K$ $(6.19)^K$ and $(6.29)^K$ we find that the boundary layer approximations for the variance of the arrival time may be written as

$$\sigma^2_{bound} = \frac{1}{\nu^2_\rho(0,0)}\left(\frac{IT^{(2)}}{Iu} - \left(\frac{IT^{(1)}}{Iu}\right)^2\right) + \frac{1}{Iu}\int_A^\infty \sigma^2_{sep}\left(\rho,\upsilon - \frac{s}{q_T(\rho)}\right)e^{-\frac{1}{2}s^2}ds \tag{32}$$

In section 7.3 we describe how the integrals Iu, $IT^{(1)}$ and $IT^{(2)}$ are computed. In section 7.5 the evaluation of the integral of σ^2_{sep} is described. We do not compute the integrals for the complete interval (A,∞). For $|s| > 10$ the value of $exp(-s^2/2)$ is so small that it can not be represented in FORTRAN REAL*4 precision (IEEE standard) anymore. To avoid numerical instabilities we already cut of the contribution for $|s| > 7.5$.

Definition of some integrals in the asymptotic method

$$Iu = \int_A^\infty (s-A)^\kappa e^{-\frac{1}{2}s^2}ds \quad , \qquad IT^{(1)} = \int_A^\infty (s-A)^\kappa \ln(s-A) e^{-\frac{1}{2}s^2}ds$$

$$IT^{(2)} = \int_A^\infty (s-A)^\kappa \ln^2(s-A) e^{-\frac{1}{2}s^2}ds$$

Table I. In (29), (31) and (32) $\kappa = 0$. In (40) and (41) $\kappa = \lambda/\nu_\rho(0,0)$

7.3 Evaluation of the integrals Iu, $IT^{(1)}$ and $IT^{(2)}$

None of the integrals in Table I can be computed analytically. So, the integration must be carried out. Because the *ln*-functions have a singularity at the endpoint $s=A$, $IT^{(1)}$ and $IT^{(2)}$ can not be solved with a simple quadrature rule. We determine the integrals in two steps.

First, at an interval $(A, A + \varepsilon)$ we expand the 'weight'-function $exp(-s^2/2)$ in a Taylor-series near $s_H = A + \varepsilon/2$. When the expansion is substituted in Iu, $IT^{(1)}$ and $IT^{(2)}$ the

integrals can be solved term by term analytically (Appendix A). We require that the error in the result is less than 10^{-5}. If we use six terms in the Taylor-expansion of $exp(-s^2/2)$ this accuracy is reached for ε=0.5. If $A > 7.5$ or $A + \varepsilon < -7.5$ the contribution of the integrals at the interval $(A, A + \varepsilon)$ is put to 0.

Second, from $s = A + \varepsilon$ the integrals are approximated with a Simpson rule. We split the interval $(A + \varepsilon, 7.5)$ into two sub-intervals: $(A + \varepsilon, M)$ and $(M, 7.5)$, where $M=\max(A + \varepsilon, -7.5)$. If $M > -7.5$ we apply the interval $(A + \varepsilon, M)$ the Simpson rule with stepsize h=0.02. If M=-7.5 the contribution of the integrals at this interval is neglected. At the interval $(M, 7.5)$ we take stepsize h=0.1. In (Stoer & Bulirsch, 1980, p. 120) an expression for the error in the Simpson approximation is given. Using this expression one may check that here the error is less then 10^{-5}.

7.4 The advective travelling time T_{sing}

When the injection point (a,b) is outside the catchment area of a well, the approximation for the mean arrival time (31) involves the evaluation of the term T_{sing}. An expression for T_{sing} has been derived by van Herwaarden (1994). From this derivation it follows that the logarithmic dependence of T_{sing} on υ (see (30)) arises from the assumption that the flow is rotational free near the stagnation point. The numerical velocity field used by ECOWELL will often not be perfectly rotational free. However, we assume that close to the separating streamline the advective travelling time to a well still approximately satisfies expression (30). Of course, the accuracy of this approximation depends on the coarseness of the discretization near the stagnation point. Therefore, we recommend to refine the discretization near the stagnation points in the flow.

From $(6.16)^K$ (or van Herwaarden, (1994), eq (4.9)) it follows that $T_{sing}(\rho,-1)$ is build up from integrals along the separating streamlines leading to and away from the stagnation point of interest. When we implemented these integrals in our computer program, it turned out that for υ small T_{sing} did not always perfectly coincide with the real advective travelling time T_{adv}. A much better results is obtained as follows. Using the (ρ,υ)-coordinates of point (a,b), we choose a point $(\tilde{\rho},\tilde{\upsilon})$ just inside the catchment area : $\tilde{\rho} = \rho$, $\tilde{\upsilon} = l/20$, where l (5) is the width of the element in which $(\rho,0)=(a_p,b_p)$ (fig. 7) is situated. With particle tracking (18) we determine the advective travelling $T_{adv}(\tilde{\rho},\tilde{\upsilon})$. Putting $T_{adv}(\tilde{\rho},\tilde{\upsilon}) = T_{sing}(\tilde{\rho},\tilde{\upsilon})$, we compute $T_{sing}(\tilde{\rho},-1)$ from eq. (30).

7.5 Evaluation of σ^2_{sep} and σ^2_{comp} .

In the asymptotic approximation for the variance of the arrival time σ^2_{comp} (32) we have a function σ^2_{sep} ($(6.24)^K$ and $(6.31)^K$) which is a (ρ,υ)-approximation for the integral of a_L/v^2 along a streamline close to the separating streamline. The expression $(6.24)^K$ consists of integrals along the separating streamlines leading to and away from the stagnation point of interest. In contrast to T_{sing} (see eq. (30)) these integrals have to be recalculated for each υ. Because in σ^2_{bound}(32) these integrals are nested in an integral to s, the evaluation of σ^2_{bound} becomes quite complicated. Moreover, since σ^2_{sep} has a singularity in υ=0, its evaluation for small υ causes numerical difficulties.

In ECOWELL these complications have been overcome as follows. Instead of applying the analytical approximation $(6.24)^K$ for $\sigma^2_{sep}(\rho,\upsilon)$, we evaluate the integral of

a_U/v^2 along the streamline through (ρ,υ) with the numerical method described in section 6. The advantage of this approach is that $\sigma^2_{catch}(\rho,\upsilon) = \sigma^2_{sep}(\rho,\upsilon)$, so that in σ^2_{comp} $(6.32)^K$ reduces to $\sigma^2_{bound}(32)$. The 'weight'-integral of σ^2_{sep} in (32) is computed with a Simpson rule with respect to s. Because of the singularity in $s=A$ we apply the Simpson rule with various stepsizes. At the interval $(A, A+0.2)$ we take stepsize $h = 0.005$, at $(A+0.2, A+1)$ $h = 0.05$ and at $(A, 7.5)$ $h = 0.1$. Let s_i be the corresponding partition points. The values

$$\sigma_i^2 = \sigma^2_{sep}(\rho, \upsilon - \frac{s_i}{q_T(\rho)}) \tag{33}$$

are stored in an array, so that they do not have to be recalculated for the arrival time distribution (34). If $|s_i| > 7.5$ the contribution of σ_i^2 to σ^2_{bound} is neglected; we put $\sigma_i^2=0$.

8. THE ARRIVAL TIME DISTRIBUTION

An approximation for the distribution for the arrival time at a well with only the effect of longitudinal dispersion incorporated is given by $(7.1)^K$. We have also derived a composite approximation that also takes into account transversal dispersion. Because in ECOWELL $\sigma^2_{catch} = \sigma^2_{sep}$ the composite approximation g_{comp} $(7.7)^K$ for the distribution of the arrival time t can be rewritten as

$$g_{comp}(x,y;t) = \frac{1}{\sqrt{2\pi}} \int_A^\infty g(\mu,\sigma^2;t) e^{-\frac{1}{2}s^2} ds \tag{34}$$

where g is given by $(5.6)^K$ and

$$\mu = \begin{cases} T^{(1)}_{catch}(x,y) + \dfrac{1}{v_\rho(0,0)} \ln(1 - \dfrac{s}{A}) & \text{if } \upsilon < 0 \\ T^{(1)}_{sep}(\rho,-1) + \dfrac{1}{v_\rho(0,0)} \ln(-\upsilon + \dfrac{s}{q_T(\rho)}) & \text{if } \upsilon \geq 0 \end{cases} \tag{35a}$$

$$\sigma^2 = \sigma^2_{sep}(-\upsilon + \frac{s}{q_T(\rho)}). \tag{35b}$$

The integral with respect to s in (35) is again computed with a Simpson rule with 3 different step sizes (see section 7.5).

To obtain an accurate description for the arrival time distribution g_{comp} should be determined for a wide range of t-values, theoretically from 0 to ∞. However, the contribution for both t small and t large will be will be almost zero. In Appendix B we show that before time

$$\tau_{min} = \mu - 4\sigma \frac{(-2\sigma + \sqrt{4\sigma^2 + \mu^2})}{\mu} \tag{36}$$

and after time

$$\tau_{max} = \mu + 4\sigma \frac{(2\sigma + \sqrt{4\sigma^2 + \mu^2})}{\mu}. \tag{37}$$

a fraction of at most 5.10^{-5} will enter the well. Therefore, we assume that it suffices to evaluate the arrival time distribution at (τ_{min},τ_{max}), where in (36) and (37) $\mu = T^{(1)}_{comp}$ and $\sigma = \sigma_{comp}$. [Note that the choice 5.10^{-5} is arbitrary. If sharper bounds are necessary, larger absolute values for r (B1) should be chosen, resulting in a smaller τ_{min} and a larger τ_{max} respectively]. At the interval (τ_{min}, τ_{max}) we choose 400 uniformly distributed times in which $g_{comp}(34)$ is evaluated. These partitions points are used in a Simpson rule for the breakthrough curve

$$b(t) = \int_0^t g_{comp}(x,y;\tau)d\tau \approx \int_{\tau_{min}}^t g_{comp}(x,y;\tau)d\tau . \tag{38}$$

9. INCORPORATION OF ADSORPTION AND DECAY

9.1 Linear equilibrium adsorption

The effect of linear equilibrium adsorption is to retard the spread of a contaminant. It does not affect the ultimate arrival fraction at a well. The effect of the retardation can be analyzed by replacing the velocity v by the retarded velocity $v^R=v/R$, where R is the retardation factor. The corresponding retarded values for the mean and variance of the arrival time are

$$\begin{aligned} T^{(1),R}_{comp} &= R\, T^{(1)}_{comp} , \\ (\sigma^R_{comp})^2 &= R^2 \sigma^2_{comp} . \end{aligned} \tag{39}$$

The retarded arrival time distribution is obtained from (34) by replacing μ and σ^2 by $\mu^R=R\mu$ and $(\sigma^R)^2=R^2\sigma^2$.

9.2 First order decay

The effect of first order decay has been studied extensively in van Kooten (1994). Using (31) we obtain that the approximation for respectively the arrival rate $(8.10)^K$ and mean arrival time $(8.11)^K$ can be rewritten as

$$u_{comp} = \begin{cases} \dfrac{1}{\sqrt{2\pi}} \exp\{-\lambda T_{adv}(x,y)\}(-A)^{\kappa} Iu & \text{if } v<0 , \\ \dfrac{1}{\sqrt{2\pi}} \exp\{-\lambda T_{sing}(\rho,-1)\}(q(\rho))^{\kappa} Iu & \text{if } v\geq 0 , \end{cases} \tag{40}$$

$$T^{(1)}_{1,comp} = \begin{cases} T_{adv}(x,y) + \dfrac{1}{v_\rho(0,0)}\left(-\ln(-A) + \dfrac{IT^{(1)}}{Iu}\right) & \text{if } v<0 , \\ T_{sing}(\rho,-1) + \dfrac{1}{v_\rho(0,0)}\left(-\ln(q(\rho)) + \dfrac{IT^{(1)}}{Iu}\right) & \text{if } v\geq 0 , \end{cases} \tag{41}$$

where $\kappa = \lambda/v_\rho(0,0)$ and Iu and $IT^{(1)}$ are again as defined in Table I. The method to

compute the integrals Iu and $IT^{(1)}$ has been described in section 7.2. In this case the asymptotic method does not give explicit expressions for the variance of the arrival time. Therefore, it is determined from the arrival time distribution $(8.1)^K$:

$$\sigma^2 \approx \int_{\tau_{min}}^{\tau_{max}} \frac{(t - T^{(1)}_{1,comp})^2 g_{comp}(x,y;t) e^{-\lambda t} dt}{u_{comp}}. \tag{42}$$

The integral with respect to t is computed with a Simpson rule ($\Delta t = (\tau_{max} - \tau_{min})/200$).

9.3 Linear kinetic adsorption

Kinetic adsorption may cause extensive tailing in the spread a contaminant. However, it does not affect the ultimate transversal spreading. Therefore, the arrival rate at a well can still approximated by (31). In van Kooten (1995b) we have shown that the arrival time distribution g_K of a kinetically adsorbing contaminant is related to the arrival time distribution of a non-adsorbing contaminant:

$$g_K(x,y;t) = g_{comp}(x,y;t) e^{-k_1 t} + \int_0^t g_{comp}(x,y;\tau) h_{ff}(\tau,t) d\tau. \tag{43}$$

where the distribution function h_{ff} is defined by van Kooten (1995b), expression (2). The integral in (43) should be evaluated with care. Below we discuss some complications we have to cope with.

Although the most important information on the arrival of a contaminant is contained in the arrival time distribution, for completeness we also compute the mean $T^{(1)}$ and variance σ^2 of the arrival time. Because no explicit expression for $T^{(1)}$ and σ^2 are available, they are computed from g_K.

9.3.1 Asymptotic behaviour

It is well known that for large k_f and k_b the kinetic model approximately predicts the same transport as the equilibrium model with retardation factor R_K=1+(k_f/k_b), i.e.

$$g_K(x,y;t) \to g_R(x,y;t) = \frac{1}{R_K} g_{comp}(x,y;\frac{1}{R_K}t) \quad \text{if } k_1, k_2 \to \infty. \tag{44}$$

In mathematical terms this implies that the function h_{ff} approaches a Dirac delta function peaked about $\tau_R = t/R_K$. The existence of this peak can be seen by rewriting h_{ff}:

$$h_{ff}(\tau,t) = (\frac{k_f k_b \tau}{t-\tau})^{1/2} I_1(z)\, e^{-z} exp\{-f(\tau)\} \tag{45a}$$

where

$$z = 2\sqrt{k_f k_b \tau (t-\tau)} \quad \text{and} \quad f(\tau) = \left(\sqrt{k_f \tau} - \sqrt{k_b (t-\tau)}\right)^2. \tag{45b}$$

From the asymptotic behaviour of the modified Bessel function

$$I_1(z) \approx \frac{e^z}{\sqrt{2\pi z}} \quad \text{for} \quad z \to \infty, \tag{46}$$

it follows that for k_f and k_b large the "Gaussian term" $exp(-f(\tau))$ dominates the behaviour of h_{ff} (45a). The width of this term vanishes if k_f, $k_b \to \infty$.

We note that Lassey (1988) has studied an integral similar to (43): his integrand g equals $(5.5)^K$ (i.e. our arrival time distribution with only the effect of longitudinal dispersion taken into account. He has developed an efficient analytical algorithm to evaluate (43) for large k_f and k_b. We have not implemented his (complete) algorithm because we need an algorithm that is also valid for small k_f and k_b. Moreover, in our integrand also the effect of transversal dispersion is incorporated. Nevertheless, some ideas of Lassey appeared to be useful in a mixed analytical-numerical approach.

9.3.2 *Mixed analytical-numerical approach*

To avoid numerical problems from the delta-function behaviour of h_{ff} and to force that g_K converges to g_R (44) if k_f, $k_b \to \infty$, we derive an analytical approximation for the integral in (43) at an ε-interval near τ_R. At the remainder of the interval $(\tau_{min}, min\{t, \tau_{max}\})$ we apply a Simpson rule with stepsize $\Delta\tau=(\tau_{min} - \tau_{max})/200$ (for $\tau < \tau_{min}$ and $\tau > \tau_{max}$ the contribution of the integrand g_{comp} is neglected, see section 8).

A Taylor-expansion for $f(\tau)$ at the interval $(\tau_R - \varepsilon, \tau_R + \varepsilon)$ is

$$f(\tau) = \frac{1}{2}\frac{(\tau-\tau_R)^2}{\sigma^2} + O(\varepsilon^3) \qquad \text{with} \quad \sigma^2 = \left\{f^{(2)}(\tau_R)\right\}^{-1} = 2\frac{k_1 k_2}{(k_1+k_2)^3}t\,. \tag{47}$$

Substituting the expansion in (43) and extracting all slowly varying terms from the integral we find the following approximation

$$\begin{aligned}\int_{\tau_R-\varepsilon}^{\tau_R+\varepsilon} g_{comp}(x,y;\tau)h_{ff}(\tau,t)d\tau &\approx [g_{comp}(x,y;\tau)(\frac{k_f k_b \tau}{t-\tau})^{1/2} I_1(z)e^{-z}]_{\tau=\tau_R}\cdot\sigma \int_{-\varepsilon/\sigma}^{\varepsilon/\sigma} exp\{-\tfrac{1}{2}\xi^2\}\,d\xi \\ &= \frac{1}{R_K} g_{comp}(x,y;\tau_R)\sqrt{2\pi z_R}\, I_1(z_R)e^{-z_R}\, erf(\frac{\varepsilon}{\sqrt{2}\,\sigma})\end{aligned} \tag{48}$$

The asymptote (46) implies that for k_f and k_b large ($\Leftrightarrow$ σ small) g_K indeed tends to g_R. For k_f and k_b small ($\Leftrightarrow$ σ large), (48) approaches a midpoint quadrature formula. For arbitrary sorption rates the mixed-method produced quite accurate results with $\varepsilon = \Delta\tau$. For the error-function in (48) we apply a polynomial approximation given in Abramowitz & Stegun (1970, eq. 7.1.26)

To compute I_1 in (45a) and (48) we use the Chebyshev approximations of Blair (1974). For $z < 15$ he gives an approximation for $z^{-1}I_1(z)$ and for $z \geq 15$ he gives an approximation for $e^{-z}I_1(z)$. For $z \geq 50$ we simply apply the asymptotic expression (46).

9.3.3 *First and last entering time*

We also have to analyze for which values of t we should compute g_K to obtain a complete and accurate description of the arrival time distribution. The first question is: at which time does the first amount of pollution enter the well? Secondly, when has all pollution reached the well? At least, the retardation effect of the kinetic process should be taken into account. So, in each case we determine g_K at the interval $(R_K\tau_{min}, R_K\tau_{max})$. However, also for $t \leq R_K\tau_{min}$ a considerable amount of pollution may enter the well, especially if the adsorption rate k_f is small. The second question is of particular interest if the desorption rate k_b is small. Due to long waiting times in the immobile phase g_K may have a long tail.

Let $b_K(t)$ be the breakthrough curve of the kinetically adsorbing contaminant. Because the arrival time distribution is the derivative of the breakthrough curve, we obtain from van Kooten (1995b, eq. 14a) that

$$b_K(t) = \int_0^t g_K(\tilde{t})\,d\tilde{t} = b(t)e^{-k_f t} + \int_0^t b(\tau)\{h_{ff}(\tau,t) + \frac{k_f}{k_b}h_{sf}(\tau,t)\}\,d\tau \,. \tag{49}$$

where $b(\tau)$ is the breakthrough curve (37) of the non-reacting solute. In Appendix B we show that for $t \in (\tau_{min}, R_K\tau_{min})$

$$b_K(t) \leq b(\tau_{min}) + [e^{-k_f t} + \tfrac{1}{2}\sqrt{k_f t\pi}\,\{erf(w_2) - erf(w_1)\}] \,, \tag{50a}$$

where

$$w_1 = \sqrt{k_f\tau_{min}} - \sqrt{k_b(t-\tau_{min})} \quad \text{and} \quad w_2 = \sqrt{k_f t} \,. \tag{50b}$$

Note that $b(\tau_{min})\approx 0$. From (50) we approximate the time at which pollution starts entering the well: t_{START} is the largest $t \in (\tau_{min}, R_K\tau_{min})$ for which the term between the brackets [ ] is less than 10^{-4}.

The lenght of the tail can be estimated in a similar way. We have the following upperbound for the amount of pollution that will enter the well after time $t \geq R_K\tau_{max}$:

$$1 - b_K(t) \leq (1-b(\tau_{max})) + [\tfrac{1}{2}\sqrt{k_f\tau_{max}\pi}\,\{erf(-w_3) - erf(-w_4)\}] \,, \tag{51a}$$

where

$$w_3 = -\sqrt{k_b t} \qquad \text{and} \quad w_4 = \sqrt{k_f\tau_{max}} - \sqrt{k_b(t-\tau_{max})} \,. \tag{51b}$$

Note that $(1-b(\tau_{max}))\approx 0$. We approximate the last entering time by t_{TAIL}: the smallest t for which the term between the brackets [ ] less than 10^{-4}.

The times $t \in (t_{START}, t_{TAIL})$ at which we evaluate g_K should be chosen with care. We distinguish two cases:

1. $k_f\tau_{min} \leq 2$ and $k_f/k_b > 1$, i.e. the mean residence time $1/k_f$ in the fluid phase is larger then or of the same order of magnitude as τ_{min}, whereas the residence time in the sorbed phase $1/k_b$ is large relative to $1/k_f$ (Note that in this case $t_{TAIL} = \tau_{min}$).
   The term $exp(-k_f t)$ will have an important effect on the shape of g_K. A considerable

amount of pollution will reach the well between (τ_{min}, τ_{max}). On the other hand, once a particle has been adsorbed it will remain immobile for a long time. So, g_K will have a long tail. A rather extreme case is shown in figure 8: 85% of the pollution enters the well between t = 110 and t= 270, whereas the tail extends from t= 270 to t= 130000.
To describe the peak and tail accurately we divide (t_{START},t_{TAIL}) into three subintervals.
- At (τ_{min}, τ_{max}) we choose n_1 = 200 points (dt_1 = (τ_{max}-τ_{min})/200).
- At (τ_{max}, $R_K\tau_{max}$) we also choose n_2 = 200 points (dt_2 = ($R_K\tau_{max}$-τ_{max})/200).
- At ($R_K\tau_{max}$, t_{TAIL}) we choose at most 100 points. If t_{TAIL}-$R_K\tau_{max}$ > 100·dt_2 we take n_3 = 100 and dt_3 = (t_{TAIL}-$R_K\tau_{max}$)/100 else n_3 = $\lfloor(t_{TAIL}$-$R_K\tau_{max})/dt_2\rfloor$ and dt_3 = dt_2.

2. In all other cases the shape of g_K is more regular (less peaked and/or tailed). Each particle will either make many transitions from the fluid to the sorbed phase before it enters the well (k_f large), or it will return rapidly to the fluid phase (k_b large) or both (equilibrium limit). Now, we divide (t_{START}, t_{TAIL}) into only two subintervals.
- We put n_1 = 0, dt_1 = 0.
- At (t_{START}, $R_K\tau_{max}$) we choose n_2 = 400 points (dt_2 = ($R_K\tau_{max}$-t_{START})/400).
- The partition point at ($R_K\tau_{max}$, t_{TAIL}) are chosen in a similar way as case 1.

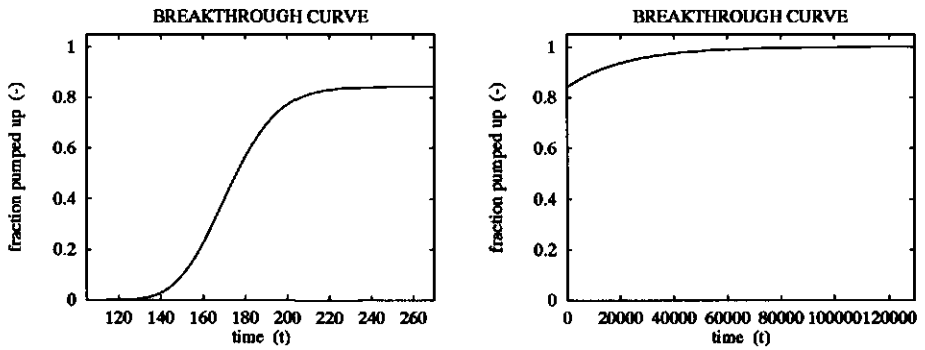

Fig. 8 Breakthrough curve of a kinetically adsorbing contaminant released in (-65,-90) (fig. 6) (a_L=0.2 (m), a_T=0.05 (m), k_f=10^{-3} (days^{-1}), k_b=5·10^{-5} (days^{-1})). Due to the small adsorption rate 85% of the solute enters the well between τ_{min}=110 and τ_{max}=270 (the first and last entering time of a non-reaction solute). The small desorption rate results in an extremely long tail.

9.4 Combined effects

The adsorption and decay phenomena discussed in the previous section may be combined (see section 2). First ECOWELL includes the retardation due to equilibrium adsorption. Next, the effect of kinetic adsorption is incorporated by computing g_K with retarded forward adsorption rate k_f^R = k_f/R_K (van Kooten, 1995b, section 3.4). The effect of decay is superposed by multiplying g_K with the survival factor $exp(-\lambda t)$. The arrival rate and the first and second moment of the arrival time are computed from respectively

$$\int_{t_{START}}^{t_{TAIL}} g_K e^{-\lambda t} dt \quad , \quad \int_{t_{START}}^{t_{TAIL}} t\, g_K e^{-\lambda t} dt \quad \text{and} \quad \int_{t_{START}}^{t_{TAIL}} t^2 g_K e^{-\lambda t} dt \; . \qquad (52)$$

10 CONTOUR LINES FOR h, u AND ARRIVAL TIMES

ECOWELL can generate contour lines of the hydraulic head h, the arrival fraction u ((29) or (40)) at a well, the mean arrival time $T^{(1)}$ ((31) or (41)) and the first and last entering time τ_{min} (36) and τ_{max} (37). For contour lines of u, $T^{(1)}$, τ_{min} and τ_{max}, ECOWELL first calculates their values in the grid points of the triangularization. The values of h in the grid points are already known because it is input for ECOWELL. The contour lines are generated with the use of barycentric coordinates. An exception is made for contour lines of u if the decay rate λ=0.

10.1 Equipotential lines

The user must first specify the point (a,b) through which he wishes to calculate an equipotential line. Because inside an element the hydraulic head is determined by linear interpolation, the equipotential line consists of element wise straight lines. The algorithm for calculating the intersection points with the edges of the elements is as follows.

- Let h_{ab}, h_1, h_2 and h_3 denote the hydraulic head in (a,b) and in the three nodal points of the element that contains (a,b). The equipotential line intersects two edges of the element. E.g. if $h_2 < h_{ab} < h_3$ the equipotential line crosses the edge at which $\beta_1 = 0$ (see fig. 3). This edge also bounds *Neighbour* 3 (fig. 4). From (6) it follows that the barycentric coordinates of the intersection points are given by

$$\beta_1 = 0\,, \qquad \beta_2 = \frac{h_{ab} - h_3}{h_2 - h_3}\,, \qquad \beta_3 = 1 - \beta_2\,. \tag{53}$$

  The other intersection point is calculated accordingly.
- To calculate the next part of the equipotential line the previous steps is repeated with h_1, h_2 and h_3 replaced by their values in one of the neighbour elements. However, now only one new intersection point has to be calculated because the other one is still known from the previous step. An exception is made for the case that the equipotential line exactly intersects a nodal point $k_{sect} = k_i$ (i = 1,2 or 3). In this case we should check all elements that surround k_{sect} to find the next part of the equipotential line.

The algorithm is repeated until the element that contains (a,b) is reached (the equipotential line is circular) or until the boundary of the domain is crossed.

10.2 Contour lines for u, $T^{(1)}$, τ_{min} and τ_{max} using a grid

In the grid points from which no contaminant can reach a specific well (u=0), the arrival time is undefined. To be able to calculate contour lines for $T^{(1)}$, τ_{min} and τ_{max}, such grid points are filled with the value T_{max}, where T_{max} is the maximum corresponding arrival time in the grid points in which the arrival time is well defined.

For any value (*VAL*) of $u \in (0,1)$ or $T^{(1)}$, τ_{min}, $\tau_{max} \in (0,T_{max})$ contour lines can be generated. First we have to search for a point in which u or the arrival time equals *VAL*. This point is searched at a line through (x_w,y_w) perpendicular to the vector $(x_w\text{-}x_{STAG},y_w\text{-}y_{STAG})^T$, where (x_w,y_w) is the position of the well and (x_{STAG},y_{STAG}) are the coordinates of a stagnation point connected with that well (An example is shown in figure 10). At this line u decreases from 1 (at the well) to 0 (far away from the well) and the arrival time increases from 0 to T_{max}. Once a point has been found in which u or the arrival time equals *VAL*, the contour line through that point is generated with the same algorithm as for the equipotential lines.

10.3 Contour lines for u if $\lambda = 0$

If the decay rate $\lambda = 0$ the contour lines for u can easily be determined from (31). We compute the value of A for which u equals a user specified value *VAL*. For a contaminant released at distance

$$v = \frac{A}{q_T(\rho)} \tag{54}$$

from a separating streamline the arrival fraction at the well equals *VAL*. The values of $q_T(\rho)$ have been stored in an array (section 5.4). Starting from a stagnation point connected with a specific well, we compute from (54) the contour lines at which u = *VAL*. An example is displayed in figure 9.

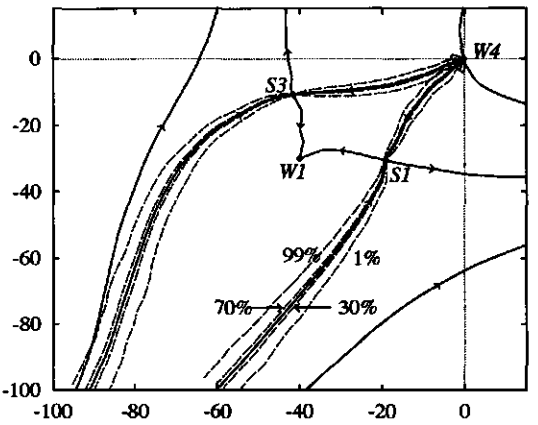

Fig. 9
Arrival rate contours for well *W1*. The dispersivities are a_L=0.2 (*m*) and a_T=0.05 (*m*).

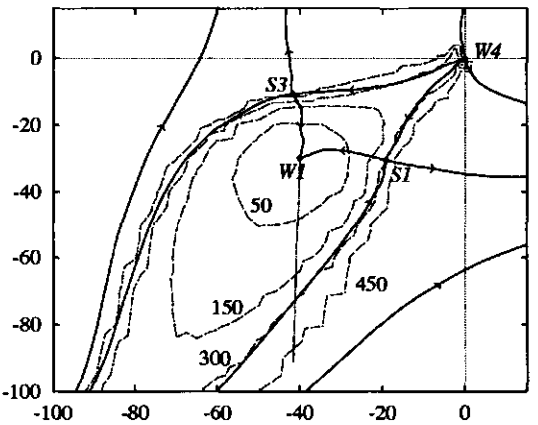

Fig. 10
Mean arrival time contours for well *W1*. First a grid with arrival times is computed. At the dashed-dotted line, which is perpendicular to *W1* - *S1*, we search for a point in which the arrival time equals a user-specified value. .

ACKNOWLEDGEMENTS

The author wishes to thank Johan Grasman and Maarten de Gee for their advices on the contents and presentation of this report. With Ed Veling I had some fruitful discussions on the evaluation of the integral in (43). He offered me computer code for (modified) Bessel functions. Oscar Buse and Adwin Vervuurt assisted me with the implementation of the algorithms in ECOWELL.

APPENDIX A: Approximations for Iu, $IT^{(1)}$ and $IT^{(2)}$ near an endpoint singularity

Let

$$Iu_\varepsilon = \int_A^{A+\varepsilon} (s-A)^\kappa e^{-\frac{1}{2}s^2} ds \,, \tag{A1}$$

$$IT_\varepsilon^{(2)} = \int_A^{A+\varepsilon} (s-A)^\kappa \ln(s-A) e^{-\frac{1}{2}s^2} ds \,, \tag{A2}$$

$$IT_\varepsilon^{(2)} = \int_A^{A+\varepsilon} (s-A)^\lambda \ln^2(s-A) e^{-\frac{1}{2}s^2} ds \,. \tag{A3}$$

Near s_H=A+ε/2 the Taylor-series of $e^{-\frac{1}{2}s^2}$ up to the sixth term reads

$$\sum_{i=0}^{5} c_i (s-s_H)^i \tag{A4}$$

where

$$c_0 = e^{-\frac{1}{2}s_H^2},$$

$$c_1 = \frac{1}{1!}\frac{d(e^{-\frac{1}{2}s^2})}{ds}\Big|_{s=s_H} = -s_H e^{-\frac{1}{2}s_H^2},$$

$$c_2 = \frac{1}{2!}\frac{d^2(e^{-\frac{1}{2}s^2})}{ds^2}\Big|_{s=s_H} = \frac{(s_H^2-1)}{2} e^{-\frac{1}{2}s_H^2},$$

$$c_3 = \frac{1}{3!}\frac{d^3(e^{-\frac{1}{2}s^2})}{ds^3}\Big|_{s=s_H} = -s_H\frac{(s_H^2-3)}{6} e^{-\frac{1}{2}s_H^2},$$

$$c_4 = \frac{1}{4!}\frac{d^4(e^{-\frac{1}{2}s^2})}{ds^4}\Big|_{s=s_H} = -\frac{(s_H^4-6s_H^2+3)}{24} e^{-\frac{1}{2}s_H^2},$$

$$c_5 = \frac{1}{5!}\frac{d^5(e^{-\frac{1}{2}s^2})}{ds^5}\Big|_{s=s_H} = -s_H\frac{(s_H^4-10s_H^2+15)}{120} e^{-\frac{1}{2}s_H^2}.$$

Substituting the Taylor-expansion in (A1), (A2) and (A3) and using that

$$(s-s_H)^j = \sum_{j=0}^{i} \binom{i}{j} (s-A)^j (-\tfrac{1}{2}\varepsilon)^{i-j} \,, \tag{A5}$$

we obtain the following approximation for Iu_ε, $IT_\varepsilon^{(1)}$ and $IT_\varepsilon^{(2)}$

$$I\tilde{u}_\varepsilon = \sum_{i=0}^{5} d_i \int_A^{A+\varepsilon} (s+A)^{i+\lambda} ds = \sum_{i=0}^{5} d_i \frac{1}{i+\lambda+1} \varepsilon^{i+\lambda+1} \tag{A6}$$

$$I\tilde{T}_\varepsilon^{(1)} = \sum_{i=0}^{5} d_i \int_A^{A+\varepsilon} \ln(s-A)(s-A)^{i+\lambda} ds = \sum_{i=0}^{5} d_i \frac{\varepsilon^{i+\lambda+1}}{i+\lambda+1}\left[\ln(\varepsilon) - \frac{1}{i+\lambda+1}\right] \tag{A7}$$

$$I\tilde{T}_\varepsilon^{(2)} = \sum_{i=0}^{5} d_i \int_A^{A+\varepsilon} \ln^2(s-A)(s-A)^{i+\lambda} ds = \sum_{i=0}^{5} d_i \frac{\varepsilon^{i+\lambda+1}}{i+\lambda+1}\left[\left(\ln(\varepsilon) - \frac{1}{i+\lambda+1}\right)^2 + \frac{1}{(i+\lambda+1)^2}\right] \tag{A8}$$

where

$$d_j = \sum_{i=j}^{5} c_i \binom{i}{j} (-\tfrac{1}{2}\varepsilon)^{i-j} \,. \tag{A9}$$

The integrals in (A7) and (A8) have been determined by (partial) integration.

$$|e^{-\frac{1}{2}s^2} - \sum_{i=0}^{5} c_i (s-s_H)^i| \le \frac{1}{6!} \max_{A<s<A+\varepsilon} |\frac{d^6(e^{-\frac{1}{2}s^2})}{ds^6}| (\tfrac{1}{2}\varepsilon)^6 \le \frac{15}{6!}(\tfrac{1}{2}\varepsilon)^6 . \tag{A10}$$

Using (A10) we can derive an upperbound for the error in $I\tilde{u}_\varepsilon$:

$$|Iu_\varepsilon - I\tilde{u}_\varepsilon| \le \frac{15}{6!}(\tfrac{1}{2}\varepsilon)^6 \int_A^{A+\varepsilon} (s-A)^\kappa ds = \frac{15}{6!}(\tfrac{1}{2}\varepsilon)^6 \frac{\varepsilon^{1+\kappa}}{1+\kappa}$$

Similar expressions can be derived for the error in $I\tilde{T}_\varepsilon^{(1)}$ and $I\tilde{T}_\varepsilon^{(2)}$. One may easily check that for ε=0.5 the errors in Iu_ε, $I\tilde{T}_\varepsilon^{(1)}$ and $I\tilde{T}_\varepsilon^{(2)}$ are less the 10^{-5}.

APPENDIX B: Bounds for the amount of pollution pumped up at a well before or after certain time

B1 Non-adsorbing contaminant

Let $r = \dfrac{(\tau-\mu)\mu^{1/2}}{\sigma\tau^{1/2}}$, (B1)

With τ_{min} and τ_{max} given by (36) and (37) ($\Leftrightarrow r = -4$ and $r = 4$, respectively) we obtain

$$\int_0^{\tau_{min}} g(\mu,\sigma^2;\tau)d\tau < \int_0^{\tau_{min}} (\frac{\tau}{\mu}+1) g(\mu,\sigma^2;\tau)d\tau = \frac{1}{\sqrt{2\pi}} \int_{-\infty}^{-4} e^{-\frac{1}{2}r^2} dr < 5\cdot 10^{-5} , \tag{B2}$$

and

$$\int_{\tau_{max}}^{\infty} g(\mu,\sigma^2;\tau)d\tau < \frac{1}{2}\int_{\tau_{max}}^{\infty} (\frac{\tau}{\mu}+1) g(\mu,\sigma^2;\tau)d\tau = \frac{1}{2\sqrt{2\pi}} \int_4^{\infty} e^{-\frac{1}{2}r^2} dr < 2.5\cdot 10^{-5} . \tag{B3}$$

It follows that

$$\int_{\tau_{min}}^{\tau_{max}} g d\tau = 1 - \int_0^{\tau_{min}} g d\tau - \int_{\tau_{max}}^{\infty} g d\tau > 0.9999 . \tag{B4}$$

B2 Kinetically adsorbing contaminant

Using that $I_0(x)e^{-x} \le 1$ and $I_1(x)e^{-x} \le 1$ (Abramowitz, 1970) we find from van Kooten (1995) (eq. A3) an upperbound for b_K (49):

$$\begin{aligned} b_K(t) &= b(t)e^{-k_f t} + \int_0^{\tau_{min}} b(\tau)\{h_{ff}(\tau,t) + \frac{k_f}{k_b} h_{sf}(\tau,t)\} d\tau + \int_{\tau_{min}}^{t} b(\tau)\{h_{ff}(\tau,t) + \frac{k_f}{k_b} h_{sf}(\tau,t)\} d\tau \\ &\le b(t)e^{-k_f t} + b(\tau_{min})(1-e^{-k_f t}) + \int_{\tau_{min}}^{t} b(\tau)\sqrt{k_f\tau}\,[(\frac{k_b}{t-\tau})^{1/2} + (\frac{k_f}{\tau})^{1/2}]e^{-w^2} d\tau \end{aligned} \tag{B5}$$

where

$$w = \sqrt{k_f\tau} - \sqrt{k_b(t-\tau)} . \tag{B6}$$

Performing a change of integration variable $\tau \rightarrow w$ we find

$$b_K(t) \le b(t)e^{-k_f t} + b(\tau_{min}) + b(t)\sqrt{k_f t}\int_{w_1}^{w_2} e^{-w^2}dw \qquad \text{(B7)}$$

where w_1 and w_2 are given by (50b). For $t < R_K\tau_{min}$, w_1 and w_2 are both positive. Because $b(t) \le 1$ we arrive at (50a).
In a similar way we obtain that for $t > R\tau_{max}$

$$\begin{aligned} 1-b_K(t) &= (1-b(t))e^{-k_f t} + \int_0^{\tau_{min}}(1-b(\tau))\{h_{ff}(\tau,t)+\frac{k_f}{k_b}h_{sf}(\tau,t)\}d\tau + \int_{\tau_{min}}^{t}(1-b(\tau))\{h_{ff}(\tau,t)+\frac{k_f}{k_b}h_{sf}(\tau,t)\}d\tau \\ &\le (1-b(\tau_{max})) + \int_0^{\tau_{min}}(1-b(\tau))\sqrt{k_f\tau}\,[(\frac{k_b}{t-\tau})^{1/2}+(\frac{k_f}{\tau})^{1/2}]e^{-w^2}d\tau \\ &\le (1-b(\tau_{max})) + \sqrt{k_f\tau_{max}}\int_{w_3}^{w_4} e^{-w^2}dw \end{aligned} \qquad \text{(B8)}$$

where w_3 and w_4 are given by (51a). Because w_3 and w_4 are less then 0 and $(1\text{-}b(t)) \le 1$. we arrive at (51b).

REFERENCES

Abramowitz, M. and I. Stegun, Handbook of mathematical functions, Ninth edition, Dover, New York, 1970.

Bear, J. and A. Verruijt, Modelling groundwater flow and pollution, Dordrecht, Reidel 1987.

Blair, J.M., Rational Chebyshev approximations for the modified Bessel functions I0(x) and I1(x), Mathematics of Computation, 28, p.581-583, 1974.

Buse, O.A. and J.J.A. van Kooten, ECOWELL, a program to Estimate the Contamination Of Wells, User manual, Department of Mathematics, Wageningen Agricultural University, 1995.

Cameron, D.R. and A. Klute, Convective dispersive solute transport with a combined equilibrium and kinetic adsorption model, Water Resour. Res., 13, 183-188,1977.

Cordes, C. and W. Kinzelbach, Continuous groundwater velocity fields and path lines in linear, bilinear and trilinear finite elements, Water Resour. Res., 28, 2903-2911, 1992.

Ewing, R.E., J.V. Koebbe, R. Gonzales, M.F. Wheeler, Mixed finite element methods for accurate fluid velocities, in *Finite Elements in Fluids, Volume 6: Finite Elements and Flow Problems*, R.H. Gallagher et al. eds., Wiley, New York, 1985, 233-249.

Kaasschieter, E.F. and A.J.M. Huyben, Mixed-hybrid finite elements and streamline computation for potential flow problem, Numerical Methods for Partial Diff. Equations, 8, 221-266, 1992.

Kaasschieter, E.F., Mixed finite elements for accurate particle tracking in saturated groundwater flow, Advances in Water Resources, 18 (5), 314-330, 1995.

van Kooten, J.J.A., Groundwater contaminant transport including adsorption and first order decay, Stoch. Hydrol. Hydraulics 8, 185-205, 1994.

van Kooten, J.J.A., An asymptotic method to predict the contamination of a pumping well, Advances in Water Resources, 18 (5), 295-313, 1995a.

van Kooten, J.J.A., A Method to solve the advection-dispersion equation with a kinetic adsorption isotherm, To appear in Advances in Water Resources, 1995b.

Lapidus, L. and G.F. Pinder, Numerical solutions of partial differential equations in science and engineering, John Wiley and Sons, 1982.

Lassey, K.R., Unidimensional solute transport incorporating equilibrium and rate-limited isotherms with First-Order-Loss, 1. Model conceptualizations and analytical solutions, 2. An approximated simulation after a pulsed input, Water Resour. Res., 24 (3), 343-355, 1988.

Stoer, J. and R. Bulirsch, Introduction to numerical analysis, Springer, New York, 1980.

CHAPTER 5

CASE STUDY: DELINEATION OF A PROTECTION ZONE NEAR PUMPING STATION LOCHEM

1. INTRODUCTION

In this chapter we apply the computer program ECOWELL to a real world problem. We searched for data of an aquifer in the Netherlands in which the flow is predominantly horizontal. Researchers of the RIVM (Rijksinstuut voor Volksgezondsheid en Milieuhygiene/National Institute of Public Health and Environmental Protection) brought to our attention an aquifer near Lochem in the Achterhoek from which groundwater is extracted by a pumping station. The pumping station is managed by Water Company Oostelijk Gelderland (WOG). We demonstrate how ECOWELL may be used to delineate a protection zone around the pumping station.

In section 2 we give a description of the (geo)hydrologic situation near Lochem. More detailed information, e.g. on the topography, the geology, geomorphology, the structure of the soil and land use, can be found in Broks (1991). The hydraulic head in the aquifer has been computed with the finite element program LGM (Landelijk Grondwater Model/National Groundwater Model) of the RIVM (section 3). With ECOWELL we analyse the effect of dispersion on the transport of a contaminant to the pumping station (section 4).

Dispersion may account for several effects. It may account for the tortuous movement of particles through the pores. In the previous chapters we have put emphasis on this interpretion. However, dispersion may also describe the uncertainty in prediction of the advective flow model. Due to the complex structure of a porous formation is often not possible to predict the actual transport of a contaminant, but rather some expected or average transport. The larger the uncertainties in the structure and parameters of the model, the larger the dispersivities should be taken. In the latter context ECOWELL may be used to get an impression of the uncertainty in the extent and shape of the catchment area and in the arrival times at a well.

2. DESCRIPTION OF THE GEOHYDROLOGICAL SYSTEM

Pumping station Lochem is situated at the foot of a hill (the Paaschberg) just south of the small town Lochem. A hydrological map of a region of 10x10 km around Lochem is shown in fig. 1. On this map all channels, brooklets and ditches in this region are indicated. The most important streams are the Berkel and the Veense Goot. The map has been drawn with the aid of GIS (Geographical Information System) and is based on a detailed invertarisation of the RGD (Rijksgeologische Dienst). From the streams water may percolate to the groundwater. Furthermore, recharge takes place by infiltration of

rainwater. Due to seasonal fluctuations in rainfall and evaporation, the infiltration is not equally distributed over a year. Because in a great part of the region the unsaturated zone is rather thick (20 à 30 m) the fluctuations are less recognizable in the groundwater head; in the period 1981-1991 changes between 0.75 and 1.5 m have been observed. Besides pumping station Lochem, four other private and industrial wells are operating in the region. The regional background flow is from south-east to north-west.

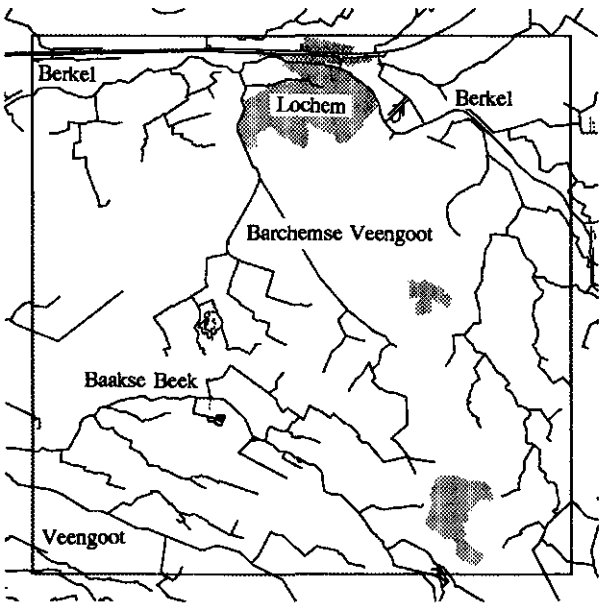

Figure 1 Hydro-geological map of a 10x10 *km* region near Lochem. The map is bounded by the coordinate lines x=220.000 *m*, x=230.000 *m*, y=455.000 *m* and y=465.000 *m* of the topographical map of the Netherlands.

3. NUMERICAL SIMULATION OF THE GROUNDWATER FLOW

We have computed the groundwater flow near Lochem with the finite element model LGM. In this national flow model the Dutch subsoil has been schematized into 4 layers. The upper layer is phreatic. The layers are separated by thin loam laminae. The lower layer has an impervious bottom. This schematization is based on bore hole data of the RGD. In each layer LGM utilizes the Dupuit-Forchheimer assumption that the variation of the head in the vertical direction is negligible. In some parts of the Netherlands, for example in the Achterhoek, the geohydrological properties of the layers only slightly differ, so that the schematization into 4 layers is redundant. The total thickness of the aquifer near Lochem, from surface level to the impervious bottom, varies between 45 and 90 m.

In fig. 2 the discretization of the region is displayed. It consists of both quadrangu-

lar and triangular elements. The two most important streams, the Berkel and the Veense Goot, are modelled separately. Near the pumping wells with the largest discharges the discretization has been refined. The topographical coordinates and the discharges of the wells are shown in table I. Actually, at pumping station Lochem eight extraction wells are operating with a total discharge of about 2.000.000 $m^3/year$. In the model these wells have been centred into one point.

Transient effects on the flow, due to seasonal fluctuations, have been neglected. Steady flow computations will already provide a good impression of the long term displacement of a water particle. As starting point has been taken the average isohypse pattern (head field) of the year 1988. By interpolation of the head, the boundary conditions for LGM have been determined. The drainage from the Berkel and the Veense Goot to the groundwater is assumed to be proportional to the area of the river bottom and the difference between the water level in the river and the groundwater head. The small streams (brooklets and ditches) have not been modelled separately. The drainage from or to the small streams has been incorporated in a recharge function. For the recharge of the groundwater due to infiltration of rain water, the average value is determined of the effective precipitation (i.e. the difference between rainfall and evaporation) over a number of years. The effective precipitation has been derived from measurements at a nearby KNMI-station and the air base Twente.

From the calculations with LGM it turned out that the hydraulic head in the four layers is exactly the same, which confirms that the flow in the aquifer is predominantly horizontal. The isohypse-pattern is displayed in fig. 3.

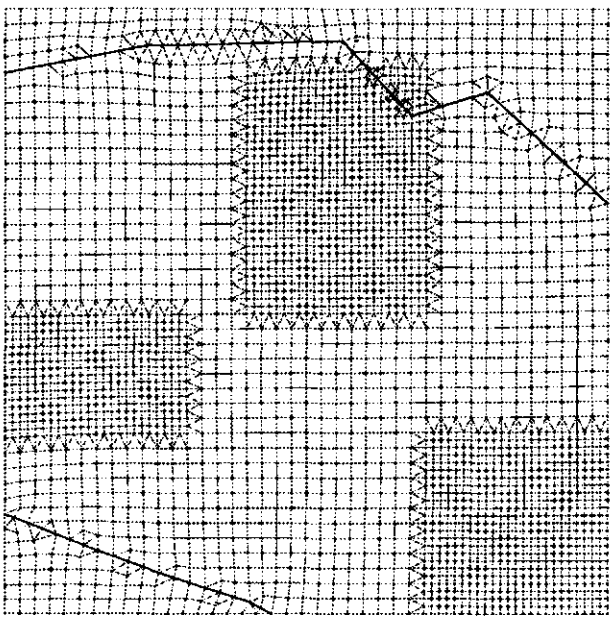

Figure 2 In the discretization that is used by LGM, special attention has been paid to the major streams, the Berkel and the Veense Goot.

Well no.	Topograghical coordinates	Discharge (m^3/year)
W1	(226025, 464565)	362988
W2	(225850, 464480)	530823
W3	(225170, 462945)	1874870
W4	(220600, 459450)	1092041
W5	(228155, 456760)	744110

Table I Topographical coordinates and discharges of the pumping wells. W3 is pumping station Lochem

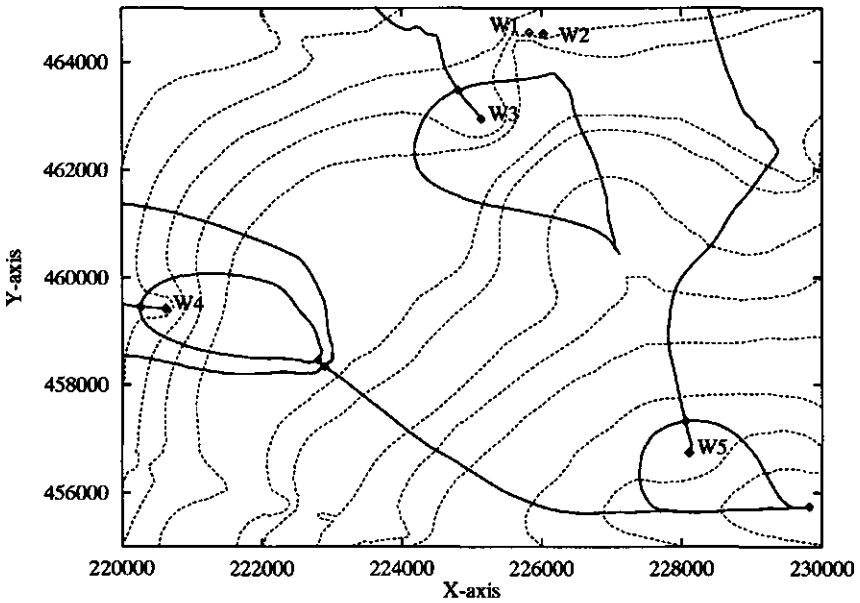

Figure 3 Isohypse pattern in the aquifer. The head field was computed with LGM. The equipotential lines have been drawn by ECOWELL.

4. ANALYSIS OF DISPERSION WITH ECOWELL

4.1 Preliminaries

ECOWELL can only be applied to strictly 2-dimensional systems: it cannot deal with multi-layer systems. Therefore we slighty adapt the output of LGM. We neglect the multi-layer structure and treat the aquifer as one phreatic system. The conductivity in a nodal point is defined as the average of the conductivity in the four layers. The average conductivity varies between 18 *m/d* and 22.5 *m/d*. Because the hydraulic head in the four layers is equal, the velocity field that is computed with the average conductivities describes the mean flow in the aquifer. Also the discretization has to be modified. ECOWELL uses a

network of triangular elements. We have split all quadrangular elements in the LGM-network into two triangles.

One of the assumptions behind ECOWELL is that the 2D flow is divergence free, which implies that the flow is not affected by recharge. Due to infiltration of rainwater and drainage from streams, the groundwater flow near Lochem is obviously not divergence free. Nevertheless, we expect that in the parts of the region where the effect of recharge is small, ECOWELL may provide a good impression of the effect of dispersion on the transport of a contaminant. One should be aware of the fact that when the recharge is large (e.g. close to a stream) unreliable results will be obtained.

4.2 Stagnation points and separating streamlines

With ECOWELL the stagnation points in the flow have been determined. Six stagnation points were found: (in mathematical terms) four sadlle points and two negative attractors. By backward integration from the saddle points the separating streamlines were determined (fig. 4). To decide with which well a stagnation point is connected also the streamlines leading away from the stagnation points were determined. For wells W1 and W2 no stagnation points were found. Most probably the stagnation points for W1 and W2 are outside the region. Furthermore the discretization near W1 and W2 should be refined. Because we are primarily interested in contaminant transport toward pumping station Lochem (W3) we have not carried out these steps.

Before we have analysed the effect of dispersion on the transport of a contaminant towards pumping station Lochem, we have used ECOWELL to compute some advective travelling time zones (fig. 5).

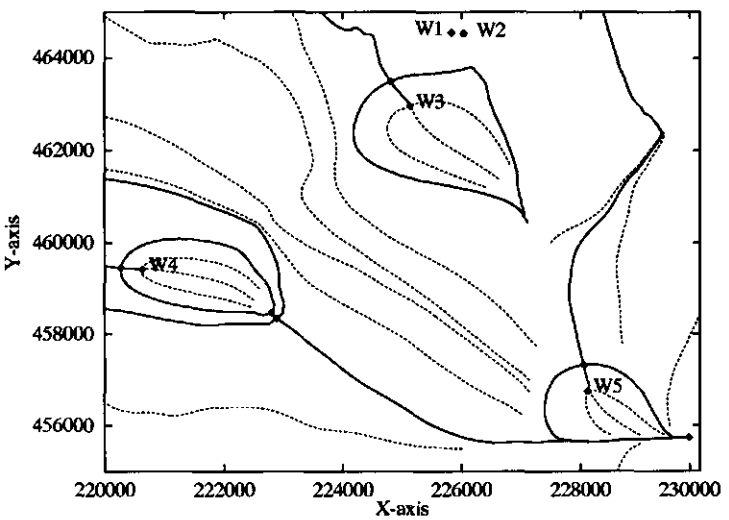

Figure 4 Stream pattern and catchment areas.

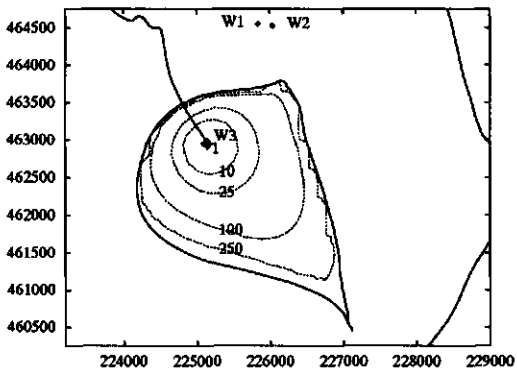

Figure 5 Advective traveling time contours: T_{adv} = 1, 10, 25, 100, 250 year.

4.3 The effect of dispersion on arrival fractions and arrival times

In practice the values of the longitudinal and transversal dispersivities are not exactly known. Dispersivities based on from laboratory experiments do not apply to field scale transport; fields scale dispersivities are a few orders of magnitude larger than those observed at laboratory scale. However, the results of field experiments are of low reliablity (Gelhar, 1986). At best, it is possible to indicate a range within which dispersivities may vary. Therefore to get an impression of what the effect of dispersion might be, the transport of a contaminant should be computed for various values of the dispersivities.

We have analysed the effect of dispersion on the ultimate arrival fraction and arrival time at pumping station Lochem for a_L=1.0 *m* and a_T=0.1 *m* (fig. 6abc) and for a_L=10.0 *m* and a_T=1.0 (fig. 6def). In fig. 6a and 6d some contours of equal arrival fraction (or probability) have been drawn. Along the separating streamline on the left hand side of the stagnation point the asymptotic approximations are smooth. However, along the separating streamline on the right hand side of the stagnation point the contours are very irregular, especially along the part where the separating streamline passes the Berkel closely. Along this part the flow velocity is very low and highly divergent. Because of the low velocity the term $q(\rho)$ (chapter 2, (6.14)) becomes small, so that the width of the error-function (chapter 2, (6.13)) that describes the transition of the arrival probability from 1 to 0 increases. The same effect is observed in the arrival time contours. Since the flow is highly divergent the asymptotic method is inaccurate in the neighbourhoud of this separating streamline.

Protection zones are often based on 1, 10 and 25 year mean travelling zones. However, due to dispersion a considerable fraction of a contaminant may reach the well before its mean arrival time $T^{(1)}$, so that mean arrival time contours may be unreliable measures for the protection zone. In the Technical Documentation of ECOWELL we have derived an approximation for the first arrival time τ_{min} in which the variance in the arrival time due to dispersion is taken into account. We have shown that before τ_{min} (Chapter 4, eq. (36) and Appendix B) at most a 5.10^{-5} fraction of a contaminant will reach the well. So τ_{min} may be a more reliable measure for the delineation of protection zones than $T^{(1)}$. Therefore in fig. 6c and 6f we have drawn contours of τ_{min}. Examples of arrival time distributions for a contaminant spilled in (226500, 461500) are shown in fig. 7. The figure clearly illustrates that dispersion may cause large spreading in the arrival time at the well.

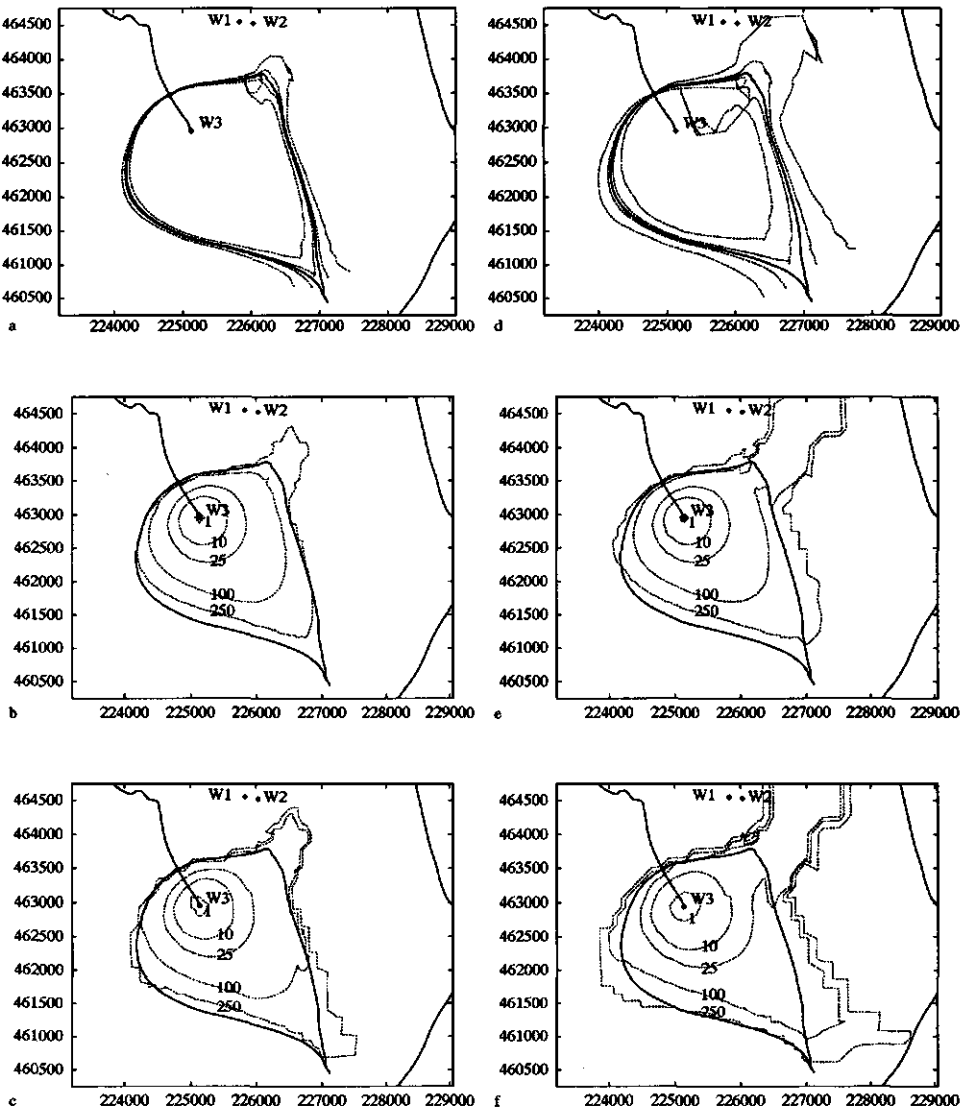

Fig. 5 In a, b, c, a_L=1.0 *m* and a_T=0.1 *m*. In d, e, f, a_L=10.0 *m* and a_T=1.0 *m*
a and d: Arrival fraction/probability contours: u = 0.001, 0.25, 0.75. 0.999.
b and e: Mean/Expected arrival time contours: $T^{(1)}$= 1, 10, 25, 100, 250 year.
c and f: First arrival time contours: τ_{min} = 1, 10, 25, 100, 250 year.

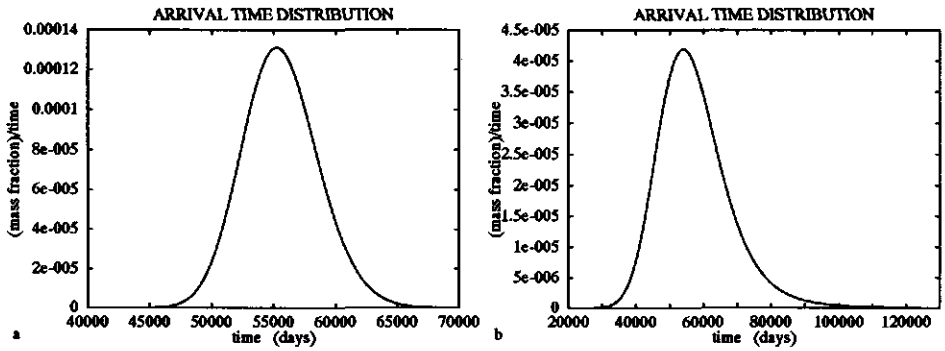

Fig. 7 Arrival time distributions at pumping station Lochem for a contaminant spilled in (226500, 461500). In fig. (a) a_L=1.0 *m* and a_T=0.1 *m*. In fig. (b) a_L=10.0 *m* and a_T=1.0 *m*.

CONCLUSIONS

The simulations confirmed that ECOWELL is a flexible and easy to use package for groundwater modellers. We were able to run ECOWELL after only slight modification of the conductivities and the finite element mesh used by the flow model LGM. In most applications the values of the dispersivities are uncertain. Because ECOWELL provides its results quickly, it is a helpful tool to analyse the effect of dispersion for various values of the dispersivities.

Close to the river the Berkel the results of ECOWELL are unreliable. This is not surprising. ECOWELL is based on the assumption that the flow is divergence free. Therefore only realible results may be expected when the recharge is small.

From fig. 6a and 6d we may conclude that due to transversal dispersion even from about 300 *m* outside the catchment area contamination may reach pumping station Lochem. However, from the time-contours it is seen that it will take more than 100 years before such contamination reaches the well. Fig. 6c and 6f illustrate the effect of dispersion on the arrival time of a contaminant. The radii of the 1, 10 and 25 year first arrival time contours are about 200 *m* larger than the corresponding contours of the mean arrival time.

ACKNOWLEDGEMENTS

The author thanks Rien Pastoors of the RIVM for carrying out the calculations with LGM and for patiently answering my many questions. Theo Reuling of the WOG in Doetinchem sent me some reports with geohydrolgical information on the aquifer near pumping station Lochem. I am also grateful to Maarten de Gee, Johan Grasman and Pieter Raats for their suggestions for improving the text.

REFERENCES

Broks Onderzoek & Ontwerp, Geohydrologisch onderzoek winplaats Lochem, Den Bosch, 1992.

Gelhar, L.W., Stochastic subsurface hydrology from theory to applications, Water Resour. Res., 22, 135S-145S, 1986.

SAMENVATTING

In grote delen van de wereld is grondwater de belangrijkste bron voor de drinkwatervoorziening. In Nederland wordt ongeveer 70% van het drinkwater uit de grond opgepompt. Bij het beheersen van de kwaliteit van het grondwater vormen wiskundige modellen een onmisbaar hulpmiddel. Hiermee kan een voorspelling verkregen worden van het transport van een verontreiniging naar een pompstation. Veel huidige modellen houden slecht rekening met het meebewegen van een verontreiniging met de macroscopische stroming (advectie). Bij het vaststellen van een beschermingsgebied gaat men dan uit van het zogenoemd intrekgebied rond een pompstation. De werkelijkheid is echter gecompliceerder. Op microscopische schaal maken deeltjes kronkelige bewegingen door de poriën van de grond, waardoor de verspreiding in zowel longitudinale als transversale richting versterkt wordt. Dit proces heet dispersie. Als gevolg van dispersie kan een fractie van een verontreiniging, welke buiten het intrek gebied werd losgelaten, de grens van het intrekgebied passeren en alsnog worden opgepompt. Longitudinale dispersie beïnvloedt de tijd dat deeltjes in de put blijven sijpelen.

Er bestaan reeds eindige elementen en eindige differentie methoden om het advectie-dispersie model op te lossen. Een nadeel van deze numerieke methoden is dat ze een groot computer geheugen en veel rekentijd vereisen. Bovendien kunnen discretisatiefouten tot grote onnauwkeurigheden leiden, vooral als de dispersie heel klein is. Een alternatief is gevonden in de random walk methode, welke de stochastische wandeling van de deeltjes door de poriën nabootst. Door de wandeling vele malen te herhalen wordt een benadering verkregen voor de fractie van de deeltjes die in de put komen, alsmede voor de aankomsttijdenverdeling. Deze methoden is echter erg tijdrovend.

Door collega-onderzoekers van de vakgroep Wiskunde van de Landbouwuniversiteit is een begin gemaakt met de ontwikkeling van een analytische benaderingsmethode die bovengenoemde nadelen niet heeft. De methode gaat er van uit dat de macroscopische stroming in de waterhoudende formatie (aquifer) reeds bekend is. Deze stroming wordt verondersteld voornamelijk stationair en horizontaal te zijn. Met behulp van perturbatie technieken wordt het effect van dispersie berekend. In dit proefschrift wordt de methode verder ontwikkeld.

In hoofdstuk 1 bestuderen we het transport van een stof die (als gevolg van radioactief verval of chemische reacties) exponentieel afgebroken wordt. Allereerst leiden we randwaardeproblemen af voor de kans en de te verwachten tijd waarop een deeltje via een stochastische wandeling de rand van een gebied bereikt. De achterwaartse Kolmogorov vergelijking speelt hierin een sleutelrol. Gegeven de huidige plaats van een deeltje beschrijft de achterwaartse vergelijking de plaats waar een deeltje vandaan gekomen kan zijn. Deze randwaarde problemen zijn toegepast op een gebied met een put en vervolgens asymptotisch opgelost. De dispersie wordt beschouwd als een verstoring die in eerste instantie verwaarloosd kan worden. Rond een scheidende stroomlijn, die het intrekgebied van een put begrenst, zal transversale dispersie echter een belangrijke rol spelen. In een grenslaag rond een scheidende stroomlijn is dus een correctie nodig. Hiertoe voeren we langs de scheidende stroomlijn nieuwe coördinaten in. Met storingstechnieken is aange-

toond dat de correctie uit error-achtige functies bestaat. Omdat longitudinale dispersie slechts een zeer klein effect heeft op de aankomstfractie en gemiddelde aankomsttijd, kan deze nog steeds buiten beschouwing worden gelaten. De asymptotische benadering zijn vergeleken met de resultaten van random walk simulaties waarin deeltjes op exponentieel verdeelde tijdstippen worden afgebroken. De overeenkomst is zeer goed.

In hoofdstuk 2 leiden we benaderingen af voor de variantie van de aankomsttijd en voor de aankomsttijden verdeling. Nu is het van belang om ook het effect van longitudinale dispersie mee te nemen. We ontwikkelen de momenten van de aankomsttijd in een machtreeks van de longitudinale dispersiecoëfficiënt. De termen van de machtreeks kunnen iteratief bepaald worden. Longitudinale dispersie is een 1-dimensionaal proces; een deeltje verandert hierdoor niet van baan. De waarschijnlijkheidsverdeling voor de aankomst van een deeltje aan het eindpunt van een kolom met constante snelheid gebruiken we als parameterisatie voor de aankomsttijdenverdeling in de put. Rond een scheidende stroomlijn moet opnieuw het effect van transversale dispersie worden meegenomen. De transversale dispersie maakt het verspreidingsproces essentieel 2-dimensionaal. Uit de in hoofdstuk 1 gevonden benaderingen leiden we een waarschijnlijkheidsverdeling af voor het overspringen van deeltjes naar een nabijgelegen stroombaan. Gebruikmakend van deze waarschijnlijkheidsverdeling berekenen we de verwachtingswaarde van de benaderingen die horen bij de 1-dimensionale dispersie processen langs de stroombanen waar een deeltje naar toe kan springen. De aldus verkregen benaderingen blijken opnieuw goed overeen te stemmen met de resultaten van random walk simulaties.

Hoofdstuk 3 is een meer algemeen hoofdstuk. We bestuderen de transportvergelijkingen voor een stof waarvan de deeltjes afwisselend een tijdje aan de poriewanden geadsorbeerd zijn en vrij zijn (kinetische adsorptie). Door gebruik te maken van het stochastisch karakter van de kinetiek tonen we aan de advectie-dispersievergelijking en de adsorptie isotherm ontkoppeld kunnen worden. Omdat advectie en dispersie alleen in de vrije fase plaatsvinden, kan het concentratie profiel van de adsorberende stof geschreven worden als convolutie van het concentratie profiel van een niet-adsorberende stof en een verblijftijdenverdeling voor deeltjes in de vrije fase. Hiermee kan de in hoofdstuk 2 gevonden aankomsttijdenverdeling gegeneraliseerd worden voor een kinetisch adsorberende stof. Ook demonstreren we hoe de methode simultaan met een numeriek transport model gebruikt kan worden. Vooral als het stroompatroon gecompliceerd is betekent de methode grote winst. Bij verandering van de adsorptie coëfficiënten hoeven de numerieke berekeningen niet opnieuw gemaakt te worden, slechts de postprocesslag voor het meenemen van de kinetiek dient te worden herhaald.

Hoofdstuk 4 is de technische documentatie van het computer programma ECOWELL. In dit programma zijn de resultaten van het onderzoek geïmplementeerd. ECOWELL moet gebruikt worden in combinatie met een eindige elementen of eindige differentie model voor grondwaterstroming. Zo'n model berekent het potentiaalveld voor een waterhoudende formatie waarin één of meerdere putten en bronnen werkzaam zijn. Dit potentiaalveld is input voor ECOWELL. Met ECOWELL kan het effect van dispersie, adsorptie en afbraak op het transport naar een put berekend worden. We beschrijven hoe ECOWELL de stagnatiepunten en de bijbehorende scheidende stroomlijnen in het stroompatroon bepaald en hoe de transformatie naar grenslaag coördinaten wordt uitgevoerd. Ook geven we schattingen voor het allereerste moment waarop een puntverontreiniging in de put begint te sijpelen, alsmede voor het moment waarop vrijwel alles is opgepompt. ECOWELL kan

worden toegepast bij

- het zo nauwkeurig mogelijk afbakenen van een grondwater beschermingsgebied,
- het ontwerpen van een schoonspoel-strategie van een vervuilde aquifer,
- het uitvoeren van een risico-analyse, bijv. betreffende het plaatsen van een afvaldepot op een zekere locatie,
- het schatten van de effectieve poreusiteit en/of dispersiviteiten, door in tracertests theoretisch en waargenomen doorbraak curves te fitten.

In hoofdstuk 5 beschouwen we een praktijk voorbeeld. We demonstreren hoe ECOWELL toegepast kan worden bij afbakenen van een beschermingsgebied rond pompstation Lochem in de Achterhoek. Het stroompatroon rond Lochem is berekend met het eindige elementen pakket LGM (Landelijk Grondwater Model) van het RIVM. Met ECOWELL hebben we het effect van dispersie bestudeerd op de aankomstfractie van een verontreiniging in het pompstation en op de 1, 10, 25, 100, en 250-jaars aankomsttijden zones.

Curriculum Vitae

Jaco Johannes Adriaan van Kooten werd op 29 mei 1968 geboren te Almkerk. In 1986 behaalde hij het VWO-diploma aan het Buys Ballot College te Goes. Daarna is hij Wiskunde gaan studeren aan de Rijksuniversiteit Utrecht. In augustus 1991 studeerde hij af in de toegepaste analyse met bijvakken in de informatica en econometrie. Het afstudeerwerk werd uitgevoerd onder supervisie van prof.dr.ir. W. Eckhaus en dr. A. Doelman. Voor de studierichting Cognitieve Kunstmatige Intelligentie is hij tweemaal als studenten-assistent werkzaam geweest. Bij Jaco van Leeuwen (thans organist te Noordwijk) en Stephen Taylor (organist van de Nicolaykerk te Utrecht) heeft hij orgellessen gevolgd. Gedurende heel zijn studententijd is hij actief geweest voor de reformatorische studentenvereniging Depositum Custodi.

Van 1 september 1991 tot en met 1 september 1995 is hij Onderzoeker in Opleiding (OiO) geweest aan de vakgroep Wiskunde van de Landbouwuniversiteit Wageningen. Het onderzoeksproject werd gefinancierd door de Stichting Technische Wetenschappen en was getiteld "Mathematische modellering van het transport van verontreinigd grondwater". Om in het onderzoeksonderwerp thuis te raken, heeft hij van januari tot en met mei 1992 stage gelopen aan het RIVM (Rijksinstituut voor Volksgezondheid en Milieuhygiëne) te Bilthoven. De stage-begeleider was dr. G.J.M. Uffink. Aan de LUW behoorde het geven van onderwijs en het begeleiden van een afstudeerstudent tot zijn taken. Het promotieonderzoek werd uitgevoerd onder leiding van prof.dr.ir. J. Grasman en Dr. M. de Gee.

De resultaten van het onderzoek zijn gepresenteerd op conferenties in Wageningen, Waterloo (Canada), Heidelberg, Lunteren en Praag.